

## ABSTRACT

Toxicological Response to Nanomaterial Exposure  
in *In Vitro* Lung Cells are Determined by Cell-Type

Henry Lujan Jr., Ph.D.

Mentor: Christie M. Sayes, Ph.D.

Nanotechnology is an advancing field that continually introduces new nano-enabled products into consumer products thereby increasing the risk of nanoparticle exposure to humans and the surrounding environment. The increased rate of nanoparticle exposure to humans requires the field of nanotoxicology to rapidly screen for markers of toxicity after nanomaterial exposure. To properly screen for markers of toxicity, this study aims to address gaps in the *in vitro* nanotoxicology literature. First, the most common biochemical pathways investigated in the nanotoxicology literature were outlined to build a landscape of the *in vitro* nanotoxicology literature to find the gaps in the literature. Next, ill-defined cell culture parameters were examined to outline the appropriate methodology required to generate proper cytotoxicological models. Lastly, a suite of microscopy techniques was used to examine novel mechanisms through which aluminum (Al) nanomaterials exert their toxicity. Results showed that no two cell lines are alike as each cell-type exhibits differential baseline characteristics. Furthermore, the cell-type and inherent morphological and biochemical differences between all cells

influences the toxicological response to nanomaterials. This research will advance the field of nanotoxicology by highlighting the importance of proper characterization for *in vitro* cell culture systems and nanoparticle test systems to increase the complexity and impact of conclusions drawn from past, current, and future pulmonary nanotoxicological studies.

Toxicological Response to Nanomaterial Exposure  
in *In Vitro* Lung Cells are Determined by Cell-Type

by

Henry Lujan, Jr., B.S.

A Dissertation

Approved by the Department of Environmental Science

---

George P. Cobb, Ph.D., Chairperson

Submitted to the Graduate Faculty of  
Baylor University in Partial Fulfillment of the  
Requirements for the Degree  
of  
Doctor of Philosophy

Approved by the Dissertation Committee

---

Christie M. Sayes, Ph.D., Chairperson

---

Erica D. Bruce, Ph.D.

---

Ramon Lavado, Ph.D.

---

Joseph H. Taube, Ph.D.

---

Leigh K. Greathouse, Ph.D.

Accepted by the Graduate School  
December 2020

---

J. Larry Lyon, Ph.D., Dean

Copyright © 2020 by Henry Lujan Jr.

All rights reserved

## TABLE OF CONTENTS

LIST OF FIGURE .....	vi
LIST OF TABLES.....	viii
ACKNOWLEDGMENTS.....	ix
DEDICATION.....	x
CHAPTER ONE.....	1
Cytotoxicological pathways induced after nanoparticle exposure: studies of oxidative stress at the ‘nano–bio’ interface.....	1
Abstract .....	1
Introduction .....	2
Discussion .....	25
Conclusions .....	29
References .....	31
CHAPTER TWO.....	41
Refining In Vitro Toxicity Models: Comparing Baseline Characteristics of Lung Cell Types .....	41
Abstract .....	41
Introduction .....	42
Materials and Methods.....	45
Results .....	53
Discussion .....	67
References .....	71
CHAPTER THREE .....	76
Lung Cell Disease State Directly Impacts Aluminum Nanoparticle Uptake and Fluctuations in Mitochondrial Morphology In Vitro.....	76
Abstract .....	76
Introduction.....	77
Results and Discussion.....	79
Conclusion.....	95
Methods.....	98
References .....	104
CHAPTER FOUR .....	108
General Discussion and Conclusions .....	108
Future Direction .....	112

References .....	119
BIBLIOGRAPHY .....	120

## LIST OF FIGURES

Figure 1.1. The possible nanoparticle uptake mechanisms described in the current Literature .....	5
Figure. 1.2. The number of papers reporting nanoparticle-induced pathway perturbations in the peer-reviewed literature.....	6
Figure 1.3. Overview of common pathways induced after nanoparticle exposure .....	26
Figure 2.1. The design of the in vitro experiments.....	46
Figure 2.2. Fluorescent microscopy shows distinct growth patterns, degrees of contact inhibition, and respiratory capacity.....	55
Figure 2.3. Cellular proliferation and mitochondrial activity are different among the six cells .....	57
Figure 2.4. Heatmap of mRNA expressions.....	58
Figure 2.5. Cells produce similar amounts of p53 but differing amounts of p21, IL-6, and GSR.....	60
Figure 2.6. Whole cell analysis of cell cycle distributions and general oxidative Stress.....	61
Figure 2.7. Comparative change in oxidative stress after exposure to tert-butyl Hydroperoxide .....	62
Figure 2.8. Boxplots for the protein, cytokine, and enzyme concentrations measured in experimental datasets.....	63
Figure 2.9. Interaction plots for the protein, cytokine, and enzyme concentrations measured in experimental datasets showing the sample mean for each treatment connected by a line .....	65
Figure 2.10. Proposed pathway linking ROS generation to induction of Inflammatory cascades, decreased viability, and cell cycle disruption.....	69
Figure 3.1. Mechanisms of mitochondrial dysregulation after aluminum nanoparticle exposure .....	81

Figure 3.2. Characterization of mitochondrial morphology in untreated primary, cancer, and asthma lung cell-types .....	83
Figure 3.3. Confirmation of aluminum nanoparticle intracellular internalization .....	87
Figure 3.4. Morphological changes in mitochondria among aluminum nanoparticle treated cell-types.....	88
Figure 3.5. Cross comparisons within each cell-type before and after aluminum nanoparticle exposure .....	91
Figure 3.6. Colocalization of lysosomes and mitochondria .....	94
Figure 4.1. Building a mitochondrial structure function relationship .....	113
Figure 4.2. Experimental design for mechanistic pathway analysis.....	115
Figure 4.3. Overview of the electron transport chain and processes that can be Measured .....	116
Figure 4.4. Extracellular flux analysis of A459 lung cancer cells after exposure to aluminum nanoparticles.....	117

## LIST OF TABLES

Table 1.1. Summary table of the pathways reviewed in this paper .....	21
Table 1.2 Assays used in the reviewed papers to probe cellular toxicity endpoints after nanoparticle exposure.....	22
Table 2.1. Comparison of culture conditions .....	47
Table 2.2. Two-way ANOVA results for each response.....	65
Table 2.3. Tukey's Honestly Significant Difference (HSD) for each pair of Treatments .....	67
Table 3.1. Statistical analysis of mitochondrial size and shape among different cell-types.....	85
Table 3.2. Statistical analysis of mitochondrial size and shape before versus after aluminum nanoparticle exposure among different cell-types.....	92
Table 3.3. Physiological consequences of altered mitochondrial properties.....	97
Table 4.1. Techniques used to characterize indices of metabolic health.....	113

## ACKNOWLEDGMENTS

I would like to thank my supervisor, Dr. Christie Sayes, for giving me the opportunity to conduct research in her laboratory and for providing me with opportunities that have allowed me to develop as a scientist that is ready to continue in my career. Your support and dedication throughout my time at Baylor University is greatly appreciated. I would like to also thank Dr. Erica Bruce, Dr. Ramon Lavado, Dr. Joseph Taube, and Dr. Leigh Greathouse for the key part they played in enhancing my research projects and aiding in completing my dissertation work. I would like to acknowledge and thank Dr. Bernd Zechmann for always assisting my research goals and for his extensive knowledge of microscopy that I was always happy to learn from. To my girlfriend and fellow lab mate, Marina George, thank you for your unwavering support of me and my research; I would not have made it through graduate school without you. Thank you to all of the other graduate and undergraduate students in the Sayes lab for your support. I would also like to thank Grace Aquino for her willingness to assist me throughout my time at Baylor University. I would also like to thank the Oak Ridge Institute for Science and Education, the Air Force Research Labs and Dr. Saber Hussain for the summer research opportunities and mentorship that was invaluable to my current and future research.

## DEDICATION

To my parents, Henry and Irene Lujan, for your unwavering support throughout my entire life that has allowed me to accomplish the things you always believed I could.

To my girlfriend, Marina George, for being there whenever I needed help and for constantly pushing me to want to do better. Without my family, none of this would be possible.

## CHAPTER ONE

### Cytotoxicological Pathways Induced After Nanoparticle Exposure: Studies of Oxidative Stress at the ‘Nano–Bio’ Interface

This chapter published as: Lujan, H. and Sayes, C.M., 2017. Cytotoxicological pathways induced after nanoparticle exposure: studies of oxidative stress at the ‘nano–bio’ interface. *Toxicology research*, 6(5), pp.580-594.

#### *Abstract*

Nanotechnology is advancing rapidly; many industries are utilizing nanomaterials because of their remarkable properties. As of 2017, over 1800 “nano-enabled products” (i.e. products that incorporate a nano- material feature and alter the product’s performance) have been used to revolutionize pharmaceutical, transportation, and agriculture industries, just to name a few. As the number of nano-enabled products continues to increase, the risk of nanoparticle exposure to humans and the surrounding environment also increases. These exposures are usually classified as either intentional or unintentional. The increased rate of potential nanoparticle exposure to humans has required the field of ‘nanotoxicology’ to rapidly screen for key biological, biochemical, chemical, or physical signals, signatures, or markers associated with specific toxicological pathways of injury within in vivo, in vitro, and ex vivo models. One of the common goals of nanotoxicology research is to identify critical perturbed biological pathways that can lead to an adverse outcome. This review focuses on the most common toxicological pathways induced by nanoparticle exposure and provides insights into how these perturbations could aid in the development of nanomaterial specific adverse

outcomes, inform nano-enabled product development, ensure safe manufacturing practices, promote intentional product use, and avoid environmental health hazards.

### *Introduction*

The use of supra-molecular chemistry, lithography, and other advanced synthesis methods employed to create engineered nano-enabled products has advanced in a myriad of industries, including biomedical, energy, and agriculture to name a few. Nano-enabled products are defined as manufactured products that contain pristine engineered nanomaterials (Sayes, Aquino, and Hickey 2017; Sayes and Child 2015). As the use of nano-enabled products increase in consumer and industrial applications, the risk of nanomaterial-related exposure to humans and the environment also increases. This increased risk of nanomaterial exposure necessitates more human health and ecological quantitative risk assessments (i.e. hazard and exposure data) due to potentially escalating adverse health effects to environmental health (Warheit et al. 2007; Oberdörster et al. 2005b; Nel et al. 2006). It is important to identify the potential adverse hazards and associated exposure doses that unintentionally occur with the use of nanomaterials and their enabled products.

Nanoparticles have the potential to induce adverse outcome pathways in biological and ecological systems due to their ability to penetrate and permeate through small pores and vacuoles (as little as 1 nanometer in size), absorb hydrophilic or hydrophobic molecular species onto the particle's large surface area (when compared to the same volume-to-volume ratio as their micrometer sized counterparts), and react with either active or inert agents through surface chemistry (due to the unique and concentrated surface functional groups of the particle-type) (Donaldson et al. 2004).

Currently, as of the date of this publication, over 1800 consumer or industrial use products from 622 companies in 32 countries contain engineered nanoparticles (Vance et al. 2015). The Woodrow Wilson International Center for Scholars and the Project on Emerging Nanotechnologies created the Nanotechnology Consumer Products Inventory (CPI) in 2005 to document the marketing and distribution of nano-enabled products in the commercial marketplace. Recent research efforts assessed the utility of the database and concluded that a diverse group of stakeholders from academia, industry, and government had become dependent on the inventory as an important resource of determining nanotechnology in society. In summary, the database indicates that the Health and Fitness category contains the most products (762, or 42% of the total) and that silver nanoparticles are the most frequently used nano-component in products (435 products, or 24%). About 29% of the recorded products (528) contain nanomaterials suspended in a liquid media and dermal contact is the most likely exposure scenario from their use. These findings provide quantitative data describing human and environmental exposure needed for life cycle and risk assessments (Vance, et al. 2015). An important factor in quantitatively assessing human and environmental health exposures is determining the nano-particle-specific cellular uptake mechanism. However, these specific mechanisms of cellular uptake are largely unknown. The nanoparticle size, surface coating, and surface charge are known factors that influence endocytosis (Zhang et al. 2009; Harush-Frenkel et al. 2007). Negatively charged nanoparticle surfaces (particles coated with unsaturated fatty acids such as oleic acid or linoleic acid) and positively charged nanoparticles (particles coated with polymers such as polyethylenimine (PEI) or cationic micro-fibrillated cellulose) are more capable of incorporation into human cells than

particles with no surface charge (Albanese, Tang, and Chan 2012; Farokhzad and Langer 2009; Chithrani, Ghazani, and Chan 2006). The surface coating of a nanoparticle can also influence the uptake by cells. Endocytosis includes pinocytosis, macropinocytosis, clathrin/caveolae-mediated endocytosis, or phagocytosis (Salatin, Maleki Dizaj, and Yari Khosroushahi 2015). Phagocytosis in mammalian immune cells often leads to NF- $\kappa$ B activation, which is one of the most common nano-particle-induced perturbed pathway (Akira, Uematsu, and Takeuchi 2006). Another factor that influences nanoparticle cellular uptake and subsequent induced cellular pathway is protein adsorption onto the surface particles. For example, proteins have been shown to form a “corona” on the surface of nanoparticles when placed in cell culture media, serum, and lung fluid (Podila et al. 2012; Lundqvist et al. 2008). Figure 1.1 shows some of the cellular uptake mechanisms involved after nano-particle cellular exposure.

As efforts to quantitatively measure exposure concentrations continue to mature, the need to determine potential adverse effects of nanomaterial exposure does not diminish. In fact, the need to interpret biological and ecological responses at the cellular and molecular level increases. Research papers that study these adverse effects normally compare nanoparticles against conventional particle toxicological “knowns”, such as hazard profiles of silica and asbestos. These particle-types have been extensively studied and provide useful correlations. The propensity of nanomaterials to penetrate through cell barriers, enter cells, and interact with subcellular structures is well established in the literature (Zhang et al. 2015; Verma et al. 2008; Lin et al. 2010; Chou, Ming, and Chan 2011).

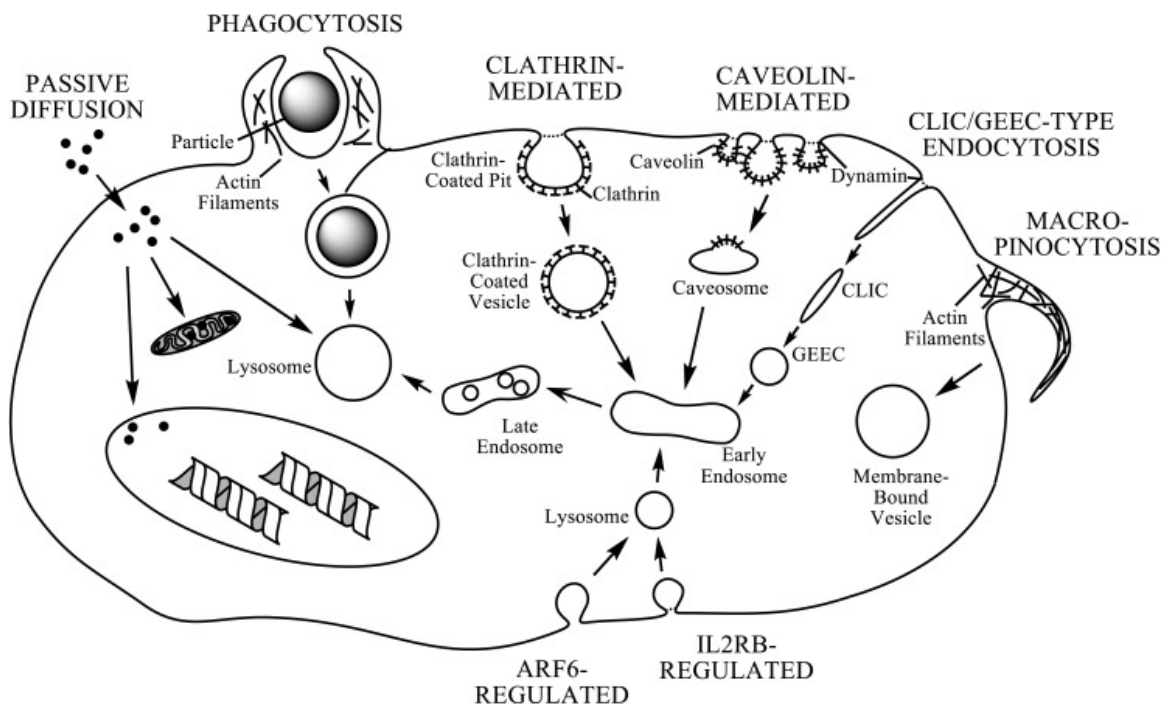
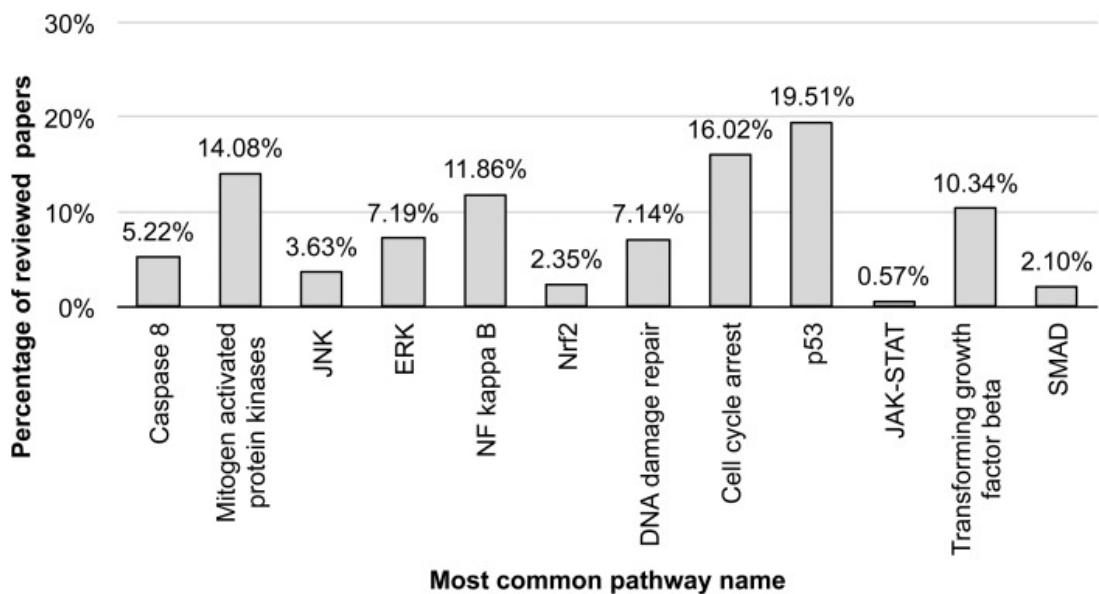


Figure 1.1. The possible nanoparticle uptake mechanisms described in the current literature. Mechanisms can either be facilitated by passive or active processes. Individual particles are more likely to enter cells passively, while aggregates or agglomerates of particles are more likely to enter cells actively.

Induction of oxidative stress and cell cycle arrest are the majority of mechanistic explanations of the stated conclusions (Figure 1.2). However, the specific adverse outcome pathways perturbed after exposure to nanomaterials—especially those perturbed in the arguably more realistic low-dose exposure scenarios—is now an active area of research. Combining the quantitative exposure data with the hazards related to more realistic exposure concentrations facilitates an active nanotoxicology research community and the desire to ensure that nano-enabled products are made safe and effective (Oberdörster, Stone, and Donaldson 2007).

Nanotoxicology research is a rapidly evolving field that was simultaneously developed from two different research communities around 2003: the toxicological/epidemiologic studies of airborne ultrafine particles and the chemistry-



Most common pathway keyword(s)	Scopus results	PubMed results	Web of Science results
Caspase 8	435	15	315
Mitogen activated protein kinases	1,555	78	428
JNK	259	32	240
ERK	491	61	501
NF kappa B	457	63	1216
Nrf2	171	27	146
DNA damage repair	458	114	473
Cell cycle arrest	1154	79	1113
p53	1466	114	1276
JAK-STAT	39	1	43
Transforming growth factor beta	991	86	437
SMAD	161	16	131

Figure. 1.2. The number of papers reporting nanoparticle-induced pathway perturbations in the peer-reviewed literature. The pathway-related keywords and abbreviated pathway-related keywords were searched against the keyword “nano\*” using Scopus, PubMed, and Web of Science search engines (bottom). From these results, the most common name for each pathway was selected, averaged, and displayed in the bar graph (top).

driven implication studies of nanotechnology (Oberdörster, Oberdörster, and Oberdörster 2005; Colvin 2003). Since that time, researchers have placed emphasis on identifying unique modes of action (MOA), i.e. characterizing the perturbation of cellular pathways due to nanoparticle exposure. The goal of testing pathway perturbation, a.k.a. toxicological pathways or molecular initiating events is to pinpoint the biological (or

ecological) mechanisms of adversity associated with low-dose (and non-lethal) nanomaterial exposure. Using cell-based systems with animal-based models, biochemical testing has unveiled tangible methods for higher throughput testing specifically aimed at identifying MOAs (Betts 2013). This review focuses on summarizing the most commonly probed cellular and molecular pathways triggered after such exposures. While the MOAs reviewed in the paper include only the most commonly screened pathway perturbations, new insights can be gleaned from this assimilation of knowledge and may help researchers gain a wider scope when looking at possible endpoints for application and implication studies.

#### *In vitro toxicity mechanisms of action*

After exposing in vitro cell systems to nanoparticles, the most common observation reported upon in the literature is the generation of reactive oxygen species (ROS) (Xia et al. 2008; Xia et al. 2006; Stone and Donaldson 2006; Yang et al. 2009; Sayes, Banerjee, and Romoser 2009; Limbach et al. 2007). The generation of ROS leads to probing activated differential pathways that is dependent on the nanomaterial (i.e. metal colloid or carbon-based) as well as the cell-type. For instance, most of the exposure scenarios included metal nanoparticles; when assessing the induced toxicities, metallothionein (MT) concentration, presence of heme oxygenase-1 (HMOX1), and super-oxide dismutase 2 (SOD2) are the commonly probed bio-markers (Xu et al. 2012). The generation of ROS leads triggers the cell system to promote different oxidative stress repair pathways. After nanoparticle exposure and concordant ROS generation, multiple adverse outcomes (AOs), in addition to oxidative stress, are seen within cells. These AOs include inflammatory response, apoptosis, cell cycle arrest, mitochondrial damage, or a

combination of effects. Inflammatory response (as measured by cytokine expression) is a fairly common screen for injury and includes interleukin-8 (IL8), interleukin-6 (IL6), interleukin-1beta (IL1 $\beta$ ), macrophage inflammatory protein-1 alpha (MIP1 $\alpha$ ), tumor necrosis factor-alpha (TNF $\alpha$ ), interferon gamma (IFN $\gamma$ ), intercellular adhesion molecule-1 (sICAM1) regulated upon activation normal T-cell expressed and secreted (RANTES), and monocyte chemoattractant protein-1 (MCP1) biomarkers. When a pathway is probed, basal level expression of the bio-markers related to that pathway should be predetermined before particle exposure. It is important that genes and proteins are probed upstream and downstream in order to better understand the origin of the changes that are seen in the cell. Organelle health is important, as seen in the Caspase-8 (CASP8) pathway, when it is necessary to assess the mitochondria, which then leads to additional which may be released due to the leaky membrane (e.g. cytochrome c). An increased understanding of the perturbed pathway allows for a broader, yet more focused array of genes and proteins. There is suite of endpoint analyses used in nanotoxicology studies. Table 1.2 summarizes the types of endpoints, the assay, tool or technique, and the data gained from each analysis.

### *Caspase-8*

Apoptosis in human cells is triggered by DNA damage, internal damage to organelles, or suppression of survival signals. The process usually follows one of two distinct routes that involve Caspase-8 (CASP8), a member of the cysteine protease family that is vital to initiating, amplifying, and executing apoptosis (Grossmann et al. 1998). The first of the two pathways is extrinsic and involves the stimulation of death receptors on the surface of cells, activation of CASP8, activation of Caspase-3, and leads to cell

death. The second pathway is intrinsic and involves Caspase-8 cleaving BH3 interacting-domain (BID) and truncated BID (tBID), disrupting mitochondrial membranes, and causing the release of pro-apoptotic factors such as cytochrome C. Cytochrome C will then activate Caspase-3 leading indirectly to cell death. This intrinsic pathway does not usually require external stimuli to lead to apoptosis; instead apoptosis is activated indirectly either through mitochondrial damage or change in mitochondrial membrane permeability (MMP) and the subsequent release of cytochrome C. One study investigated an apoptotic pathway induced by titanium dioxide (TiO<sub>2</sub>) nanoparticle exposure in human bronchiole epithelial cells (BEAS-2B) (Shi et al. 2010). In this study, a dose-dependent increase of reactive oxygen species (ROS) levels was related to the induction of morphological apoptosis and increased CASP3 activity. There was also a dose-dependent decrease in cell viability following TiO<sub>2</sub> nanoparticle exposure. The apoptotic activity was thought to be intrinsic because CASP8 and BID were not perturbed after TiO<sub>2</sub> exposure. This evidence was supported through the observed changes inactivity of B-cell lymphoma protein-2 (BCL2), BCL2-associated X protein (BAX), cytochrome C (cyt-C), and p53 (Shi, et al. 2010). Shi's study provided strong evidence that the intrinsic apoptotic pathway is controlled through mitochondrial changes when exposed to TiO<sub>2</sub> nanoparticles. A study by Zhao et al., looked at the effect of metallic nickel (Ni) nanoparticles versus Ni microparticles on primary cultures of neonatal BALB/c epidermal (JB6) cells with a focus on apoptotic signaling pathways (Zhao et al. 2009). An MTT assay was utilized to establish a dose-dependent cytotoxic response to the Ni nanoparticles. A dose-dependent cytotoxic response was seen in the cells exposed to either the nano-sized or fine-sized particles, but the Ni nanoparticle resulted in significantly higher

cytotoxicity levels. A green-fluorescent YO-PRO®-1 (YP) stain was used to study apoptosis and, similarly, the nanoparticle-exposed cells were described as apoptotic. The most notable difference between the nano-sized and fine-sized particle samples was seen at a concentration of  $5 \mu\text{g cm}^{-2}$ , where a 4-fold increase in apoptosis was observed. Western blot analysis found that the upstream protease Caspase-8 had been activated by the Ni nanoparticle induced apoptosis. Immunoprecipitation (IP) western blot was also used to probe the formation of death-inducing signaling complex (DISC, the binding of Fas, Fas-Associated protein with Death Domain (FADD), and CASP8) and its role in apoptosis. Through the use of anti-Caspase-8 IP, it was found that exposure to Ni nanoparticles caused Fas, FADD, and CASP8 to bind and form DISC, subsequently initiating the Fas-induced apoptotic pathway. Other research describing nanoparticle induced Caspase-8 pathways are included in Table 1.1.

### *MAPK/JNK*

C-Jun-N-terminal kinase (JNK) is one of the three main mitogen-activated protein kinases (MAPKs) and is commonly activated through mitogens, inflammatory cytokines, onco-genes, and inducers of cell differentiation and morphogenesis. Another trigger for the activation of MAPK and the JNK signaling cascade is the generation of ROS from varying sources of oxidative stress (Martindale and Holbrook 2002; Simbula et al. 2007). When activated, JNK has the potential to modify the activity of other proteins such as p53, c-Jun, and ATF-2 through phosphorylation, thus increasing the transcriptional activity (Johnson and Lapadat 2002). Once activated, JNK will translocate to the nucleus where phosphorylation of the p53 transcription factor occurs. p53 is a tumor suppressant protein that serves to regulate the normal cell growth cycle following DNA damage

(Kastan et al. 1992). p53 has the ability to activate DNA repair by halting cell growth at the G1/S checkpoint and can also initiate apoptosis if DNA repair is not possible. In one study, silica (SiO<sub>2</sub>) nanoparticles were tested on human umbilical vein endothelium cells (HUVECs) at over a dose–response experimental design. SiO<sub>2</sub> nanoparticles are currently used to target cells in drug delivery and their primary administration is through intravenous injections (Liu and Sun 2010). Due to this route of exposure, human endothelial cells are one of the primary cell-types immediately exposed to the SiO<sub>2</sub> nanoparticles. The results of the study showed a dose-dependent increase in the uptake of SiO<sub>2</sub> nanoparticles by HUVECs. In lower concentrations, cell viability was not significantly changed (i.e. viability was maintained between 97–99%); however, at the highest exposure concentration (200µg mL<sup>-1</sup>), cell viability dropped to 82%. Investigations into the damage of the cell membrane via lactate dehydrogenase (LDH) leakage found that only the highest concentration of SiO<sub>2</sub>-exposed cells impacted the release of LDH. The study also found that ROS generation was greatly increased within 3h at concentrations of 50 µg mL<sup>-1</sup> and higher. Due to the generation of ROS, mitochondrial membrane integrity was also investigated. Mitochondrial depolarization occurred due to SiO<sub>2</sub> nanoparticle exposure in a dose-dependent manner. It was also found that SiO<sub>2</sub> nanoparticles activated JNK, c-Jun, p53, CASP3 and NFκB. Activation of JNK and p53 were analyzed through western blot. The western blot analysis showed a dose-dependent increase in the phosphorylation of JNK and c-Jun, however the total expression of JNK and c-Jun was unchanged(Liu and Sun 2010)

## MAPK induced NFκB

When under oxidative conditions, it has been reported that the NFκB is regulated by MAPK. The NFκB pathway is important because of its regulation of programmed cell death, normal cellular proliferation rate, and tumorigenesis. The NFκB pathway is also considered the classic pro-inflammatory signaling pathway, which makes this pathway a prime target for toxicological studies (Lawrence 2009). One study that aimed to characterize the relationship between MAPK and the NFκB pathway exposed normal human dermal fibroblast (HDF) cells and NFκB-knockdown HDF cells to a variety of nanoparticles. The nanoparticles selected for the exposure studies included cadmium selenide/zinc sulfide quantum dots (QDs), titanium dioxide (TiO<sub>2</sub>), silver (Ag), and fullerol (C<sub>60</sub>OH<sub>24</sub>). Romoser et al., used NFκB-knockdown cells to block NFκB translocation into the nucleus. Both cell models were assayed after a low-dose exposure (5 μg mL<sup>-1</sup>) to nanoparticles over a short period of time. The assay probed glutathione, which is a protein involved in antioxidant defense via transformation into an oxidized state when exposed to intra-cellular oxidants. The assay showed a greater antioxidant response in the NFκB-knockdown cells than in the normal cells, which implies that NFκB can lessen the antioxidant response and allow oxidative stress to damage the cell. Western blot comparisons between the NFκB-knockdown and normal HDF cells concerning downstream responses of the IL1 family of cytokines showed that NFκB has a major part in controlling a part of the inflammatory response in the tested HDF cells (Romoser et al. 2012). Another study that focused on the effects of COOH-capped QD exposure also used HDF cells and found that there was a concentration and time-dependent gene regulation of the NFκB pathway at low doses (Romoser et al. 2011). It

was also found that there was an up-regulation of genes and proteins indicative of oxidative stress, apoptosis, inflammation, and other immune responses. These included genes and proteins such as chemokine ligands and interleukins.

### *MAPK/ERK*

Extracellular signal-regulated kinases (ERK) is the third of the three groups of MAPKs and is a major participant in the regulation of cell growth and differentiation. G-protein-coupled receptor kinases (GPCRs), receptor tyrosine kinases (RTKs), integrins, or ion channels trigger ERK activation. In 2005, Ding et al. tested multi-walled carbon nanotubes (MWCNTs) and multi-walled carbon nano-onions (MWCNOs) on human skin fibroblast (HSF42) and embryonic skin fibroblast (IMR-90) (Ding et al. 2005). These two cell lines were selected because the respiratory tract and the skin have both been indicted as likely routes of exposure to these nanomaterials. The nanomaterials were found to induce cell cycle arrest and cell death at cytotoxic doses ( $6 \mu\text{g mL}^{-1}$ ). MWCNTs were found to induce genes related to immune and inflammatory responses in the HSF42 cells. MWCNOs up-regulated genes that are usually induced in a response to external stimuli. A promoter analysis of a micro-array showed that perturbation of the critical pathways, i.e. interferon and MAPK/ERK cascades, caused signal transduction that contributed to the adverse effect seen after particle exposure. The differential expression patterns of cells exposed to MWCNTs and MWCNO demonstrate upstream signaling events that cause changes in cellular transcription (Ding, et al. 2005). Park et al. examined the effects of “biocompatible” iron oxide nanoparticles on cells due to their presumed chronic persistence that causes a continuous stimulation of the immune system (Park et al. 2014). Macrophages are a key mediator in this persistent stimulation, so a

mouse peritoneal macrophage cell line, RAW264.7, was selected for the study. After a 24-hour exposure, the iron oxide particles distributed within the cellular autophagosome-like vacuoles. RAW264.7 cells decreased in viability and went through cell cycle arrest in the G1 phase. The study also reported an increase in the generation of reactive oxygen species (ROS), nitric oxide (NO), and tumor necrosis factor alpha, (TNF $\alpha$ ). In addition, investigators observed a decrease in mitochondrial calcium levels and adenosine triphosphate (ATP) production. Autophagy-related proteins (i.e. p62, Beclin 1, ATG5, and LC3B) and the phosphorylated ERK protein also increased; while phosphorylated JNK protein decreased. This study showed that iron oxide nanoparticles induced autophagy in RAW264.7 cells due to oxidative stress and activated the ERK pathway (Park, et al. 2014). Taken together, SiO<sub>2</sub>, QD, and iron oxide nanoparticles studies by Liu, Romoser, and Park, respectively, reveal similar trends in that the MAPK pathways are perturbed after nano-particle exposure. The QD study showed differential cellular responses between keratinocytes and fibroblasts emphasizing the need to investigate potential mechanisms of action in different cell-types within the same target organ. Other research describing nanoparticle induced MAPK family of pathways (i.e. JNK, NF $\kappa$ B, and/or ERK) are included in Table 1.1

#### *Nrf2 induced antioxidant response*

The nuclear factor (erythroid-derived 2)-like 2 (Nrf2) pathway is thought to be the primary cellular defense against the cyto-toxic effects of oxidative stress (Gold et al. 2012). When a cell is exposed to electrophilic and other oxidative stressors, a reactive cysteine residue, Kelch-like ECH-associated protein 1 (Keap1), becomes modified, reduces E3 ligase activity, and stabilizes Nrf2 (Taguchi, Motohashi, and Yamamoto

2011). This activity leads to a dynamic series of cyto-protective gene up-regulation. Due to the strong link between oxidative stress and nanoparticle exposures reported in the scientific literature, the Nrf2 pathway has become a hallmark indicator of toxicity in nanotoxicology research (Berg et al. 2013; Delgado-Buenrostro et al. 2015; Guo et al. 2015; Aueviriyavit, Phummiratch, and Maniratanachote 2014; Gui et al. 2013; S.J. Kang et al. 2012; Piao et al. 2011; Zhang et al. 2012; Su Jin Kang et al. 2012; Wilhelmi et al. 2013). Berg et al. assessed the effect of SiO<sub>2</sub> nanoparticles exposed to two pulmonary cell lines, adenocarcinomic human alveolar basal epithelial cells (A549) cells and human pleural meso-thelial cells (MeT-5A) (Berg, et al. 2013). In the study, both cell lines exhibited a dose-dependent increase in ROS generation and a decrease in glutathione (GSH) levels after 24 h of low-dose SiO<sub>2</sub> nano-particle exposures (1 µg mL<sup>-1</sup>). The MeT-5A response was observed at lower SiO<sub>2</sub> concentrations than the A549 cells suggesting that the MeT-5A cells are susceptible to oxidative stress and/or nanoparticle exposure. In addition to viability and oxidative stress measurements, both cell lines showed a time-dependent increase in Nrf2 expression after exposure to SiO<sub>2</sub>. MeT-5A cells were tested for Nrf2 mRNA expression to evaluate the post-transcriptional regulation. It was determined that the increase was not caused by transcriptional activity, but rather by post-transcriptional regulation. Catalase (CAT) expression was also measured to determine activation of downstream antioxidants. Downstream antioxidant activation, such as CAT expression, is a known characteristic of the Nrf2 pathway (Itoh et al. 1997; Nguyen, Nioi, and Pickett 2009; Kobayashi and Yamamoto 2005). CAT expression increased in both cell lines after SiO<sub>2</sub> exposure. The increase in CAT suggests that the Nrf2 pathway is inducible by nanoparticle exposure. Aueviriyavit et al. studied the toxicities of gold (Au)

nanoparticles and silver (Ag) nanoparticles in human gastrointestinal tract (GI) tract cells, Caco-2 (Aueviriyavit, Phummiratch, and Maniratanachote 2014). An 3-(4,5-dimethylthiazol-2-yl)-2,5-diphenyltetrazolium bromide (MTT) assay and a trypan blue exclusion (TBE) assay were used to determine the acute cytotoxicity after exposure to the two different particle systems. There was a dose-dependent cytotoxic effect to Ag particle exposure and the LC<sub>50</sub> values for the MTT and TBE assay were 16.7 and 14.9  $\mu\text{g ml}^{-1}$ , respectively. The Au particles did not significantly reduce cell viability. The dichlorofluorescein (DCF) assay was used observe oxidative stress, but data was inconclusive due to possible particle interferences with the fluorescein dye (Aueviriyavit, Phummiratch, and Maniratanachote 2014). GSH was measured and showed that Ag particles, and not Au particles, caused depletion of intracellular GSH levels in a dose-dependent manner. To further quantify the biological responses to the stresses seen in this study, the authors probed for up-regulation of genes involved in the Nrf2 pathway activation. Gene expression levels for Nrf2, HO-1, GSTP1, and ABCC1 were measured via quantitative real-time polymerase chain reaction (qRT-PCR). Only two mRNA expression levels, i.e. Nrf2 and HMOX1, were significantly up-regulated after a few hours of Ag exposure; these genes dropped to normal levels by the 24-h post-exposure time point. Au nanoparticles caused no change in the mRNA expression level of genes along the Nrf2 pathway. To determine if this mRNA up-regulation caused changes at the protein level, a western blot analysis of Nrf2 and HMOX1 proteins was also performed. The protein expression level after Ag exposure of HMOX1 was also upregulated at the 6 h post-exposure time points, but returned to normal levels at by 24 h. Nrf2 protein

expression levels were elevated at the 12 h timepoint. Other research describing nanoparticle induced Nrf2 pathways are included in Table 1.1

### *DNA damage response and cell cycle regulation*

The DNA damage response (DDR) is another mechanism that is affected by oxidative stress. DDR is a complex mechanism that attempts to repair and minimize lethal or permanent genetic damage with a suite of signal transduction pathways involved in cell cycle regulation (CCR) and/or apoptosis. This process is primarily driven by the activities of cyclin-dependent kinases (CDKs) and CDK inhibitors, such as CDKN1B (Tenderenda 2005). Duan et al. investigated the impact of SiO<sub>2</sub> nanoparticle exposure on apoptosis and cell cycle checkpoints in human umbilical vein endothelial cells (HUVECs) (Duan et al. 2013). After SiO<sub>2</sub> nanoparticle exposure, a dose-dependent increase in intracellular ROS generation was found. ROS generation caused oxidative damage, malondialdehyde (MDA) production, and the inhibition of superoxide dismutase (SOD) and glutathione peroxidase (GPx). Analysis of apoptotic versus necrotic events in HUVECs suggested an increase in both of these cell death mechanisms after low-dose exposures to SiO<sub>2</sub> (25 µg mL<sup>-1</sup>). The investigators also measured DNA damage; damage increased as the dose of SiO<sub>2</sub> nanoparticles increased (up to 100 µg mL<sup>-1</sup>). Endpoints measured included the percentage of tail DNA, tail length, and Olive tail moment (i.e. the product of the tail length and the fraction of total DNA in the tail). Flowcytometry was used to analyze cell cycle arrest. Results indicated a significant increase in the G2/M phase arrest in the SiO<sub>2</sub>-exposed groups. In addition, G2/M checkpoint regulator expression was perturbed (i.e. chk1, Cdc25C, and cyclinB1/Cdc2). This study demonstrates that SiO<sub>2</sub> nanoparticle exposure induces ROS generation and DDR though

the Chk1-dependent G2/M damage checkpoint signaling pathway. Another study examined the cytotoxicity of titanium dioxide (TiO<sub>2</sub>) nanoparticles rat dopaminergic neuronal cells (PC12) (Wu, Sun, and Xue 2010). Three (3) different types of TiO<sub>2</sub> particles were tested. The first two differ from each other in crystallinity, i.e. one form is anatase (tetragonal) crystal structure and the other is rutile (needlelike) crystal structure. The third particle is amorphous micrometer-sized titanium dioxide. Cell proliferation and mitochondria activity was assessed through the (3-(4,5-di-methylthiazol-2-yl)-5-(3-carboxymethoxyphenyl)-2-(4-sulfohenyl)-2H-tetrazolium) (MTS) assay after particle exposure. Dosing concentrations of 100 to 200 µg mL<sup>-1</sup> of the anatase TiO<sub>2</sub> nanoparticles resulted higher cytotoxicity as compared to cells dosed with either of the other two particle-types. At the highest concentration (i.e. 200 µg mL<sup>-1</sup>), the anatase nanoparticles induced LDH leakage, which indicated the impact of the anatase nanoparticle on the cellular membrane integrity. Using DCF fluorescence as a reporter of ROS generation, anatase nanoparticles produced the greatest increase in relative fluorescence units (RFUs), when compared to the other two particles. PC12 cells were tested for mitochondrial health using tetraethylbenzimidazolylcarbocyanine iodide (JC-1) due to the ROS generation. The most significant reduction of mitochondrial membrane potential (MMP) was observed at 200 µg mL<sup>-1</sup> anatase particle dose. The amorphous micrometer-sized titanium dioxide resulted in no MMP adverse effect. In order to quantify the rate of apoptosis and necrosis, fluorescein iso-thiocyanate (FITC) conjugated Annexin V and propidium iodide (PI) dyes were validated against flow cytometry. In the control group, there was no sign of apoptosis or necrosis; however, after exposure to the anatase nanoparticles, the rate of apoptosis and necrosis increased significantly. In the rutile

nanoparticle exposures, only the rate of apoptosis increased. In the amorphous micrometer-sized titanium dioxide exposures, the rate of necrosis increased. Anatase nanoparticles were also found to cause significant accumulation of cells in the G2/M phase in a dose-dependent manner (Wu, Sun, and Xue 2010). The rutile nanoparticles also caused accumulation of cells in the G2/M phase, but to a lesser degree. The amorphous micrometer-sized titanium dioxide particles did not affect the cell cycle distribution. This study also found that the anatase nanoparticles caused the expression of JNK and c-Jun phosphorylation, p53 activation, and G2/M DNA damage in the PC12 cells. To test the downstream effects of p53 activation, western blot analysis of p21, GADD45, BAX, and BCL2 proteins was performed. The anatase nanoparticles were more effective at activating the apoptosis and cell cycle-related proteins than the rutile nanoparticles.

### *DNA damage and p53*

Tumor protein p53 exists in many different types of cells at a basal level expression (i.e. the default expression level of a gene or protein). It is usually expressed at low concentrations through continuous stabilization including ubiquitylation, phosphorylation, and acetylation (Levine 1997; Donehower and Harvey 1992). However, stress signals such as DNA damage, hypoxia, perturbation of cytokines, and metabolic changes can cause an increase in p53 activation. These stress signals are received by p53 through post-transcriptional modifications where p53 then act as a transcriptional factor (Harris and Levine 2005). As a transcriptional factor, p53 initiates a program of cell cycle arrest and apoptosis. The activation of p53 can also initiate genetic repair. The diverse functions of p53 are put under a multitude of regulatory mechanisms in order to keep the

protein in check until it is needed (Prives and Hall 1999). Due to the potential imbalance of p53 activation caused cell stress, some studies have been performed to determine effect of nanoparticle exposure on p53 activation. In 2008, Kang et al. published a study investigating the DNA damage cause by TiO<sub>2</sub> nanoparticles using the alkaline single cell gel electrophoresis Comet assay (Kang et al. 2008). DNA damage was seen in the lymphocyte extracts via western blots of p53. TiO<sub>2</sub> caused an increase in p53; however, none of its downstream targets were affected suggesting that p53 does not translocate. The DNA damage caused a cell-cycle checkpoint response through the cell's activated p53. Other research describing nanoparticle induced cell cycle regulation and DNA damage response are included in Table 1.1 Romoser et al. examined primary human dermal fibroblasts (HDF) exposed to three different, but commonly used engineered nanoparticles (i.e., cerium dioxide (CeO<sub>2</sub>), titanium dioxide (TiO<sub>2</sub>), and zinc oxide (ZnO)) in an attempt to determine the potential DNA damaging effects through the analysis of ROS generation, heme oxygenase-1 and phosphorylation of p38 protein up-regulation, and single and double DNA strand breaks using low dose exposures (as low as 1 ppb). Immunocytochemistry and western blotting showed ZnO-treated cells induced DNA double strand breaks as evidenced by a marked increase in the presence of  $\gamma$ -H2AX foci and was validated against the cell cycle arrest endpoint, phosphorylation of cyclin-dependent kinase 1. These data suggest that the three particle-types induce DNA damage, but at different doses, and of the three particle-types tested, exposure to ZnO nanoparticles induced the most significant DNA damage (Romoser, Criscitiello, and Sayes 2014).

Table 1.1. Summary table of the pathways reviewed in this paper. Table includes the pathway induced, the nanoparticle-type, description of the pathway, the hypothesized adverse outcome, and the original source of information. The most notable pathways describing in the table include CASP8/tBID pathways, the MAPK family of pathways, Nrf2 induced antioxidant response, cell cycle arrest, and DNA damage and checkpoint induced response

Pathway	Nanoparticle	Pathway description	Adverse outcome
CASP8/BID	Titanium dioxide	Increases activation of CASP8, BID, BAX, and CASP3	Leads to apoptosis
CASP8	Carbon black, titanium dioxide	Induces morphological and biochemical alterations	Leads to apoptosis
CASP8/MAPK	Arsenic sulfide	Inhibits cell growth, causes cell morphological changes, and induces DNA fragmentation	Leads to apoptosis
CASP8	Cobalt oxide	Elevates TNF $\alpha$ , activates CASP8, and phosphorylates p38MAPK	Leads to apoptosis
NF $\kappa$ B ERK JNK	Single-walled carbon nanotubes	Increases ROS generation	Induces DNA damage and causes oxidative stress
NF $\kappa$ B	Cadmium selenide/zinc sulfide	Up-regulates apoptotic, inflammatory, and immunoregulatory proteins	Induces DNA damage
p38/MAPK NF $\kappa$ B Nrf2	Silver	Induces cell cycle arrest	Induces DNA damage and leads to apoptosis
MAPK	Gold	Stresses cell membrane and induces cell differentiation	Induces DNA damage and leads to apoptosis
Nrf2	Multi-walled carbon nanotubes	Increases translocation of Nrf2 and expression of HMOX1 and IL1	Causes oxidative stress
Nrf2	Silver	Induces PI3K and p38MAPK	Causes oxidative stress
p38/Nrf2	Cerium dioxide	Increases ROS production and induces HMOX1	Causes oxidative stress
Nrf2	Nickel	Increases expression of HMOX1, c-Myc, and decreases expression of Nrf2	Causes oxidative stress
Cell cycle arrest	Gold (glucose-capped)	Accumulates cancer cells in the G2/M phase	Cell division stops
Cell cycle arrest	Silver	Increases G1 fraction	Cell division stops
DNA damage	Zinc oxide, silicon dioxide	Oxidative damage to DNA base	DNA mutations and genomic instability

Table 1.2 Assays used in the reviewed papers to probe cellular toxicity endpoints after nanoparticle exposure. Table includes the endpoint, assay, and the type of data retrieved

Endpoint	Assay	Data retrieved
Cell proliferation rate	3-(4,5-Dimethylthiazol-2-yl)-5-(3-carboxymethoxyphenyl)-2-(4-sulfophenyl)-2H-tetrazolium (MTS)	The metabolic activity and number of viable cells
Cell membrane integrity	Lactate dehydrogenase (LDH)	Increased LDH concentration in the surrounding media relates to increased cytoplasmic membrane permeability
Cytotoxicity or cell death	Trypan blue exclusion (TBE)	Stain will absorb onto dead cells, only
	3-(4,5-Dimethylthiazol-2-yl)-2,5-diphenyltetrazolium bromide (MTT)	Assesses cell metabolic activity
ROS generation	2',7'-Dichlorofluorescein diacetate (DCFDA)	Fluorescence dye reacts with ROS within cells
	Glutathione (GSH)	Measures total GSH levels and relates to antioxidant protection
	MitoTracker® Red CMXRos	Red dye stains active mitochondria indicating ROS production
Mitochondrial membrane potential	Tetraethylbenzimidazolylcarbocyanine iodide (JC-1)	Detects changes & abnormalities in mitochondria
Apoptosis	Fluorescein isothiocyanate conjugated Annexin V (Annexin V-FITC)	Fluorescence probe stains cell membranes expressing phosphatidylserine indicating apoptosis
	YO-PRO®-1 (YP)	Stain used to identify apoptotic cells, only
Necrosis	Propidium iodide (PI)	Stain used in to differentiate necrotic, apoptotic, and healthy cells
DNA damage	Comet assay (or single cell gel electrophoresis)	Used to quantify and analyze DNA damage of individual cells
Cell cycle arrest	Vybrant DyeCycle family	Cell cycle assays for flow cytometry to assess cells in G0/G1 phase <i>versus</i> S phase, G2, or polyploidy

## *JAK-STAT*

The Janus kinase/signal transducers and activators of transcription (JAK-STAT) pathway is a cascade that sends multiple signals necessary for cellular development and homeostasis (Rawlings, Rosler, and Harrison 2004). The JAK-STAT pathway is one of the primary signaling mechanisms for a wide array of cytokines, interferon (IFN) family of activators, and growth factors—all of which activate JAK and stimulate proliferation, differentiation, and apoptosis in the cell population (Rawlings, Rosler, and Harrison 2004) (O'Shea, Gadina, and Schreiber 2002). This pathway known to be relatively simple, when compared to other signaling pathways, due to its relative ease in observing perturbation along membrane-to-nucleus signaling (O'Shea, Gadina, and Schreiber 2002). In a study by Xu, et al., a DNA microarray tailored for global gene expression analysis was used to measure up- or down-regulated genes after silver nanoparticle hydrogel matrix exposure in human cervical cancer cells (HeLa) (Xu, et al. 2012). Results showed 1258 genes up-regulated and 788 genes were down-regulated at 24 h exposure time point. At 48 h, the silver hydro-gel matrix-exposed cells maintained 21.7% gene up-regulated and 19.16% gene down-regulated. The genes perturbed coincided with genes in the JAK-STAT pathway, such as many interferon-induced proteins in the interleukin (IL) and tetratricopeptide (TP) families. Snyder-Talkington et al. used human small airway epithelial cells (SAEC) and human microvascular endothelial cells (HMVEC) grown in a co-culture model system to analyze the JAK-STAT pathway after multi-walled carbon nanotubes (MWCNT) exposure. The epithelial cells were dosed with the nanotubes and acted as a barrier for the vascular endothelial cells. Transmission electron microscopy confirmed that the vascular endothelial cells were protected from nanotube exposure.

Using a panel of inflammatory biomarkers via ELISA, the researchers found that intracellular inflammatory signals (e.g. phospho-NF- $\kappa$ B p65 and phospho-Stat3) were up-regulated (Snyder-Talkington et al. 2013).

### *TGF- $\beta$ and SMAD*

Perturbation of transforming growth factor-beta (TGF- $\beta$ ) signaling is linked to autoimmunity, inflammation, pulmonary hypertension, and cancer (Attisano and Wrana 2002). Mothers against decapentaplegic (SMAD) proteins transduce signals from growth factor ligands to the nucleus where downstream gene transcription occurs (Attisano and Wrana 2002). Either SMAD2 or SMAD3 proteins are phosphorylated as a downstream target of TGF- $\beta$  and forms a complex with SMAD4 that translocates into the nucleus. Gene interactions occurs at the promoter site in order to regulate gene expression in a cell-specific manner (Elliott and Blobel 2005). SMAD complexes regulate transcriptional responses with DNA-binding proteins. Activation can either suppress or stimulate tumorigenesis. Khan et al. used a unique method to determine gene perturbation in HeLa cells after magnetite (Fe<sub>3</sub>O<sub>4</sub> iron oxide) nanocrystals (Khan et al. 2011). Cells were imaged via transmission electron microscopy (TEM) to determine particle endocytosis. Whole genome microarrays were used to assess transcriptional profiling of the cells after Fe<sub>3</sub>O<sub>4</sub> exposure. Results showed that 68 genes were down-regulated and one gene was up-regulated. TGF- $\beta$  signaling was a key perturbed mechanism as it specifically contains 5 of the 69 genes closely associated with the study's observed signaling. Five (5) genes (i.e. ID1, ID2, ID3, SMAD6, and SMAD7) were quantified using RT-PCR and the results of this test verified results from the microarray data analysis. ID1, ID2, and SMAD6 had an average of a 4-fold down-regulation when compared to ID3 and SMAD7. The TGF- $\beta$

family is also involved in cell cycle regulation and apoptosis; therefore, CASP9 was also selected for further analysis due to its role in apoptosis. A luminescence-based assay (Caspase-Glo® assay) showed that CASP9 activity decreases in the HeLa cells exposed to Fe<sub>3</sub>O<sub>4</sub> nanocrystals. Mishra et al. exposed human lung bronchial epithelial (BEAS-2B) cells and lung fibroblasts (CRL-1490) to low-dose, and physiologically relevant, concentrations of single-walled and multi-walled carbon nanotubes, ranging 0.02 to 0.6 µg cm<sup>-2</sup>. Using western blotting and ELISA techniques, it was determined that both forms of nanotubes triggered over-expression of TGF-β1, TGF-βR1 and Smad2/3 proteins in both lung cell-types, which in turn caused an increase in collagen production. By inhibiting collagen production via ALK5 inhibitor, or shRNA knockdown of TGF-βR1 and Smad2, the researchers showed that TGF-β/Smad signaling plays an important part in nanotube-induced fibrogenesis (Mishra et al. 2015).

### *Discussion*

This review focuses on the most common toxicological pathways induced by nanoparticle exposure. Data collected from these types of studies have the potential to provide insights into how gene and protein perturbations could aid in the development of nanomaterial specific AOPs, inform nano-enabled product development, ensure safe manufacturing practices, promote intentional product use, and avoid environmental health hazards.

The pathways presented in this paper follow a similar series of trends as represented in Figure 1.3. Molecular reactions begin with nanoparticle extracellular exposure. After particle endocytosis, reactive oxygen species are generated and initiate cascading events. MAPK, Nrf2, DNA, and mitochondrial damage can begin with

increased ROS production; cell cycle arrest, apoptosis, and inflammatory responses are the results. Through translocation, suppression, transcription, and phosphorylation processes, individual cells can experience multiple cascading events after nanoparticle exposure. There is not enough available data to correlate each nanoparticle to one specific adverse reaction; current data suggests that multiple particle-types can result in multiple cytotoxicities.

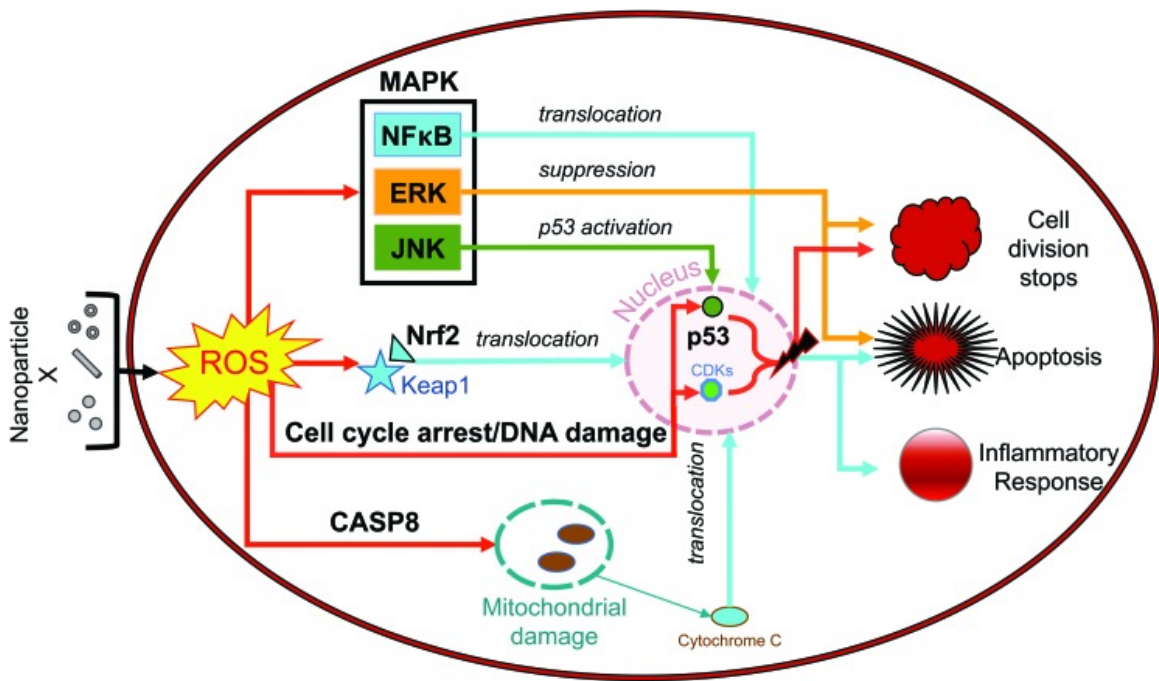


Figure 1.3. Overview of common pathways induced after nanoparticle exposure. The names of the pathway (i.e. MAPK, NFκB, ERK, JNK, Nrf2, p53, cell cycle arrest/DNA damage, and CASP8) are bolded in the figure. Red arrows represent ROS generation, the blue arrows represent translocation into the nucleus, the orange arrow represents suppression, and the green arrow represents activation. Most arrows lead to the nucleus and all arrows eventually lead to one or more adverse outcomes (i.e. cell division stops, apoptosis, and/or inflammatory response). Most metal-based engineered nanomaterials (i.e. Ni, Ag, Au, TiO<sub>2</sub>, SiO<sub>2</sub>, Fe<sub>3</sub>O<sub>4</sub>, ZnO, CdSe/ZnS) and a few carbon-based engineered nanomaterials (i.e. fullerenes, carbon nanotubes, nano onions, carbon black) follow one or more of these cellular pathways.

Most papers reviewed in this manuscript did not consider the effect of the particle's surface functional group on the induced biochemical signaling. These functional groups can range from phospholipids (i.e. biocompatible molecular chains, such as polyethelene glycol (PEG)) to terminating linear molecules (i.e. carboxylic groups, such as mercaptocarboxylic acid) (Sperling and Parak 2010). The type of surface functionalization varies depending on the intended application of the nanomaterial. Common biomedical uses of surface functionalization include avoiding the immune system (i.e. stealth nanoparticles), cell-specific targeting (i.e. cancer drug delivery), and improved medical imaging techniques (i.e. superior contrast agents) (Storm et al. 1995; Huynh et al. 2010; Shenoy et al. 2006). It is not common for nanotoxicology research papers to comment on how the perturbed pathway may change if the surface coating changes. This may prove to be an oversight and should be addressed in papers investigating the mechanisms of toxicity in the future. There are many papers in the literature speculating that the nanoparticle surface chemistry will ultimately influences the ADME and toxicokinetic/dynamic properties (Slowing, Trewyn, and Lin 2006; Mout et al. 2012; Villanueva et al. 2009). Toxicokinetic properties describe the uptake and elimination of the material over time; while toxicodynamics is the effects of the nanomaterial on the organism over time (Topuz and van Gestel 2015). These two physiological properties inform the critical quality attributes needed in successful product development. Another cellular-based nanoparticle-induced toxicological pathway analyses model that is gaining more attention in recent years is the three-dimensional (3D) or co-culture model. Co-culture, in this context, is defined as a cell culture containing growths of at least two distinct cell types. Co-cultures are useful in

understanding the interaction among and between the different cell-types as well as providing the ability to measure cross talk in cell–cell interactions. Some people have suggested that 3D co-culture models are able to capture more sensitive endpoints for different exposure scenarios, and that these more sensitive endpoints allow for more accurate in vitro-to-in vivo toxicology correlations (Snyder-Talkington, et al. 2013; Cho et al. 2013). Organ systems that are recapitulated using 3D co-cultures include liver, blood brain barriers, gastrointestinal tract, lung, and vascularization. These systems have demonstrated utility in drug design, drug safety testing, wound healing, and permeability studies (Kostadinova et al. 2013; Kirkpatrick, Fuchs, and Unger 2011; Deli et al. 2005). Some of the major goals from reviewing perturbed pathways is to link the data together to aid in biomarker development or aid in the creation of Adverse Outcome Pathways (AOPs) of nanoparticle exposure. Biomarkers can range from DNA/RNA, proteins, and can also be image based. These biomarkers are either only related with disease or the biomarker can also be classified as a mechanism of action (Vargas and Harris 2016). Outside of biomarkers of exposure some nanoparticles also have the ability to functions as precise biomarkers when they target specific cells (Li et al. 2007). An AOP is a representation of biological events that uses existing data to create a relationship from a molecular initiating event that goes through several key events that lead to an adverse outcome (Ankley et al. 2010). As biomarker development increases so too does AOP development as AOPs employ these biomarkers in order to predetermine the impacts an exposure may have on a population. While most of the pathways examined in the paper are not unique to nanoparticle exposure, the type of uptake mechanism induced for nanoparticles is different than those relevant for chemicals or larger micrometer sized

materials (Chithrani and Chan 2007; Monopoli et al. 2012). Differential uptake mechanisms lead to different lethal concentrations and post-exposure time points. For example, silver nanoparticles that are less than 30 nm in diameter tend to induce a toxicological response much sooner than silver particles in the micrometer size scale (i.e. 1–5  $\mu\text{m}$  in diameter). When comparing silver nanoparticles to silver chloride salt (i.e. AgCl), the induced toxic dose ( $\text{LC}_{50}$ ) of the silver nanoparticles is an order of magnitude less than the  $\text{LC}_{50}$  of AgCl (Marambio-Jones and Hoek 2010; Liu and Hurt 2010; Gliga et al. 2014). In all cases, however, the induced adverse pathway is often reported as MAPK induced NF $\kappa$ B (Parnsamut and Brimson 2015; Stepkowski, Brzóska, and Kruszewski 2014; Hyun-Jeong Eom and Jinhee Choi 2010).

### *Conclusions*

This paper reviews the most common toxicological pathways induced by nanoparticle exposure. Understanding these gene and protein perturbations could aid in multiple aspects of environmental health. By identifying and evaluating the potential adverse health effects at the molecular and cellular level, scientists will be more informed when measuring and assessing hazards, recommending protective measures, setting acceptable exposure levels, developing guidelines, policies, and regulations, and communicating health and safety educational and training materials to workers and consumers of nano-enabled products. While limiting the unintended and accidental exposures to hazardous agents should be the ultimate goal, interpreting the results of nanotoxicological experiments can be critical in protecting both healthy and susceptible human (and animal) populations. To this end, studying the cytotoxicological pathways induced after nanoparticle exposures aids in the development of nanomaterial-specific

adverse outcome pathways (AOPs) by linking molecular initiating events (MIEs) to adverse outcome (AOs) health effects. Pathway analysis is related to nano-enabled product development by establishing a framework for optimizing product efficiency, ensuring safe manufacturing practices, promoting the product's intentional use, and avoiding environmental health hazards. The following chapter investigates multiple pathways outlined in chapter 1 in a wide range of *in vitro* cell lines from the upper and lower airway with varying phenotypes. The rationale of this study design was to determine the similarities and differences among common cell lines used in pulmonary toxicology to increase translatability across the body of literature.

## References

- Akira, Shizuo, Satoshi Uematsu, and Osamu Takeuchi. 2006. "Pathogen Recognition and Innate Immunity." *Cell* 124, no. 4: 783-801.
- Albanese, Alexandre, Peter S Tang, and Warren CW Chan. 2012. "The Effect of Nanoparticle Size, Shape, and Surface Chemistry on Biological Systems." *Annual review of biomedical engineering* 14: 1-16.
- Ankley, G.T., R.S. Bennett, R.J. Erickson, D.J. Hoff, M.W. Hornung, R.D. Johnson, D.R. Mount, J.W. Nichols, C.L. Russom, and P.K. Schmieder. 2010. "Adverse Outcome Pathways: A Conceptual Framework to Support Ecotoxicology Research and Risk Assessment." *Environmental Toxicology and Chemistry* 29, no. 3: 730-741.
- Attisano, L., and J.L. Wrana. 2002. "Signal Transduction by the Tgf-B Superfamily." *Science* 296, no. 5573: 1646-1647.
- Aueviriyavit, Sasitorn, Duangkamol Phummiratch, and Rawiwan Maniratanachote. 2014. "Mechanistic Study on the Biological Effects of Silver and Gold Nanoparticles in Caco-2 Cells—Induction of the Nrf2/Ho-1 Pathway by High Concentrations of Silver Nanoparticles." *Toxicology letters* 224, no. 1: 73-83.
- Berg, J.M., A.A. Romoser, D.E. Figueroa, C.S. West, and C.M. Sayes. 2013. "Comparative Cytological Responses of Lung Epithelial and Pleural Mesothelial Cells Following in Vitro Exposure to Nanoscale SiO<sub>2</sub>." *Toxicology in Vitro* 27, no. 1: 24-33.
- Betts, K.S. 2013. "Tox21 to Date: Steps toward Modernizing Human Hazard Characterization." *Environmental Health Perspectives* 121, no. 7: A228.
- Chithrani, B Devika, and Warren CW Chan. 2007. "Elucidating the Mechanism of Cellular Uptake and Removal of Protein-Coated Gold Nanoparticles of Different Sizes and Shapes." *Nano letters* 7, no. 6: 1542-1550.
- Chithrani, B Devika, Arezou A Ghazani, and Warren CW Chan. 2006. "Determining the Size and Shape Dependence of Gold Nanoparticle Uptake into Mammalian Cells." *Nano letters* 6, no. 4: 662-668.
- Cho, Wan-Seob, Rodger Duffin, Mark Bradley, Ian L Megson, William MacNee, Jong Kwon Lee, Jayoung Jeong, and Ken Donaldson. 2013. "Predictive Value of in Vitro Assays Depends on the Mechanism of Toxicity of Metal Oxide Nanoparticles." *Particle and fibre toxicology* 10, no. 1: 55.

- Chou, L.Y.T., K. Ming, and W.C.W. Chan. 2011. "Strategies for the Intracellular Delivery of Nanoparticles." *Chemical Society Reviews* 40, no. 1: 233-245.
- Colvin, V.L. 2003. "The Potential Environmental Impact of Engineered Nanomaterials." *Nature Biotechnology* 21, no. 10: 1166-1170.
- Delgado-Buenrostro, N.L., E.I. Medina-Reyes, I. Lastres-Becker, V. Freyre-Fonseca, Z. Ji, R. Hernández-Pando, B. Marquina, J. Pedraza-Chaverri, S. Espada, and A. Cuadrado. 2015. "Nrf2 Protects the Lung against Inflammation Induced by Titanium Dioxide Nanoparticles: A Positive Regulator Role of Nrf2 on Cytokine Release." *Environmental Toxicology* 30, no. 7: 782-792.
- Deli, Mária A, Csongor S Ábrahám, Yasufumi Kataoka, and Masami Niwa. 2005. "Permeability Studies on in Vitro Blood–Brain Barrier Models: Physiology, Pathology, and Pharmacology." *Cellular and molecular neurobiology* 25, no. 1: 59-127.
- Ding, L., J. Stilwell, T. Zhang, O. Elboudwarej, H. Jiang, J.P. Selegue, P.A. Cooke, J.W. Gray, and F.F. Chen. 2005. "Molecular Characterization of the Cytotoxic Mechanism of Multiwall Carbon Nanotubes and Nano-Onions on Human Skin Fibroblast." *Nano Letters* 5, no. 12: 2448-2464.
- Donaldson, K., V. Stone, C.L. Tran, W. Kreyling, and P.J.A. Borm. 2004. *Nanotoxicology*: BMJ Publishing Group Ltd.
- Donehower, Lawrence A, and Michele Harvey. 1992. "Mice Deficient for P53 Are Developmentally Normal but Susceptible to Spontaneous Tumours." *Nature* 356, no. 6366: 215.
- Duan, J., Y. Yu, Y. Li, Y. Yu, Y. Li, X. Zhou, P. Huang, and Z. Sun. 2013. "Toxic Effect of Silica Nanoparticles on Endothelial Cells through DNA Damage Response Via Chk1-Dependent G2/M Checkpoint." *PloS One* 8, no. 4: e62087.
- Elliott, R.L., and G.C. Blobe. 2005. "Role of Transforming Growth Factor Beta in Human Cancer." *Journal of Clinical Oncology* 23, no. 9: 2078-2093.
- Eom, Hyun-Jeong, and Jinhee Choi. 2010. "P38 Mapk Activation, DNA Damage, Cell Cycle Arrest and Apoptosis as Mechanisms of Toxicity of Silver Nanoparticles in Jurkat T Cells." *Environmental science & technology* 44, no. 21: 8337-8342.
- Farokhzad, Omid C, and Robert Langer. 2009. "Impact of Nanotechnology on Drug Delivery." *ACS nano* 3, no. 1: 16-20.

- Gliga, Anda R, Sara Skoglund, Inger Odnevall Wallinder, Bengt Fadeel, and Hanna L Karlsson. 2014. "Size-Dependent Cytotoxicity of Silver Nanoparticles in Human Lung Cells: The Role of Cellular Uptake, Agglomeration and Ag Release." *Particle and fibre toxicology* 11, no. 1: 1-17.
- Gold, R., L. Kappos, D.L. Arnold, A. Bar-Or, G. Giovannoni, K. Selmaj, C. Tornatore, M.T. Sweetser, M. Yang, and S.I. Sheikh. 2012. "Placebo-Controlled Phase 3 Study of Oral Bg-12 for Relapsing Multiple Sclerosis." *New England Journal of Medicine* 367, no. 12: 1098-1107.
- Grossmann, J., S. Mohr, E.G. Lapetina, C. Fiocchi, and A.D. Levine. 1998. "Sequential and Rapid Activation of Select Caspases During Apoptosis of Normal Intestinal Epithelial Cells." *American Journal of Physiology-Gastrointestinal and Liver Physiology* 274, no. 6: G1117-G1124.
- Gui, S., B. Li, X. Zhao, L. Sheng, J. Hong, X. Yu, X. Sang, Q. Sun, Y. Ze, and L. Wang. 2013. "Renal Injury and Nrf2 Modulation in Mouse Kidney Following Chronic Exposure to Tio2 Nanoparticles." *Journal of Agricultural and Food Chemistry* 61, no. 37: 8959-8968.
- Guo, C., Y. Xia, P. Niu, L. Jiang, J. Duan, Y. Yu, X. Zhou, Y. Li, and Z. Sun. 2015. "Silica Nanoparticles Induce Oxidative Stress, Inflammation, and Endothelial Dysfunction in Vitro Via Activation of the Mapk/Nrf2 Pathway and Nuclear Factor-Kb Signaling." *International Journal of Nanomedicine* 10: 1463.
- Harris, S.L., and A.J. Levine. 2005. "The P53 Pathway: Positive and Negative Feedback Loops." *Oncogene* 24, no. 17: 2899-2908.
- Harush-Frenkel, Oshrat, Nir Debotton, Simon Benita, and Yoram Altschuler. 2007. "Targeting of Nanoparticles to the Clathrin-Mediated Endocytic Pathway." *Biochemical and biophysical research communications* 353, no. 1: 26-32.
- Huynh, N.T., E. Roger, N. Lautram, J.-P. Benoît, and C. Passirani. 2010. "The Rise and Rise of Stealth Nanocarriers for Cancer Therapy: Passive Versus Active Targeting." *Nanomedicine* 5, no. 9: 1415-1433.
- Itoh, Ken, Tomoki Chiba, Satoru Takahashi, Tetsuro Ishii, Kazuhiko Igarashi, Yasutake Katoh, Tatsuya Oyake, Norio Hayashi, Kimihiko Satoh, and Ichiro Hatayama. 1997. "An Nrf2/Small Maf Heterodimer Mediates the Induction of Phase Ii Detoxifying Enzyme Genes through Antioxidant Response Elements." *Biochemical and biophysical research communications* 236, no. 2: 313-322.
- Johnson, G.L., and R. Lapadat. 2002. "Mitogen-Activated Protein Kinase Pathways Mediated by Erk, Jnk, and P38 Protein Kinases." *Science* 298, no. 5600: 1911-1912.

- Kang, S.J., B.M. Kim, Y.J. Lee, and H.W. Chung. 2008. "Titanium Dioxide Nanoparticles Trigger P53-Mediated Damage Response in Peripheral Blood Lymphocytes." *Environmental and Molecular Mutagenesis* 49, no. 5: 399-405.
- Kang, S.J., Y.J. Lee, E.-K. Lee, and M.-K. Kwak. 2012. "Silver Nanoparticles-Mediated G2/M Cycle Arrest of Renal Epithelial Cells Is Associated with Nrf2-Gsh Signaling." *Toxicology Letters* 211, no. 3: 334-341.
- Kang, Su Jin, In-geun Ryoo, Young Joon Lee, and Mi-Kyoung Kwak. 2012. "Role of the Nrf2-Heme Oxygenase-1 Pathway in Silver Nanoparticle-Mediated Cytotoxicity." *Toxicology and applied pharmacology* 258, no. 1: 89-98.
- Kastan, M.B., Q. Zhan, W.S. El-Deiry, F. Carrier, T. Jacks, W.V. Walsh, B.S. Plunkett, B. Vogelstein, and A.J. Fornace. 1992. "A Mammalian Cell Cycle Checkpoint Pathway Utilizing P53 and Gadd45 Is Defective in Ataxia-Telangiectasia." *Cell* 71, no. 4: 587-597.
- Khan, J.A., T.K. Mandal, T.K. Das, Y. Singh, B. Pillai, and S. Maiti. 2011. "Magnetite (Fe<sub>3</sub>O<sub>4</sub>) Nanocrystals Affect the Expression of Genes Involved in the Tgf-Beta Signalling Pathway." *Molecular BioSystems* 7, no. 5: 1481-1486.
- Kirkpatrick, C James, Sabine Fuchs, and Ronald E Unger. 2011. "Co-Culture Systems for Vascularization—Learning from Nature." *Advanced drug delivery reviews* 63, no. 4-5: 291-299.
- Kobayashi, Makoto, and Masayuki Yamamoto. 2005. "Molecular Mechanisms Activating the Nrf2-Keap1 Pathway of Antioxidant Gene Regulation." *Antioxidants & redox signaling* 7, no. 3-4: 385-394.
- Kostadinova, Radina, Franziska Boess, Dawn Applegate, Laura Suter, Thomas Weiser, Thomas Singer, Brian Naughton, and Adrian Roth. 2013. "A Long-Term Three Dimensional Liver Co-Culture System for Improved Prediction of Clinically Relevant Drug-Induced Hepatotoxicity." *Toxicology and applied pharmacology* 268, no. 1: 1-16.
- Lawrence, T. 2009. "The Nuclear Factor Nf-Kb Pathway in Inflammation." *Cold Spring Harbor Perspectives in Biology* 1, no. 6: a001651.
- Levine, Arnold J. 1997. "P53, the Cellular Gatekeeper for Growth and Division." *cell* 88, no. 3: 323-331.
- Li, J., X. Wang, C. Wang, B. Chen, Y. Dai, R. Zhang, M. Song, G. Lv, and D. Fu. 2007. "The Enhancement Effect of Gold Nanoparticles in Drug Delivery and as Biomarkers of Drug-Resistant Cancer Cells." *ChemMedChem* 2, no. 3: 374-378.

- Limbach, Ludwig K, Peter Wick, Pius Manser, Robert N Grass, Arie Bruinink, and Wendelin J Stark. 2007. "Exposure of Engineered Nanoparticles to Human Lung Epithelial Cells: Influence of Chemical Composition and Catalytic Activity on Oxidative Stress." *Environmental science & technology* 41, no. 11: 4158-4163.
- Lin, J., H. Zhang, Z. Chen, and Y. Zheng. 2010. "Penetration of Lipid Membranes by Gold Nanoparticles: Insights into Cellular Uptake, Cytotoxicity, and Their Relationship." *ACS Nano* 4, no. 9: 5421-5429.
- Liu, Jingyu, and Robert H Hurt. 2010. "Ion Release Kinetics and Particle Persistence in Aqueous Nano-Silver Colloids." *Environmental science & technology* 44, no. 6: 2169-2175.
- Liu, X., and J. Sun. 2010. "Endothelial Cells Dysfunction Induced by Silica Nanoparticles through Oxidative Stress Via Jnk/P53 and Nf-Kb Pathways." *Biomaterials* 31, no. 32: 8198-8209.
- Lundqvist, Martin, Johannes Stigler, Giuliano Elia, Iseult Lynch, Tommy Cedervall, and Kenneth A Dawson. 2008. "Nanoparticle Size and Surface Properties Determine the Protein Corona with Possible Implications for Biological Impacts." *Proceedings of the National Academy of Sciences* 105, no. 38: 14265-14270.
- Marambio-Jones, Catalina, and Eric MV Hoek. 2010. "A Review of the Antibacterial Effects of Silver Nanomaterials and Potential Implications for Human Health and the Environment." *Journal of Nanoparticle Research* 12, no. 5: 1531-1551.
- Martindale, J.L., and N.J. Holbrook. 2002. "Cellular Response to Oxidative Stress: Signaling for Suicide and Survival." *Journal of Cellular Physiology* 192, no. 1: 1-15.
- Mishra, Anurag, Todd A Stueckle, Robert R Mercer, Raymond Derk, Yon Rojanasakul, Vincent Castranova, and Liying Wang. 2015. "Identification of Tgf-B Receptor-1 as a Key Regulator of Carbon Nanotube-Induced Fibrogenesis." *American Journal of Physiology-Lung Cellular and Molecular Physiology* 309, no. 8: L821-L833.
- Monopoli, Marco P, Christoffer Åberg, Anna Salvati, and Kenneth A Dawson. 2012. "Biomolecular Coronas Provide the Biological Identity of Nanosized Materials." *Nature nanotechnology* 7, no. 12: 779-786.
- Mout, R., D.F. Moyano, S. Rana, and V.M. Rotello. 2012. "Surface Functionalization of Nanoparticles for Nanomedicine." *Chemical Society Reviews* 41, no. 7: 2539-2544.
- Nel, A., T. Xia, L. Mädler, and N. Li. 2006. "Toxic Potential of Materials at the Nanolevel." *Science* 311, no. 5761: 622-627.

- Nguyen, Truyen, Paul Nioi, and Cecil B Pickett. 2009. "The Nrf2-Antioxidant Response Element Signaling Pathway and Its Activation by Oxidative Stress." *Journal of Biological Chemistry* 284, no. 20: 13291-13295.
- O'Shea, J.J., M. Gadina, and R.D. Schreiber. 2002. "Cytokine Signaling in 2002: New Surprises in the Jak/Stat Pathway." *Cell* 109, no. 2: S121-S131.
- Oberdörster, G., A. Maynard, K. Donaldson, Vi. Castranova, J. Fitzpatrick, K. Ausman, J. Carter, B. Karn, W. Kreyling, and D. Lai. 2005b. "Principles for Characterizing the Potential Human Health Effects from Exposure to Nanomaterials: Elements of a Screening Strategy." *Particle and Fibre Toxicology* 2, no. 1: 8.
- Oberdörster, G., E. Oberdörster, and J. Oberdörster. 2005. "Nanotoxicology: An Emerging Discipline Evolving from Studies of Ultrafine Particles." *Environmental Health Perspectives*: 823-839.
- Oberdörster, G., V. Stone, and K. Donaldson. 2007. "Toxicology of Nanoparticles: A Historical Perspective." *Nanotoxicology* 1, no. 1: 2-25.
- Park, E.-J., H.N. Umh, S.-W. Kim, M.-H. Cho, J.-H. Kim, and Y. Kim. 2014. "Erk Pathway Is Activated in Bare-Fenps-Induced Autophagy." *Archives of Toxicology* 88, no. 2: 323-336.
- Parnsamut, C, and S Brimson. 2015. "Effects of Silver Nanoparticles and Gold Nanoparticles on Il-2, Il-6, and Tnf-A Production Via Mapk Pathway in Leukemic Cell Lines." *Genet. Mol. Res* 14, no. 2: 3650.
- Piao, M.J., K.C. Kim, J.-Y. Choi, J. Choi, and J.W. Hyun. 2011. "Silver Nanoparticles Down-Regulate Nrf2-Mediated 8-Oxoguanine DNA Glycosylase 1 through Inactivation of Extracellular Regulated Kinase and Protein Kinase B in Human Chang Liver Cells." *Toxicology Letters* 207, no. 2: 143-148.
- Podila, Ramakrishna, Ran Chen, Pu Chun Ke, JM Brown, and AM Rao. 2012. "Effects of Surface Functional Groups on the Formation of Nanoparticle-Protein Corona." *Applied physics letters* 101, no. 26: 263701.
- Prives, C., and P.A. Hall. 1999. "The P53 Pathway." *Journal of Pathology* 187, no. 1: 112-126.
- Rawlings, J.S., K.M. Rosler, and D.A. Harrison. 2004. "The Jak/Stat Signaling Pathway." *Journal of Cell Science* 117, no. 8: 1281-1283.
- Romoser, A.A., P.L. Chen, J.M. Berg, C. Seabury, I. Ivanov, M.F. Criscitiello, and C.M. Sayes. 2011. "Quantum Dots Trigger Immunomodulation of the Nfkb Pathway in Human Skin Cells." *Molecular Immunology* 48, no. 12: 1349-1359.

- Romoser, A.A., D.E. Figueroa, A. Sooresh, K. Scribner, P.L. Chen, W. Porter, M.F. Criscitiello, and C.M. Sayes. 2012. "Distinct Immunomodulatory Effects of a Panel of Nanomaterials in Human Dermal Fibroblasts." *Toxicology Letters* 210, no. 3: 293-301.
- Romoser, Amelia A, Michael F Criscitiello, and Christie M Sayes. 2014. "Engineered Nanoparticles Induce DNA Damage in Primary Human Skin Cells, Even at Low Doses." *Nano Life* 4, no. 01: 1440001.
- Salatin, Sara, Solmaz Maleki Dizaj, and Ahmad Yari Khosroushahi. 2015. "Effect of the Surface Modification, Size, and Shape on Cellular Uptake of Nanoparticles." *Cell biology international* 39, no. 8: 881-890.
- Sayes, C.M., G.V. Aquino, and A.J. Hickey. 2017. "Nanomaterial Drug Products: Manufacturing and Analytical Perspectives." *AAPS Journal*.
- Sayes, C.M., and J.R. Child. 2015. "Nanotoxicology: Determining Nano-Bio Interactions and Evaluating Toxicity Using in Vitro Models." *Nanoengineering: Global Approaches to Health and Safety Issues*: 85.
- Sayes, Christie M, Nivedita Banerjee, and Amelia A Romoser. 2009. "The Role of Oxidative Stress in Nanotoxicology." *General, Applied and Systems Toxicology*.
- Shenoy, D., W. Fu, J. Li, C. Crasto, G. Jones, C. Dimarzio, S. Sridhar, and M. Amiji. 2006. "Surface Functionalization of Gold Nanoparticles Using Hetero-Bifunctional Poly (Ethylene Glycol) Spacer for Intracellular Tracking and Delivery." *International Journal of Nanomedicine* 1, no. 1: 51.
- Shi, Y., F. Wang, J. He, S. Yadav, and H. Wang. 2010. "Titanium Dioxide Nanoparticles Cause Apoptosis in Beas-2b Cells through the Caspase 8/T-Bid-Independent Mitochondrial Pathway." *Toxicology Letters* 196, no. 1: 21-27.
- Simbula, G., A. Columbano, G.M. Ledda-Columbano, L. Sanna, M. Deidda, A. Diana, and M. Pibiri. 2007. "Increased Ros Generation and P53 Activation in A-Lipoic Acid-Induced Apoptosis of Hepatoma Cells." *Apoptosis* 12, no. 1: 113-123.
- Slowing, I., B.G. Trewyn, and V.S.-Y. Lin. 2006. "Effect of Surface Functionalization of Mcm-41-Type Mesoporous Silica Nanoparticles on the Endocytosis by Human Cancer Cells." *Journal of the American Chemical Society* 128, no. 46: 14792-14793.
- Snyder-Talkington, Brandi N, Diane Schwegler-Berry, Vincent Castranova, Yong Qian, and Nancy L Guo. 2013. "Multi-Walled Carbon Nanotubes Induce Human Microvascular Endothelial Cellular Effects in an Alveolar-Capillary Co-Culture with Small Airway Epithelial Cells." *Particle and fibre toxicology* 10, no. 1: 1-14.

- Sperling, R.A., and W.J. Parak. 2010. "Surface Modification, Functionalization and Bioconjugation of Colloidal Inorganic Nanoparticles." *Philosophical Transactions of the Royal Society of London A: Mathematical, Physical and Engineering Sciences* 368, no. 1915: 1333-1383.
- Stępkowski, TM, K Brzóska, and M Kruszewski. 2014. "Silver Nanoparticles Induced Changes in the Expression of Nf-Kb Related Genes Are Cell Type Specific and Related to the Basal Activity of Nf-Kb." *Toxicology in Vitro* 28, no. 4: 473-478.
- Stone, Vicki, and Ken Donaldson. 2006. "Nanotoxicology: Signs of Stress." *Nature Nanotechnology* 1, no. 1: 23-24.
- Storm, G., S.O. Belliot, T. Daemen, and D.D. Lasic. 1995. "Surface Modification of Nanoparticles to Oppose Uptake by the Mononuclear Phagocyte System." *Advanced Drug Delivery Reviews* 17, no. 1: 31-48.
- Taguchi, K., H. Motohashi, and M. Yamamoto. 2011. "Molecular Mechanisms of the Keap1–Nrf2 Pathway in Stress Response and Cancer Evolution." *Genes to Cells* 16, no. 2: 123-140.
- Tenderenda, M. 2005. "A Study on the Prognostic Value of Cyclins D1 and E Expression Levels in Resectable Gastric Cancer and on Some Correlations between Cyclins Expression, Histoclinical Parameters and Selected Protein Products of Cell-Cycle Regulatory Genes." *Journal of Experimental & Cclinical Cancer Research* 24, no. 3: 405-414.
- Topuz, E., and C.A.M. van Gestel. 2015. "Toxicokinetics and Toxicodynamics of Differently Coated Silver Nanoparticles and Silver Nitrate in Enchytraeus Crypticus Upon Aqueous Exposure in an Inert Sand Medium." *Environmental Toxicology and Chemistry* 34, no. 12: 2816-2823.
- Vance, M.E., T. Kuiken, E.P. Vejerano, S.P. McGinnis, M.F. Hochella, D. Rejeski, and M. S. Hull. 2015. "Nanotechnology in the Real World: Redeveloping the Nanomaterial Consumer Products Inventory." *Beilstein Journal of Nanotechnology* 6: 1769-1780. <https://dx.doi.org/10.3762/bjnano.6.181>.
- Vargas, A.J., and C.C. Harris. 2016. "Biomarker Development in the Precision Medicine Era: Lung Cancer as a Case Study." *Nature Reviews Cancer* 16, no. 8: 525-537.
- Verma, A., O. Uzun, Y. Hu, Y. Hu, H.-S. Han, N. Watson, S. Chen, D.J. Irvine, and F. Stellacci. 2008. "Surface-Structure-Regulated Cell-Membrane Penetration by Monolayer-Protected Nanoparticles." *Nature Materials* 7, no. 7: 588-595.

- Villanueva, A., M. Canete, A.G. Roca, M. Calero, S. Veintemillas-Verdaguer, C.J. Serna, M. del Puerto Morales, and R. Miranda. 2009. "The Influence of Surface Functionalization on the Enhanced Internalization of Magnetic Nanoparticles in Cancer Cells." *Nanotechnology* 20, no. 11: 115103.
- Warheit, D.B., R.A. Hoke, C. Finlay, E.M. Donner, K.L. Reed, and C.M. Sayes. 2007. "Development of a Base Set of Toxicity Tests Using Ultrafine TiO<sub>2</sub> Particles as a Component of Nanoparticle Risk Management." *Toxicology Letters* 171, no. 3: 99-110.
- Wilhelmi, V., U. Fischer, H. Weighardt, K. Schulze-Osthoff, C. Nickel, B. Stahlmecke, T.A.J. Kuhlbusch, A.M. Scherbart, C. Esser, and R.P.F. Schins. 2013. "Zinc Oxide Nanoparticles Induce Necrosis and Apoptosis in Macrophages in a P47phox-and Nrf2-Independent Manner." *PloS One* 8, no. 6: e65704.
- Wu, Jie, Jiao Sun, and Yang Xue. 2010. "Involvement of Jnk and P53 Activation in G2/M Cell Cycle Arrest and Apoptosis Induced by Titanium Dioxide Nanoparticles in Neuron Cells." *Toxicology letters* 199, no. 3: 269-276.
- Xia, Tian, Michael Kovichich, Jonathan Brant, Matt Hotze, Joan Sempf, Terry Oberley, Constantinos Sioutas, Joanne I Yeh, Mark R Wiesner, and Andre E Nel. 2006. "Comparison of the Abilities of Ambient and Manufactured Nanoparticles to Induce Cellular Toxicity According to an Oxidative Stress Paradigm." *Nano letters* 6, no. 8: 1794-1807.
- Xia, Tian, Michael Kovichich, Monty Liong, Lutz Mädler, Benjamin Gilbert, Haibin Shi, Joanne I Yeh, Jeffrey I Zink, and Andre E Nel. 2008. "Comparison of the Mechanism of Toxicity of Zinc Oxide and Cerium Oxide Nanoparticles Based on Dissolution and Oxidative Stress Properties." *ACS nano* 2, no. 10: 2121.
- Xu, L., X. Li, T. Takemura, N. Hanagata, G. Wu, and L.L. Chou. 2012. "Genotoxicity and Molecular Response of Silver Nanoparticle (Np)-Based Hydrogel." *Journal of Nanobiotechnology* 10, no. 1: 16.
- Yang, Hui, Chao Liu, Danfeng Yang, Huashan Zhang, and Zhuge Xi. 2009. "Comparative Study of Cytotoxicity, Oxidative Stress and Genotoxicity Induced by Four Typical Nanomaterials: The Role of Particle Size, Shape and Composition." *Journal of applied Toxicology* 29, no. 1: 69-78.
- Zhang, F., P. Durham, C.M. Sayes, B.L.T. Lau, and E.D. Bruce. 2015. "Particle Uptake Efficiency Is Significantly Affected by Type of Capping Agent and Cell Line." *Journal of Applied Toxicology* 35, no. 10: 1114-1121.

- Zhang, H., H. Liu, K.J.A. Davies, Co. Sioutas, C.E. Finch, T.E. Morgan, and H.J. Forman. 2012. "Nrf2-Regulated Phase II Enzymes Are Induced by Chronic Ambient Nanoparticle Exposure in Young Mice with Age-Related Impairments." *Free Radical Biology and Medicine* 52, no. 9: 2038-2046.
- Zhang, Sulin, Ju Li, George Lykotrafitis, Gang Bao, and Subra Suresh. 2009. "Size-Dependent Endocytosis of Nanoparticles." *Advanced materials* 21, no. 4: 419-424.
- Zhao, J., L. Bowman, X. Zhang, X. Shi, B. Jiang, V. Castranova, and M. Ding. 2009. "Metallic Nickel Nano-and Fine Particles Induce Jb6 Cell Apoptosis through a Caspase-8/Aif Mediated Cytochrome C-Independent Pathway." *Journal of Nanobiotechnology* 7, no. 1: 2.

## CHAPTER TWO

### Refining In Vitro Toxicity Models: Comparing Baseline Characteristics of Lung Cell Types

This chapter published as: Lujan, H., Criscitiello, M.F., Hering, A.S. and Sayes, C.M., 2019. Refining in vitro toxicity models: comparing baseline characteristics of lung cell types. *Toxicological Sciences*, 168(2), pp.302-314.

#### *Abstract*

There is an ever-evolving need in the field of in vitro toxicology to improve the quality of experimental design, ie, from ill-defined cell cultures to well-characterized cytotoxicological models. This evolution is especially important as environmental health scientists begin to rely more heavily on cell culture models in pulmonary toxicology studies. The research presented in this study analyzes the differences and similarities of cells derived from two different depths of the human lung with varying phenotypes. We compared cell cycle and antioxidant-related mRNA and protein concentrations of primary, transformed, and cancer-derived cell lines from the upper and lower airways. In all, six of the most commonly used cell lines reported in *in vitro* toxicology research papers were included in this study (ie, PTBE, BEAS-2B, A549, PSAE, Met-5A, and Calu-3). Comparison of cell characteristics was accomplished through molecular biology (q-PCR, ELISA, and flow cytometry) and microscopy (phase and fluorescence) techniques as well as cellular oxidative stress endpoint analyses. After comparing the responses of each cell type using statistical analyses, results confirmed significant differences in background levels of cell cycle regulators, inherent antioxidant capacity, pro-inflammatory status, and differential toxicological responses. The analyzed data

improve our understanding of the cell characteristics, and in turn, aids in more accurate interpretation of toxicological results. Our conclusions suggest that *in vitro* toxicology studies should include a detailed cell characterization component in published papers.

### *Introduction*

Over the past decade, *in vitro* toxicology testing has evolved from simply a cost-effective screening method to a viable alternative to animal testing (Cohen, Teeguarden, and Demokritou 2014; Fernandes et al. 2009; Goldberg and Frazier 1989). As with many other tools and techniques available to environmental health scientists, there are advantages and disadvantages to using cell culture-based models to gauge dose-response relationships, mechanistic analyses, and biotransformation profiles of xenobiotics exposed to mammalian systems (Blaauboer 2008; Hartung and Daston 2009; Kroll et al. 2009; Phalen, Oldham, and Nel 2006). Some experts cite resistance of regulators to use data collected from *in vitro* studies to inform decisions about chemicals and other substances due to lack of representative three-dimensional anatomical structure of human airways (Hartung and Daston 2009; Liebsch and Spielmann 2002). Others have stated that *in vitro* models fail to identify indicators of disease. Even with these oppositional arguments, there is a clear need to reduce the reliance on test animals for both new and existing substances, and *in vitro* models can provide useful data for decision-making. In fact, because the speed, ease, and low cost of cellular tests can be combined with precise gene, protein, cytokine, metabolite, and enzyme analysis tools, research teams (within industry and academia) have invested substantially in cell and tissue culture (Carere, Stamatii, and Zucco 2002; Godoy et al. 2013; Guillouzo and Guguen-Guillouzo 2008; Lin and Chang 2008; Nemmar et al. 2013). However, study designs must be created with

scrutiny to ensure the utility of the data gleaned from the in vitro experiment; namely, the choice of cells used in the culture model. Choosing the best cell type for an in vitro toxicology study requires comprehensive cell characterization.

To improve the practicality of in vitro models, immortalized cells have been created by transforming certain intracellular pathways or characteristics (Hahn et al. 1999; Hahn et al. 2002). These transformed cells are crafted by altering a selection of intracellular pathways to produce cells that will proliferate beyond primary cells while also avoiding the acquisition of a tumorigenic classification. Alterations to cellular genotypes include changes in mitogenic signaling, cell cycle checkpoint controls pRB and p53, telomerase maintenance, or signaling pathways controlled by PP2A (Mooi and Peeper 2006). Due to the dysregulation of intracellular pathways, transformed cells possess basal expression levels of “normal” cells with the immortalization of “cancerous” cells. The altered pathways resemble the pathways cancer cells are known to modify or hijack. These pathways are known as the “hallmarks of cancer” (Hanahan and Weinberg 2000).

The hallmarks of cancer originally described by Hanahan et al. included sustained angiogenesis, ability to avoid apoptosis, self-induced growth signaling, and metastasis (Hanahan and Weinberg 2000). An updated list also included dysregulation of cellular metabolism and tumor-promoting inflammation as essential pathways perturbed within cancer cells (Hanahan and Weinberg 2011). These updated pathways are vital in in vitro toxicology studies and must be taken into account for proper cell line selection and subsequent interpretation of results.

There are a few common endpoints among studies in the fields of cell biology, toxicology, and cancer research. Two overarching endpoints have significant overlap when characterizing cells: antioxidant capacity and cell cycle deregulation. In cell biology, normal cellular functions such as metabolism can generate reactive oxygen species (ROS) causing oxidative DNA damage (Finkel and Holbrook 2000; Murphy 2009; Yu 1994). Another outcome of this endogenous ROS generation is the adverse effect on the cell cycle and cytoskeleton (Boonstra and Post 2004; Menon and Goswami 2007; Sauer, Wartenberg, and Hescheler 2001). In toxicology, increasing particle dose correlates with increasing amount of ROS generation (ROS) (Foldbjerg, Dang, and Autrup 2011; Guo et al. 2009; Hussain et al. 2005; Sayes, Staats, and Hickey 2014). New studies have shown particles to cause cell cycle arrest due to ROS generation increasing cell cycle regulators such as p53 and p21 ((H. J. Eom and J. Choi 2010; Wu, Sun, and Xue 2010). In recent years, cancer research has also investigated the impact that excess reactive species, inflammation, and cell cycle regulation can have on tumorigenesis (Gupta et al. 2012) (Ishii et al. 2005) Kongara and Karantza, 2012). With these fields of research investigating oxidative stress, proinflammatory response, and cell cycle disruption, it is important to know the state of these characteristics within a selected cell culture model.

Utilizing cell culture models require characterization of the baseline cellular features and processes. Different cell types can express different levels of biomolecules (eg, mRNAs and proteins), thus influencing oxidative capacity, cellular adhesion, proliferation rate, metabolic activity, and sensitivity to exogenous materials (Diamond et al. 2000; Liu 2001; Thierry et al. 2009). When assessing the available literature, 1000+

research papers between 2015 and 2017 have cited “in vitro toxicology.” Within those papers, almost half used “lung” cells. Currently available primary cell types consist of primary tracheal/bronchial epithelial (PTBE) or primary small airway epithelial (PSAE) cells. When conducting toxicological assessments, the four most common cell types used include human bronchial epithelial cells (BEAS-2B), which are transformed from the upper airway; human alveolar epithelial cells (A549), which are cancer-derived from the upper airway; human mesothelial cells (MeT-5A), which are transformed from the lower airway; and human mesothelial epithelial cells (Calu-3), which are cancer-derived from the lower airway.

The purpose of this manuscript is 2-fold: Our first objective was to compare the antioxidant capacity of each of these cell types. Our second objective was to compare the cell cycle population distribution of the same six cell types. It is anticipated that information regarding appropriate cell type use for mechanistic pulmonary toxicology studies will be acquired by examining the comparative baseline expressions of commonly utilized lung cells. Furthermore, statistical analysis allows for testing for differences in means of the cell types separated by phenotype and lung location.

## *Materials and Methods*

### *General experimental design*

The general approach to this study was to characterize cells in culture (Figure 1.1). Specifically, we conducted substantial cellular assessments (ie, whole cell, protein, cytokine, enzyme, and gene expression analyses) of six human lung cell types (ie, PTBE cells; BEAS-2B normal lung epithelial adenovirus 12-SV40 virus-transformed cells;

A549 lung epithelial carcinoma cells; PSAE cells; Met-5A lung mesothelial pRSV-T plasmid-transfected cells; and Calu-3 lung epithelial adenocarcinoma cells from the pleural effusion) used in pulmonary toxicology studies. Figure 2.1 lists the types of cells, incubation time points, and endpoint analyses.

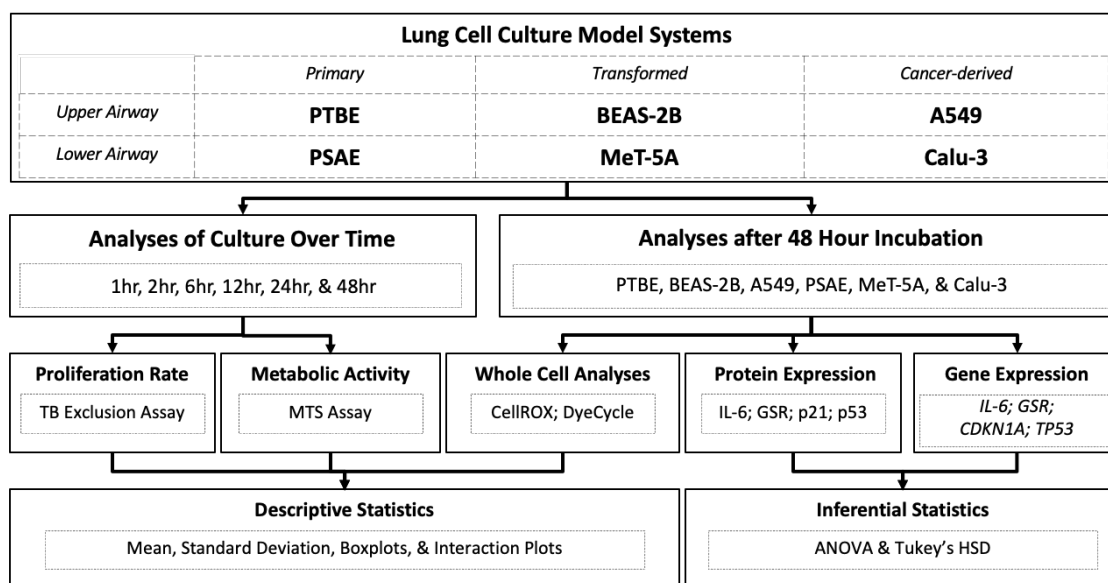


Figure 2.1. The design of the in vitro experiments. Six different cell types were used (PTBE, BEAS-2B, A549, PSAE, MeT-5A, and Calu-3). Six incubation time points were used for the proliferation rate and metabolic activity endpoints (1, 2, 6, 12, 24, and 48 h). Antioxidant capacity and cell cycle regulation were analyzed using whole cell, protein expression, and gene expression at the 48 h incubation time point.

### *Maintaining cell culture*

PTBE (PCS-300-010, American Type Culture Collection [ATCC], Manassas, Virginia) and PSAE (PCS-301-010, ATCC) were cultured in “Airway Epithelial Cell Basal Medium” supplemented with the “Bronchial Epithelial Cell Growth Kit” (PCS-300-040, ATCC), as described by ATCC. A549 cells (CCL-185, ATCC), BEAS-2B cells (CRL-9609, ATCC), and Calu-3 cells (HTB-55, ATCC) were cultured using the same media (Table 2.1). Medium consisted of a 1:1 mixture of Dulbecco’s Modified Eagle’s Medium

and Ham's F-12 Nutrient Mixture (DMEM/F12; Gibco, Waltham, Massachusetts) supplemented with 10% fetal bovine serum (FBS; Equitech-Bio, Inc. Kerrville, Texas) and 1% antibiotic cocktail of penicillin-streptomycin (MP Biomedical, Solon, Ohio). Met-5A cells were cultured using Media 199 (Gibco, Adair, Oklahoma) supplemented with 10% FBS, 1% antibiotic cocktail, 3.3 nM epidermal growth factor (Invitrogen, Waltham, Massachusetts), 400 nM hydrocortisone (ACROS Organics, Geel, Belgium), 870 nM insulin (Cell Applications, San Diego, California), 20 mM HEPES (Gibco), and "Trace Elements B" (Corning, Pittsburgh, Pennsylvania). All cells were cultured at 37°C in an air-jacketed humidified incubator with 5% CO<sub>2</sub>. All cells were tested at a passage number 3 or 4 after receipt from the ATCC stock.

Table 2.1. Comparison of culture conditions. Characteristics of the cells used in this study that are available from the source/vendor. All six types of cells are derived from *Homo sapiens* (human), have a morphological appearance as epithelial-like, are adherent, and were cultured with 5% CO<sub>2</sub>, 90% humidity at 37°C.

Cell Name	Lung Location	Phenotype	Culture Medium	Doubling Time	Other details
PTBE	Upper Airway	Primary	Airway epithelial cell basal medium	72 h	Not diseased, normal
BEAS-2B	Upper Airway	Transformed	DMEM/F12	26 h	Immortalized via adenovirus 12-SV40 virus hybrid
A549	Upper Airway	Cancer-derived	DMEM/F12	22 h	Diseased, carcinoma
PSAE	Lower Airway	Primary	Airway epithelial cell basal medium	>72 h	Not diseased, normal
MeT-5A	Lower Airway	Cancer-derived	Media 199	30 h	Immortalized via pRSV-T plasmid
Calu-3	Lower Airway	Primary	DMEM/F12	72 h	Diseased, carcinoma

### *Cell proliferation*

All cell types were collected at ~70% confluency using trypsin/EDTA 0.25% (Gibco) to detach cells, pelleted, and re-suspended in appropriate media. A trypan blue exclusion assay (Gibco) was performed using a Countess automated cell counter

(Invitrogen). Cell seeding densities were carefully measured and recorded. After seeding approximately 30 000 cells/ml in each well of a 6-well plate, the exclusion assay was repeated after 1, 2, 6, 12, 24, and 48-h incubation time points.

In addition, a [3-(4,5-dimethylthiazol-2-yl)-5-(3-carboxymethoxyphenyl)-2-(4-sulfophenyl)-2H-tetrazolium assay (MTS; Promega, Fitchburg, Wisconsin) was used to determine growth rate and mitochondrial activity. Briefly, cells were collected, counted, and seeded at the same density as before. At 1, 2, 6, 12, 24, and 48-h incubation time points, the MTS solution was added, incubated for 2 h, and spectroscopically measured at 490 nm on a Synergy H1 microplate reader (BioTek, Winooski, Vermont).

#### *Cell morphology*

All cells types were seeded and incubated into one of 4 wells of a chamber slide (Lab-Tek II, Rochester, New York) for 48 h to allow adhesion and acclimation. Subsequently, the cells were fixed and permeabilized as described in the Image-it Fix-Perm kit (Molecular Probes, Eugene, Oregon). Cells were then washed (3×) with wash buffer and incubated in the dark at room temperature with ActinGreen 488 ReadyProbes reagent (Invitrogen) for 15 min, followed by the addition of MitoTracker Red CM-H2XRos and NucBlue Live Cell Stain Ready Probes reagent (Molecular Probes).

Samples were incubated, again, in the dark at room temperature for 15 min. Each well was then washed with PBS solution (3×) and fixed with two drops of ProLong Diamond Anti-fade Mountant (Molecular Probes). A glass cover slip was then carefully placed on the slide and set for 24 h. Images of the cells were taken using fluorescence microscopy (CytoViva Inc., Auburn, Alabama) with the accompanying Ocular software

(Advanced Scientific Camera Control Version 1.0), and the 3-colored probes were stitched together.

### *mRNA expression*

Specific mRNA concentration was measured to determine the baseline level of gene expression within each cell culture. CDKN1A, TP53, IL-6, and GSR mRNA content was analyzed using Real-Time quantitative Polymerase Chain Reaction (RT-qPCR). All work areas, gloves, and pipettes were wiped down with RNaseZap to avoid contamination. RNA was harvested using a PureLink RNA mini kit (Invitrogen), followed by the generation of cDNA and DNase treatment using a SuperScript IV VILO master mix with ezDNase (Invitrogen). Concentrations of RNA and DNA were calculated and kept consistent across all cell types using a Qubit high sensitivity RNA assay (Invitrogen) and NanoDrop One/One Microvolume UV-Vis Spectrophotometer (Thermo Scientific, Waltham, Massachusetts) set at 260 nm wavelength, respectively. TaqMan fast advanced master mix (Applied Biosciences, Beverly Hills, California) was substituted for the master mix in the SuperScript kit to allow for more rapid data acquisition. TaqMan gene expression assays were used to perform qPCR. A TaqMan gene expression assay of  $\beta$ -actin was also included and used as an endogenous control. The reactions were analyzed on a Step-One Real-Time PCR system (Applied Biosystems). Upper airway cell types BEAS-2B and A549 were compared with PTBE as a control, whereas lower airway cell types MeT-5A and Calu-3 cell types were compared with PSAE as a control. Data are presented as Expression Fold Change ( $2^{-\Delta\Delta Ct}$ ).

*Cell cycle regulation: protein expression*

To collect the baseline level of p21 and p53 within the cells, the cells were collected and lysed using the same methodology, and then the protein levels were measured using either a p21 or p53 ELISA kit (Invitrogen). Cells were collected, pelleted, and re-suspended in PBS. The cells were again pelleted and re-suspended in cell extraction buffer (Invitrogen) containing protease inhibitor cocktail (Millipore-Sigma, St. Louis, Missouri) and phenylmethylsulfonyl fluoride (PMSF; Thermo Scientific). Samples were placed on ice and vortexed 3X over a 30-min period. Samples were centrifuged at 13 000 RPM for 10 min. The standards and samples were added to the well plate and read at an absorbance of 450 nm on a Synergy H1 (BioTek, Broadview, Illinois) microplate reader.

*Antioxidant capacity: cytokine expression*

The baseline levels of IL-6 within the cells were measured using a human IL-6 enzyme-linked immunosorbent assay (ELISA; Invitrogen). Cells were washed with cold phosphate-buffered saline solution (2×) before being covered with ice-cold radioimmunoprecipitation cell lysis buffer (RIPA; Pierce, Rockford, Illinois) for 10 min. A cell scraper was used to detach the cells before the lysis solution was transferred into a microcentrifuge tube. The tube was spun at 18 705 RCF for 10 min and kept on ice until use. The plate layout, standards, controls, and samples were performed following the kit's protocol. Immediately after the addition of the stop solution, the plate was read at an absorbance of 450 nm on a Synergy H1 microplate reader.

#### *Antioxidant capacity: enzyme analyses*

The glutathione reductase (GSR) activity within the cells was measured using the OxiSelect glutathione reductase assay kit (Cell Biolabs Inc., San Diego, California). Following the OxiSelect protocol, cells were collected, pelleted, and re-suspended in ice-cold assay buffer. Cell suspension was transferred and homogenized. After the addition of the glutathione disulfide (GSSG) solution, the absorbance of the plate was read using the kinetic assay reading at 405 nm every minute for 10 min on the Synergy H1 microplate reader.

#### *Whole cell analysis: cell cycle distribution*

The cell cycle population distribution was analyzed among the six cell types using a Vybrant DyeCycle stain (Invitrogen) analyses via FACSVerse flow cytometer (BD Biosciences). Cells were pelleted, re-suspended in sheath fluid, stained, and briefly vortexed at room temperature. Samples were then incubated in the dark at 37°C for 20 min. Flow cytometer performance QC was run using 2 µm polystyrene research beads (BD Biosciences). All samples were vortexed prior to analysis. Analyses at 488 nm excitation and 670 nm emission corresponded to the APC-Cy7-A filter. The range was first optimized while previewing the cells, and then 10 000 cells/run were acquired. Each sample was run in triplicate before the data was saved and analyzed using FlowJo software (FlowJo LLC, Ashland, Oregon). Histograms were created in FlowJo by comparing counts versus APC-Cy7-A, and then gates were placed over the two peaks or the valley to calculate the percent of cells in that range. The data from each triplicate were averaged.

*Whole cell analysis: general oxidative stress*

Endogenous antioxidants (ie, the capacity of the cell to neutralize free radicals using basal levels of antioxidants) in each of the six cell lines were analyzed using a general oxidative stress CellROX Deep Red Flow Cytometry Assay Kit (Invitrogen) and a FACSVerse flow cytometer (BD Biosciences, San Jose, California). Cells were collected, pelleted, and re-suspended in complete media. A prepared aliquot of CellROX dye was added; after 45 min, SYTOX dead cell stain was added and incubated for 15 min. Prior to testing samples, a flow cytometer performance QC was run using 2  $\mu$ m polystyrene research beads (BD Biosciences). All samples were vortexed prior to analysis to reduce aggregation. The CellROX dye had an excitation at 644 nm and emission at 665 nm, which corresponded to the APC-Alexa Flour filter. The SYTOX dead cell stain had an excitation at 444 nm and emission at 480 nm, which corresponded to the SSC-A filter. The range was first optimized while previewing the cells and then 10 000 cells/run were acquired. These data were saved and analyzed using FlowJo software (FlowJo LLC, Ashland, Oregon). Flow cytometry graphs were generated by comparing the CellROX and SYTOX emissions. Gates were placed to discriminate dead cells without oxidative stress, dead cells with oxidative stress, alive cells with oxidative stress, and alive cells without oxidative stress.

*Whole cell analysis: change in oxidative stress after tert-butyl hydroperoxide exposure*

Change in the amount of detectable ROS in each of the six cell types were analyzed using a general oxidative stress as described previously (ie, CellROX Deep Red Flow Cytometry Assay Kit). Cells were collected, pelleted, and re-suspended in complete media. Tert-butyl hydroperoxide was used as a positive ROS generating control and was

added to each of the cell cultures and subsequently incubated at 37°C for 1 h at a concentration of 250 µM. A prepared aliquot of CellROX dye was added and analyzed via flow cytometry.

### *Statistical analysis*

For each cellular response, a 2-way analysis of variance (ANOVA) in lung location and phenotype was performed (Kuehl, 2000). When the interaction between lung location and phenotype is found to be highly significant (with p-values less than .01), follow-up tests to identify those pairs of treatments that are significantly different from each other were done with Tukey's Honest Significant Differences (HSD). To confirm results for responses where the assumption of constant variance across treatments was not met, a nonparametric ANOVA was also implemented to confirm the parametric 2-way ANOVA results (Wobbrock et al., 2011). All statistical analyses were performed in the open-source software package R (R Core Team, 2016).

## *Results*

### *Cell Culture Growth and Morphology*

Figure 2.2 shows the differential cellular densities via microscopy. Each color in the fluorescence image represents a different component of an individual cell's structure. The blue shade is a nuclear stain (Hoechst), the red shade preferentially enters the mitochondria and only fluoresces upon oxidation (MitoTracker), and the green shade illuminates the F-actin in the cytoskeleton (ActinGreen). Each nucleus appears as a different shade of blue to purple to pink based on the differences in mitochondrial density/oxidative state among the cells. The upper airway primary and transformed cells

have a more blue to purple shade of nuclei than the A549 cells, which have a higher density of mitochondria as indicated by the pink shade. BEAS-2B and MeT-5A cells have a lower density of mitochondria as indicated by the purple shade. The primary cells have large areas of red indicating large amounts of mitochondria when compared with Calu-3 cells, which have the least amount of mitochondria as indicated by the distinct and de-convoluted blue versus red-stained areas (nuclei vs mitochondria, respectfully).

In addition to color saturation differences, each cell type exhibit differences in confluency. PTBE, BEAS-2B, and A549 cells create uniform monolayers with rounded cytoskeletons; however, A549 cells can continue to proliferate past plate saturation, demonstrating the absence of contact inhibition. In contrast, the PTBE cells will grow isolated from one another and become quiescent if 100% confluency is reached. PSAE and MeT-5A cells also create uniform monolayers but depict an elongated cytoskeleton. These cells proliferate more slowly compared with upper airway cell types. Results also indicate that Calu-3 cells grow in colony formations (rather than uniform monolayers) as indicated by the clustering of multiple nuclei co-located within a dense cytoskeleton. Together, these cell adhesion images demonstrate that integrin cell signaling pathways are likely activated soon after initial seeding and create connections to extracellular matrix for either monolayer or colony formations. Calu-3 cells have a metastatic phenotype and may have overactive integrin signaling as demonstrated by both the bright green cytoskeleton and colony structure.

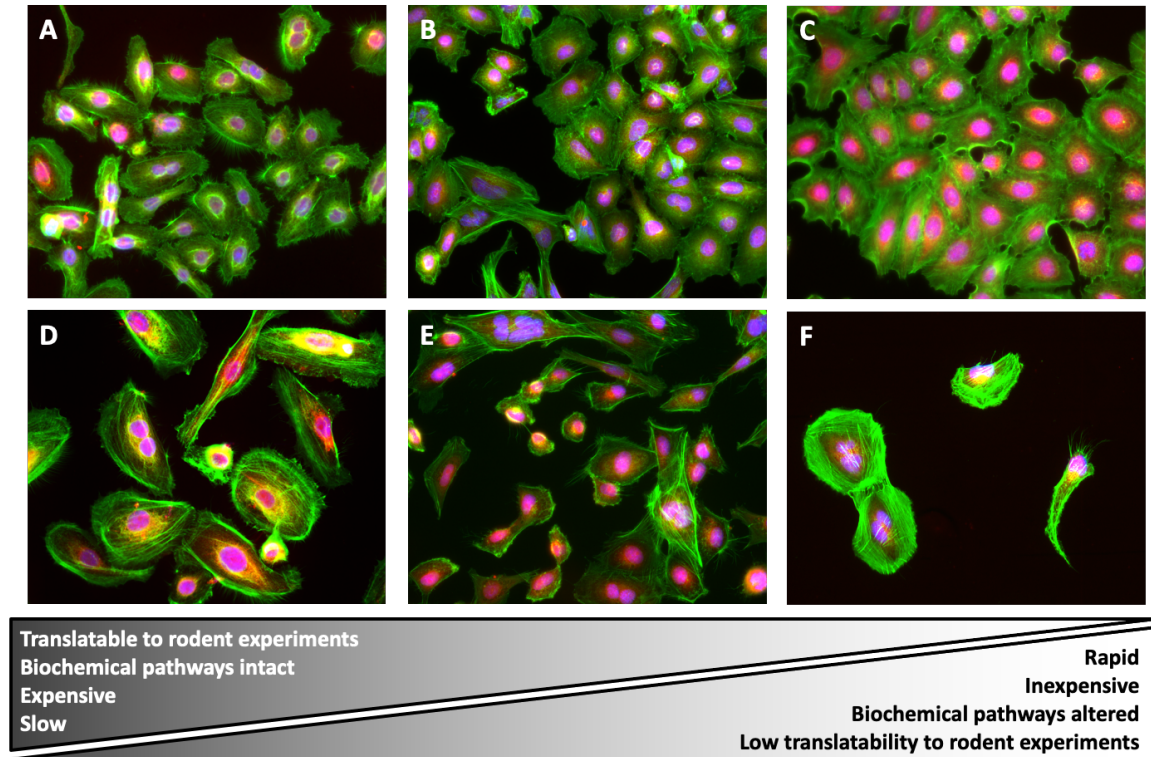


Figure 2.2. Fluorescent microscopy shows distinct growth patterns, degrees of contact inhibition, and respiratory capacity. Image of (A) PTBE cells, (B) BEAS-2B, (C) A549, (D) PSAE, (E) MeT-5A, and (F) Calu-3 cell types. Fluorescent dyes highlight F-actin (ie. the cytoskeleton), mitochondria (and fluoresces when oxidized), and DNA. The bottom figure suggests that these cell types lie on a spectrum of translatability and cost where primary cell types are the most translatable and most expensive. The cancer cell types are the least translatable and least expensive. The transformed cell lines represent a middle ground for translatability and cost.

Figure 2.3. shows the differential proliferation rate and metabolic activity of the six cell types used in this study (PTBE, BEAS-2B, A549, PSAE, MeT-5A, and Calu-3). Line graphs include mean value over multiple observations with standard deviations. The cell proliferation data showed that the bronchial epithelial cells (BEAS-2B and A549) proliferate faster than mesothelial cells (MeT-5A and Calu-3) while transformed and cancerous phenotypes grow more rapidly than their primary cell counterparts (PTBE and PSAE). It is important to note that all cells were seeded at the same density and normalized to the 1-h incubation time point. The mitochondrial activity data showed that

the primary cells and cancer-derived cell types are much more metabolically active when compared with transformed cells. The primary cells are under stress while growing in culture plates and may have overactive mitochondria to counteract this stress. The cancer cells have altered metabolic pathways (ie, the “Warburg effect”), which may be indicative of a higher MTS assay reading (Heiden, Cantley, and Thompson 2009; Warburg 1956). This phenomenon occurs because the MTS is cleaved via aerobic glycolysis; the same pathway commonly perturbed in cancer cells. Together, these results imply that proliferation rates may be dependent on location of the cell type in the lung, whereas mitochondrial activity assays can be utilized as a multifaceted approach to determining cell growth and mitochondrial health.

#### *Differential mRNA Expressions*

Figure 2.4. shows a heatmap of the transformed and cancer cell lines normalized to the primary cell line from their respective area of the lung. In the upper airway cell types (BEAS-2B and A549), the probed mRNAs CDKN1A, TP53, and IL-6 are drastically under expressed when compared with the primary cell line. The GSR mRNA is also under expressed, but less so than the others. In the lower airway cells, CDKN1A is downregulated in both cell types (MeT-5A and Calu-3). MeT-5A cells expressed relatively the same amount of mRNA for TP53, IL-6, and GSR. Calu-3 cells had downregulated TP53, upregulated IL-6, and slightly upregulated levels of GSR.

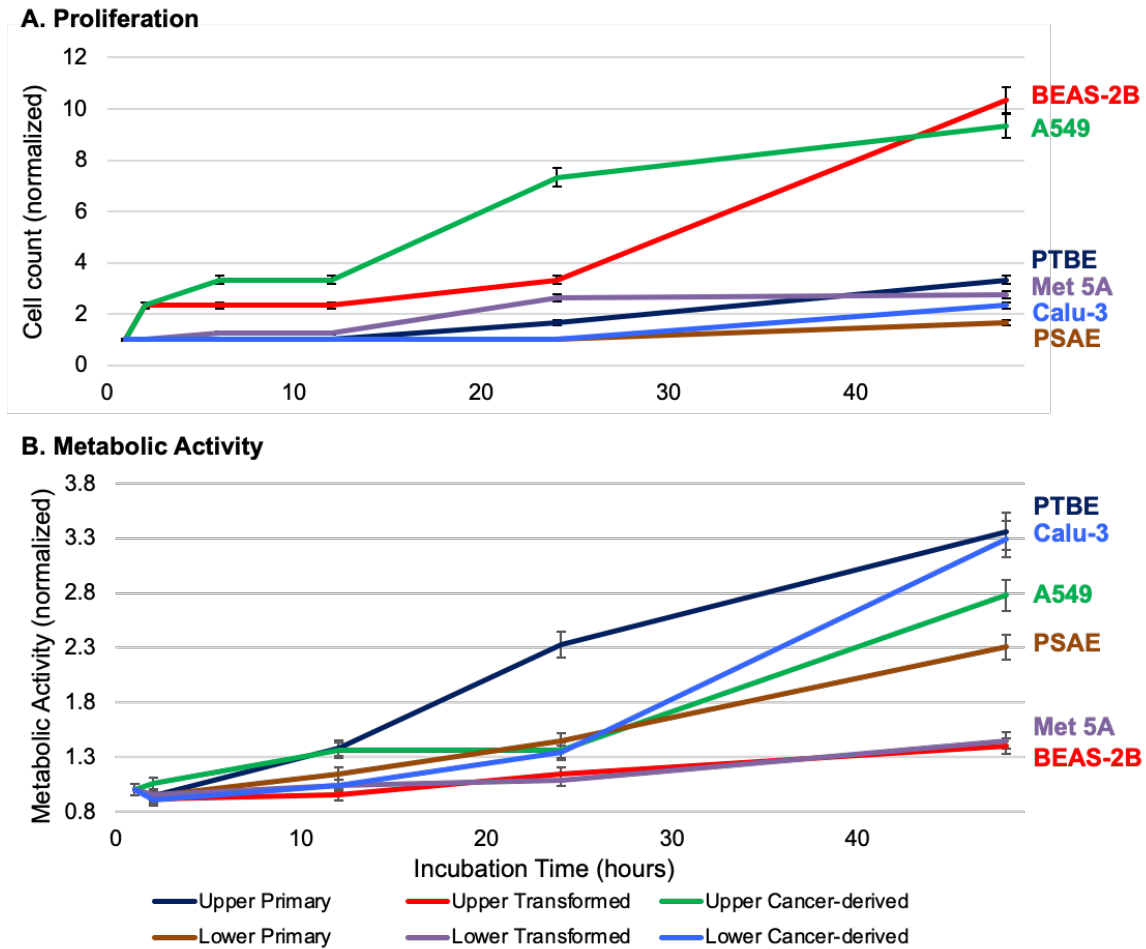


Figure 2.3. Cellular proliferation and mitochondrial activity are different among the six cells. A, PTBE, BEAS-2B, A549, PSAE, MeT-5A, and Calu-3 cells were collected and counted via a cell counter at 1, 2, 6, 12, 24, and 48 h time points. All cells were normalized to their first cell count at the 1 h time point. B, The six cell types were seeded at the same density, and at the designated time point, MTS was added to the well, incubated for 2 h, and then the absorbance of the solution was collected.

Normalized to Upper Primary (PTBE)		GENE	Normalized to Lower Primary (PSAE)	
Upper Transformed (BEAS-2B)	Upper Cancer-derived (A549)		Lower Transformed (Met-5A)	Lower Cancer-derived (Calu-3)
0.0033	0.0055	<i>CDKN1A</i>	0.1175	0.0704
0.0776	0.1027	<i>TP53</i>	1.0467	0.7870
0.0300	0.1250	<i>IL-6</i>	1.0626	6.8446
0.5685	0.3611	<i>GSR</i>	0.9922	1.3365

Figure 2.4. Heatmap of mRNA expressions. The upper airway cells BEAS-2B and A549 are normalized to PTBE, and the lower airway cells MeT-5A and Calu-3 are normalized to PSAE. Values ranging 0 to 0.99 indicate a decreased expression of the corresponding mRNA target, while values ranging 1.1 to 7 indicate an increased expression. Values between 0.99 to 1.1 indicate an expression similar to the primary cell mRNA expression (ie. 1.0).

#### *Protein/Cytokine Expression and Enzyme Activity*

Figure 2.5A shows the concentration of cyclin-dependent kinase inhibitor 1 (p21) and tumor (suppressor) protein (p53). The primary cells have larger concentrations of p53 than the other cells with MeT-5A expressing this protein the least. PTBE cells also express more p21 protein than the other upper airway cell lines. In contrast, MeT-5A cells express the most p21 out of all the different cell types. This could be attributed to the method of transformation used in MeT-5A cells, which is hypothesized to increase p21 protein expression. Figure 2.5B shows the concentration of interleukin 6 (IL-6) and enzyme activity of GSR. There is an inverse relation seen with the enzyme activity of GSR and the subsequent expression of IL-6. In all cell types, the level of GSR activity and IL-6 are either clustered in the same area, or the reduction of GSR activity correlates to the level of IL-6 expression. Both primary cell types have higher levels of IL-6 than the other cell types and also exhibit lower GSR activity. In contrast, the BEAS-2B cell type has highly active GSR activity and a low IL-6 expression. A549, MeT-5A, and

Calu-3 cell types exhibit a GSR activity level that correlates to a reduced IL-6 expression compared with the primary cells.

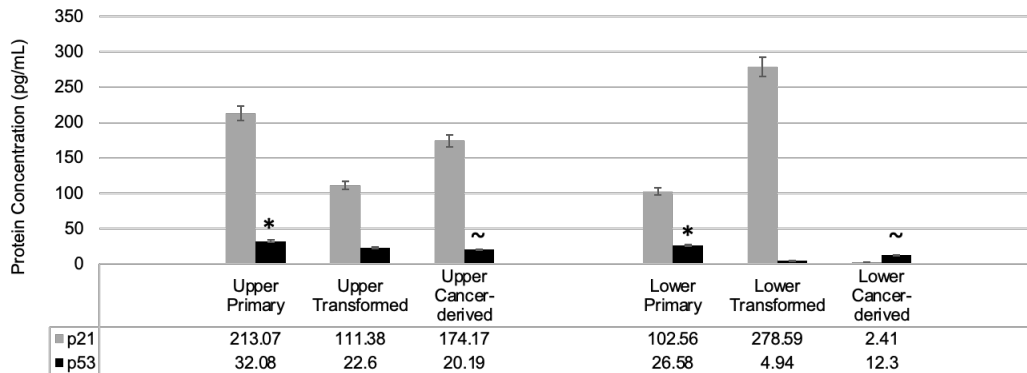
### *Whole Cell Analysis*

Figure 2.6A shows the whole cell analyses data of the six cell types, demonstrating varying oxidative states. Primary cells PTBE and PSAE as well as MeT-5A cells have a percentage of their population that is experiencing high enough levels of endogenous ROS to be detected by flow cytometry. In contrast, BEAS-2B, A549, and Calu-3 cell populations are not experiencing high enough levels of endogenous ROS to be detected via flow cytometry. These results support the premise that primary cell types and lower airway cells (MeT-5A) are more sensitive to exogenous exposures, such as ambient light, change in temperature/humidity, and cleavage processes. All cell types have a low percentage of dead cells (<5%). Induced oxidative stress could be related to the sample preparation procedure; however, sample preparation used in this study is identical among all cell types.

Figure 2.6B demonstrates the cell cycle distributions of the six cell types. The upper airway primary and transformed cell types (PTBE and BEAS-2B) show a similar cell cycle distribution, whereas the lower airway primary and transformed cell lines (PSAE and MeT-5A) also exhibit the same pattern. The cancer phenotypes, A549 and Calu-3, cells have similar cell cycle distributions that are different from that of the primary or transformed cells. The upper airway primary and transformed cell populations have slightly more than 50% of the cells in the G2/M phase, with the transformed cell line having less cells in the G2/M phase and more cells in the G0/G1 phase. The same pattern is seen in the lower airway primary and transformed cells, with the only

difference being the larger ratio of cells in the G0/G1 phase (about 75%). The cancer phenotypes, A549 and Calu-3, are mostly in the G2/M phase. As expected, none of the populations have a large number of cells in the S phase.

**A. p21 & p53 protein analyses**



**B. IL-6 protein concentration & GSR enzyme activity**

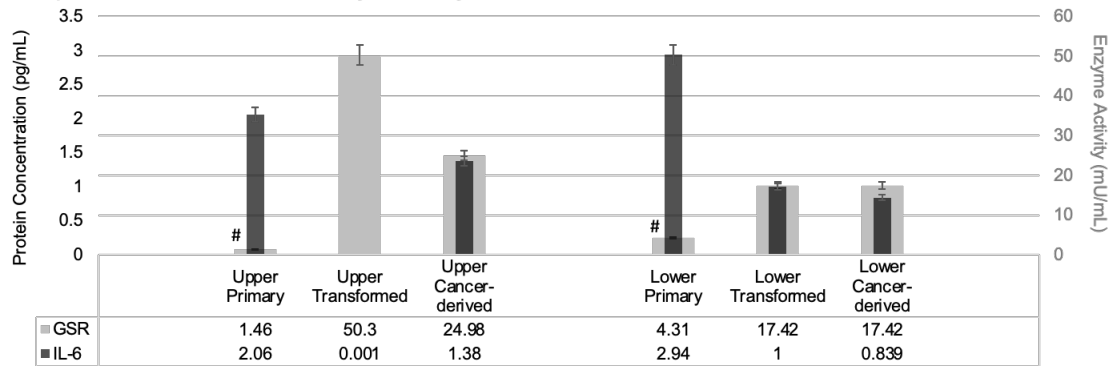


Figure 2.5. Cells produce similar amounts of p53 but differing amounts of p21, IL-6, and GSR. A, Comparison of p21 and p53 protein expression in each cell type determined using an ELISA. B, Comparison of IL-6 protein concentration and GSR enzyme activity in each cell type determined using ELISA and enzyme activity kits.

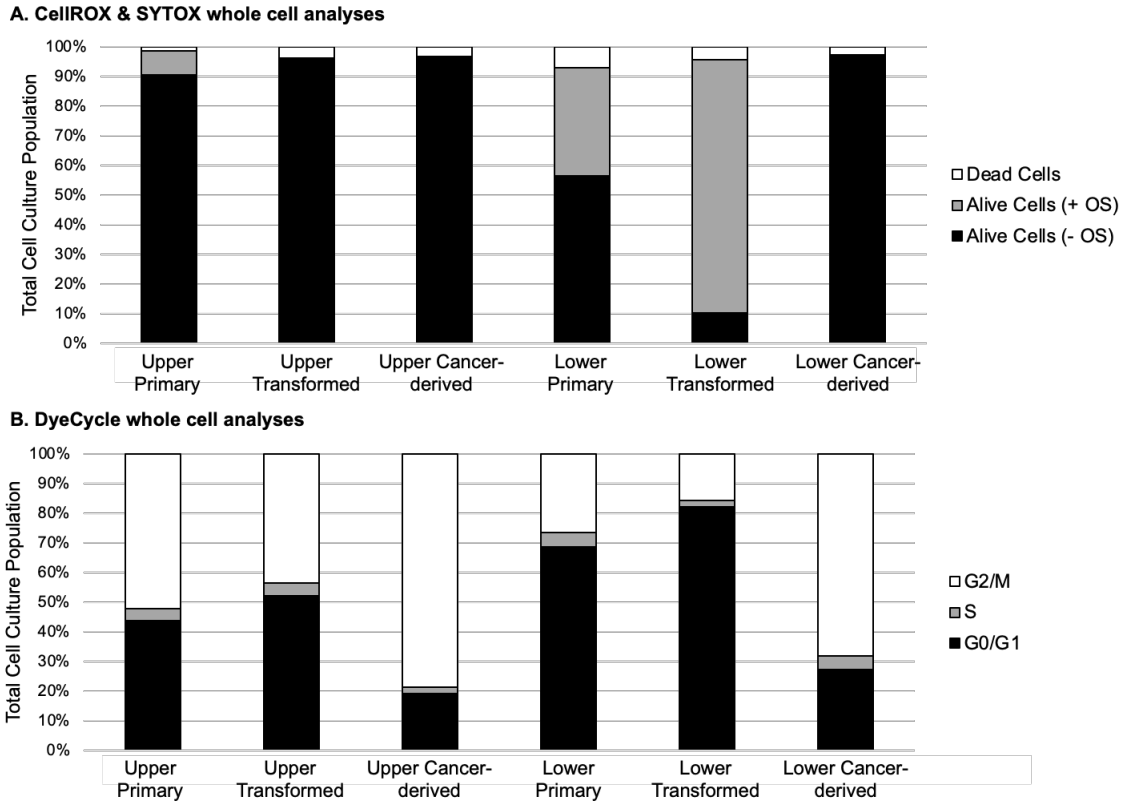


Figure 2.6. Whole cell analysis of cell cycle distributions and general oxidative stress. FACS flow cytometry data comparing (A) the florescence of dead cells (SYTOX), cells undergoing oxidative stress (CellROX), and healthy cells. Florescence-activated cell sorting (FACS) flow cytometry data comparing (B) cell cycle distributions.

Figure 2.7 shows the change in the cell cultures' oxidative stress. Overall, the lower airway cell types showed an increase in the amount of ROS as compared with their un-exposed counterparts. Furthermore, the lower primary cells demonstrated the highest amount of oxidative stress, as compared with the lower transformed and lower cancer derived cells. Similarly, the upper primary cell type also demonstrated the highest amount of oxidative stress, as compared with the upper transformed and upper cancer-derived cells. However, the upper primary cells showed a significantly elevated oxidative stress level as compared with the increased observed in the lower primary cells (1.4 $\times$ ).

**Comparative change in oxidative stress after exposure to tert-butyl hydroperoxide**

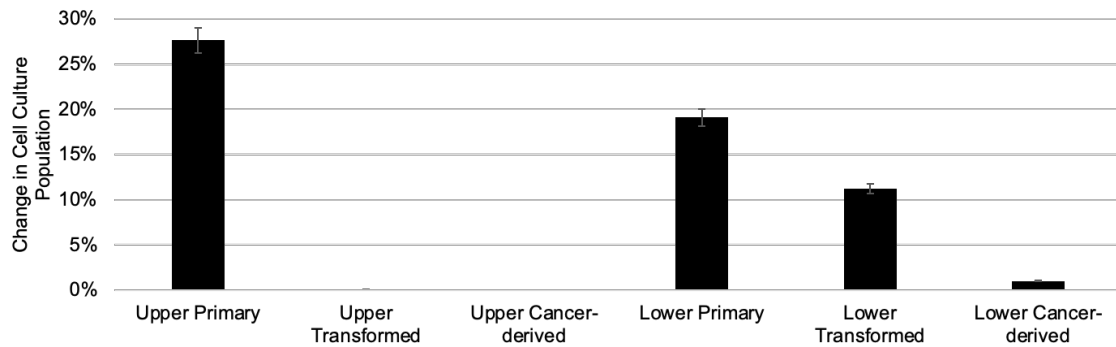


Figure 2.7. Comparative change in oxidative stress after exposure to tert-butyl hydroperoxide. Florescence-activated cell sorting (FACS) flow cytometry data comparing the ROS detected after incubation with a positive oxidative stress control (tert-butyl hydroperoxide) among the 6 cell types used in the study. Change in oxidative stress was normalized against each cell's baseline ROS concentration.

### *Statistical Analysis*

Boxplots are useful in visualizing variation as part of preliminary exploratory data analysis. Figure 2.8 shows that the measured cell-type markers have different ranges of values, including both their centers and spreads. The distributions of expression vary within each marker expression panel. However, in each cell-type marker, the majority of the distributions appear to be symmetric around the median. Each marker is scale-wise comparable, as measured by original experimental parameters. Reading across the biomarker expressions, it is clear that some cells do not express some proteins. For example, lower cancer-derived cells (A549) do not express p21; upper primary cells (PTBE) do not express GSR; and upper transformed cells (Met-5A) do not express IL-6 when cultures are maintained in normal, healthy conditions.

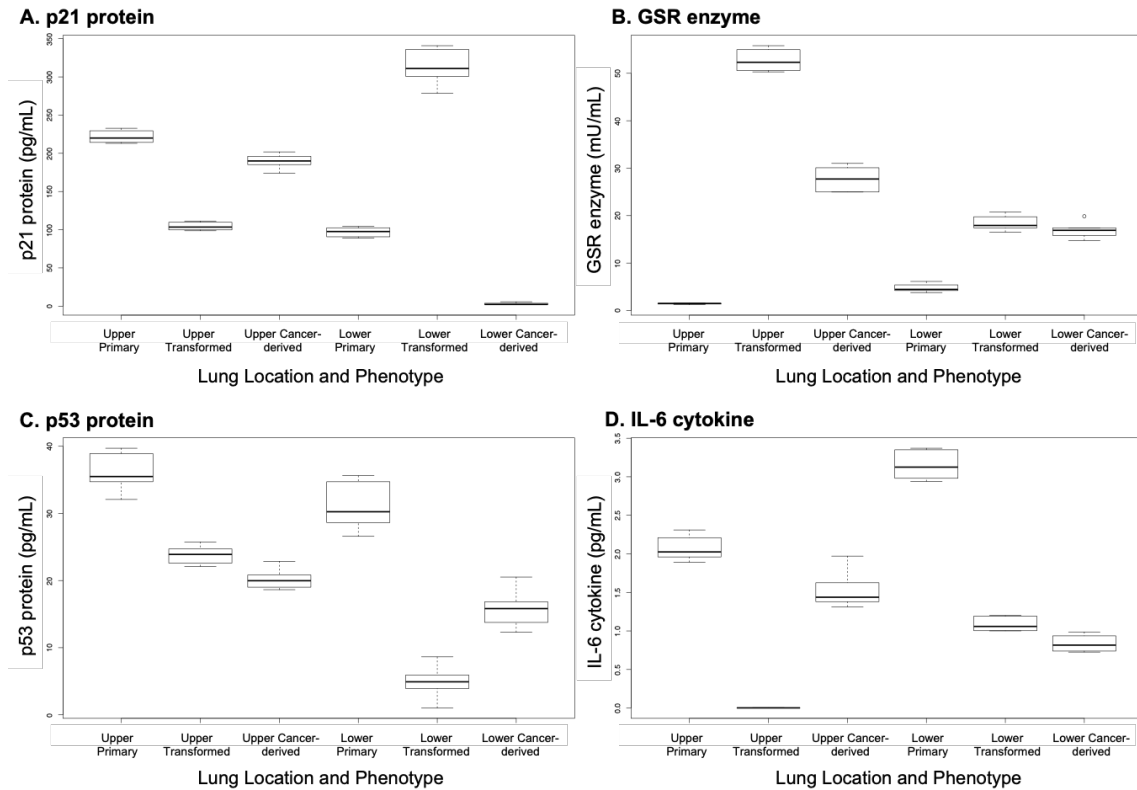


Figure 2.8. Boxplots for the protein, cytokine, and enzyme concentrations measured in experimental datasets. A, p21 protein, B, GSR enzyme, C, p53 protein, and D, IL-6 cytokine. The cell types include PTBE (upper primary), BEAS-2B (upper transformed), A549 (upper cancer derived), PSAE (lower primary), Met-5A (lower transformed), and Calu-3 (lower cancer derived).

Visual comparisons can be made in 3 ways: first, upper airway cells (PTBE, BEAS-2B, and A549) can be compared with corresponding lower airway cells (PSAE, Met-5A, and Calu-3, respectively). Second, primary cells can be compared against transformed or cancer-derived cells (eg, PTBE against BEAS-2B or A549); and third, cell type can be compared across the biomarkers (eg, compare p21, p53, GSR, and IL-6 expressions for PTBE). In p21 protein expression, lower transformed (Met-5A) have the largest distribution while lower cancer (Calu-3) have the smallest distribution. Upper cancer cells (A549) express p21 protein most similarly to upper primary cells (PTBE), whereas upper transformed cells (BEAS-2B) express p21 at lower concentrations than

PTBE. Lower transformed cells (Met-5A) express p21 protein higher than lower primary cells (PSAE), whereas lower cancer cells (Calu-3) express p21 at lower concentrations than PSAE. When comparing CDKN1A mRNA data against p21 protein expression data (results not shown), the upper airway cells follow a similar pattern of primary cells expressing higher concentrations of p21 gene and protein as compared with transformed or cancer derived. When reading across the protein expression data, PTBE cells express a large amount of p53, moderate amount of p21 and IL-6, and low amount of GSR as compared with the other cell types.

The interaction plots in Figure 2.9 show that the measured cell-type markers appear to be dependent upon both lung location and type of cell and are useful in visualizing the effect of one factor in conjunction with another. Generally, lines with differing slopes indicate the possible presence of an interaction, indicating that the effect of lung location on the protein expression differs depending on the cell type. Conversely, parallel lines indicate that the effect of lung location does not depend on the cell type.

Based on the interaction plots and the test for significance of the interaction in a 2-way ANOVA (both parametric and nonparametric versions), a strongly significant interaction effect is present for each protein (all p-values less than .0001), implying that conclusions must be made that are specific to combination of lung location and cell type (Table 2.2). For example, when comparing the primary cells to the transformed cells in the p21 protein panel, lung location does have a strong effect on p21 protein expression, but its effect depends on the cell type. Cell type also has a strong effect on p21 protein expression, but its effect depends on the lung location. Follow-up analysis to test the null hypothesis that the means of each possible pair of treatments (15 total pairs of means to

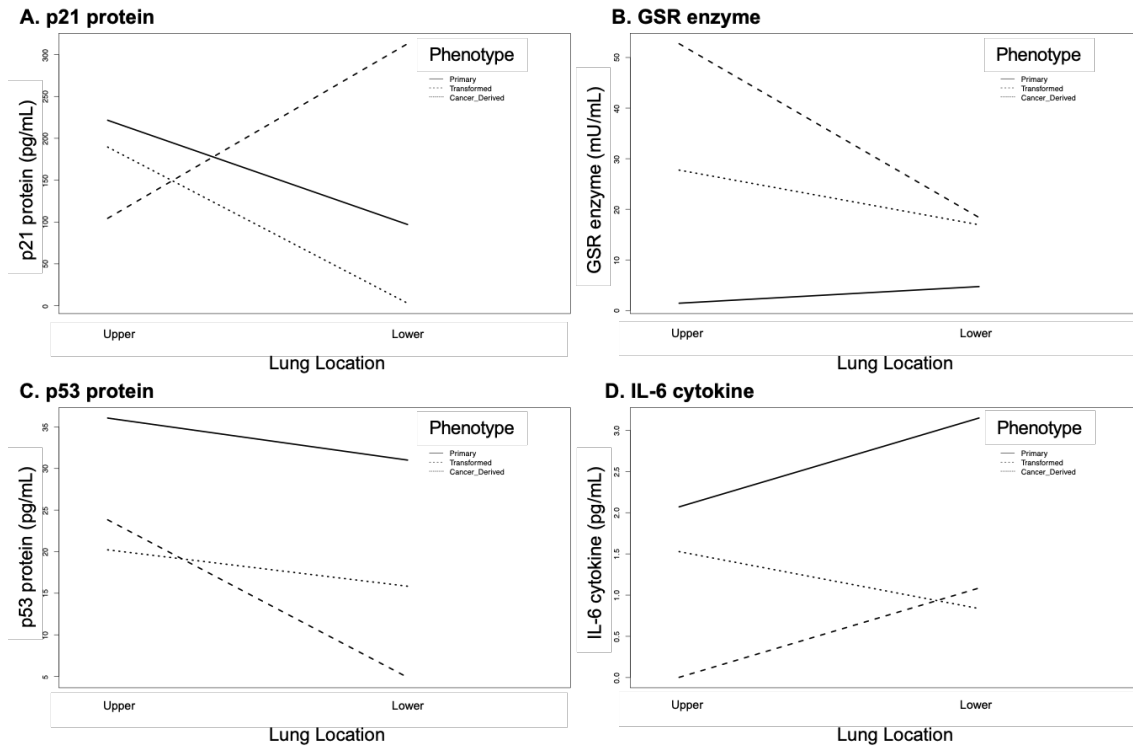


Figure 2.9. Interaction plots for the protein, cytokine, and enzyme concentrations measured in experimental datasets showing the sample mean for each treatment connected by a line. A, p21 protein, B, GSR enzyme, C, p53 protein, and D, IL-6 cytokine. The cell types include PTBE (upper primary), BEAS-2B (upper transformed), A549 (upper cancer derived), PSAE (lower primary), Met-5A (lower transformed), and Calu-3 (lower cancer derived).

Table 2.2. Two-way ANOVA results for each response. “LL” stands for “Lung Location,” and “PT” stands for “Phenotype.”

Effect	p21 protein	p53 protein	IL6 cytokine	GSR enzyme	<i>CDKN1A</i> mRNA	<i>TP53</i> mRNA	IL6 mRNA	GSR mRNA
LL	< 0.0001	< 0.0001	< 0.0001	< 0.0001	< 0.0001	< 0.0001	< 0.0001	< 0.0001
PT	< 0.0001	< 0.0001	< 0.0001	< 0.0001	< 0.0001	< 0.0001	< 0.0001	0.0109
LL × PT	< 0.0001	< 0.0001	< 0.0001	< 0.0001	< 0.0001	< 0.0001	< 0.0001	< 0.0001

compare) are the same indicate that only the upper transformed and lower primary cells do not have significantly different average p21 protein expression (p-value .8711). All other p21 treatments have significantly different mean protein expression (p-values less than .001).

Table 2.3 lists a subset of 6 of the 15 possible pairwise comparisons for each biomarker expression (ie, p21 protein, p53 protein, IL-6 cytokine, and GSR enzyme). Comparisons across (i) lung locations with the same phenotype and (ii) between transformed and cancer-derived with primary for the same lung location are listed. The first set of comparisons is chosen to draw inference across lung locations with the same phenotypes, and only three of these comparisons (ie, Lower: Primary vs Upper: Primary for p53 protein and GSR enzyme and Lower: Cancer derived and Upper: Cancer-derived for the p53 protein) have p-values that are larger than .01. The remainder of the comparisons in mean biomarker expression across lung location have p-values less than .01, indicating that the mean biomarker expression differs significantly depending on the location from which the cells were extracted from the lung. The “Diff” column in Table 3 gives difference in the means between the two treatments and gives a sense of the scale of the differences detected and which combination of phenotype and lung location results in stronger gene expression. Note, a positive (negative) difference in means indicates that the mean in column T1 (T2) is larger than the mean in column T2 (T1).

The second set of comparisons in Table 2.3 controls for location in the lung and compares the transformed and cancer-derived phenotypes to the “gold standard” primary phenotype. If indeed the transformed and cancer derived phenotypes are equivalent to the primary cell type, then there should be no difference in the mean expression of each of

Table 2.3. Tukey's Honestly Significant Difference (HSD) for each pair of treatments with the difference in the means between the two groups listed along with the associated p-value for the biomarker expression (i.e., protein, cytokine, and enzyme). The p-values of those pairs whose means are not significantly different at the 0.01 level are in bold.

Comparable	Pair		p21 protein		p53 protein		IL-6 cytokine		GSR enzyme	
	T1	T2	Diff	p-value	Diff	p-value	Diff	p-value	Diff	p-value
Across same phenotype; different lung location	Lower: Primary	Upper: Primary	-124.58	0.00	-5.06	<b>0.02</b>	1.08	0.00	3.29	<b>0.03</b>
	Lower: Transformed	Upper: Transformed	208.62	0.00	-18.94	0.00	1.08	0.00	-34.33	0.00
	Lower: Cancer Derived	Upper: Cancer Derived	-186.59	0.00	-4.37	<b>0.06</b>	-0.69	0.00	-10.80	0.00
Across same lung location; different phenotype	Upper: Transformed	Upper: Primary	-117.20	0.00	-12.24	0.00	-2.07	0.00	51.28	0.00
	Upper: Cancer Derived	Upper: Primary	-32.04	0.00	-15.85	0.00	-0.54	0.00	26.30	0.00
	Lower: Transformed	Lower: Primary	216.01	0.00	-26.12	0.00	-2.06	0.00	13.65	0.00
	Lower: Cancer Derived	Lower: Primary	-94.04	0.00	-15.17	0.00	-2.31	0.00	12.21	0.00

these four biomarkers; however, the opposite conclusion is reached with this data. Every comparison indicates a significant difference between the mean expression for the transformed or cancer-derived cells and the primary cells, evidence that the transformed and cancer-derived cells cannot be substituted for primary cells with the expectation that the gene expressions will remain, on average, the same.

### *Discussion*

Spontaneous generation of ROS produced during normal cell culture and proliferation can create low levels of oxidative stress within cells. These endogenous sources of ROS generation include cellular respiration (ie, mitochondrial activity) and integrin-signaled adhesion (Murphy 2009; Nohl, Gille, and Staniek 2005; Ravuri et al. 2011; Sauer, Wartenberg, and Hescheler 2001). Endogenous ROS has the potential to trigger multiple adverse cellular effects through oxidative stress pathways and cell cycle arrest if the cell does not have the proper antioxidant compensation mechanisms.

Intracellular oxidation is connected to the cell's cycle. Cell cycle regulation requires a balance of different cyclins at different phases. For instance, G0/G1 is dependent on cyclin D, G1/S is dependent on cyclin E, S/G2 is dependent on cyclin A, and G2/M is dependent on cyclin B. However, research has shown that each of these cyclins are vulnerable, and oxidation of complementary proteins and genes impair the cell cycle progress from one phase to another. Increases in certain proteins (such as p21 and p53) and genes (such as TP53 and CDKN1A) contribute to cell cycle arrest as demonstrated in this and other studies (Agarwal et al. 1995; Brugarolas et al. 1995) (Bunz et al. 1998; Vousden and Lu 2002). However, oxidation of cyclins and/or their associated cofactors also causes cell cycle dysregulation. For instance, the MAPK family members JNK, ERK, and p38 respond to ROS and can further affect the cell cycle (Burhans and Heintz 2009; Menon and Goswami 2007; Wei and Liu 2002).

Two of the most commonly reported causes of subcellular molecular oxidation are direct (through mitochondrial respiration) or indirect (through metabolism of an engulfed xenobiotic) (Oberdörster et al. 2005a). In either direct or indirect mechanism, multiple ROS species can be involved, including H<sub>2</sub>O<sub>2</sub>, •OH<sub>2</sub>, •OH, or •O<sub>2</sub><sup>-</sup>. Once ROS generation overcomes the antioxidant capacity of the cell, oxidative stress is induced. Some of the adverse effects that are especially responsive to this induction are DNA damage (at the molecular level), cell cycle arrest (at the cell level), inflammation (at the tissue level), and cancer (at the organism level) (Figure 2.10).

To date, the six cell types presented in this study are cited as the most commonly utilized cell lines in in vitro toxicology, which include reports on pulmonary hazards, nanomaterial exposures, workplace scenarios, and particulate matter health effects. Each

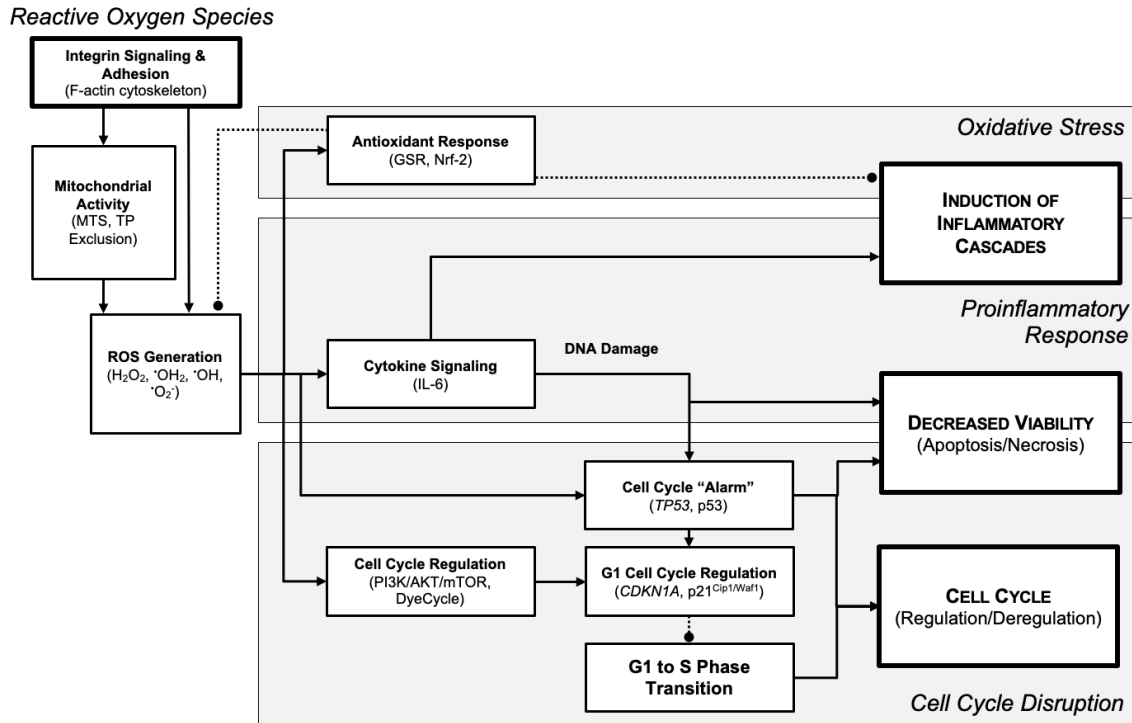


Figure 2.10. Proposed pathway linking ROS generation to induction of inflammatory cascades, decreased viability, and cell cycle disruption. The flowchart lists the descriptions, steps, and the associated proteins and genes involved along the pathway.

of these cell lines have major differences. PTBE, BEAS-2B, A549, PSAE, MeT-5A, and Calu-3 are not just limited to differing phenotypes, but also are unlike in their morphologies, proliferation rates, mRNA and protein expressions, antioxidant capacities, pro-inflammatory states, and cell cycle distributions. Furthermore, the elevated oxidative stress of each cell type is not equally perturbed after exposure to the same concentration of the oxidative stress control used in this study. In general, the results of the oxidative stress challenge can be analyzed in two different ways. First, the primary cells responded to the oxidative stress more pronouncedly than either the transformed or cancer-derived counterparts. As a group, the lower airway cells responded to the oxidative stress ubiquitously as compared with the group of upper airway cells. Comparing adverse

health effects is not feasible for read-across efforts without the proper baseline characterization among cell types; put simply, these cells are not interchangeable.

When designing an in vitro toxicological study, it is important to select cell cultures with unaltered cell signaling pathways relevant to the expected adverse cellular effect as well as being derived from the relevant site of injury. For the lung, studies have shown that the effects of cells and tissues in the upper airways respond differently than cells and tissues in the alveolar space and in the pleural space (Michael Berg et al. 2013; Hatch 2013; Oberdörster 2010; Pedley 1977). These differential responses can be attributed to xenobiotic dose or physicochemical properties, as well as the characteristics of the cell culture. Just as the properties of the xenobiotic agent require careful characterization in any in vitro toxicology study, similar rigor must extend to collecting and reporting data on the antioxidant capacity and cell cycle population distribution. These are key indices gauging the relative health of the cell culture before toxicant exposure and will allow for reading across various studies of similar design or will warn when the cellular data are incongruous (Figure 2.8). With this new understanding, in vitro toxicology datasets have the potential to be exponentially more translatable to other areas of science and, eventually, policy. The next chapter builds upon chapters one and two by uncovering novel mechanisms of toxicity among different cell types. Specifically, mitochondrial toxicity and endpoints of mitochondrial dysregulation are investigated using multiple forms of microscopy in normal, transformed, and cancer derived cells.

## References

- Agarwal, Munna L, Archana Agarwal, William R Taylor, and George R Stark. 1995. "P53 Controls Both the G2/M and the G1 Cell Cycle Checkpoints and Mediates Reversible Growth Arrest in Human Fibroblasts." *Proceedings of the National Academy of Sciences* 92, no. 18: 8493-8497.
- Blaauboer, Bas J. 2008. "The Contribution of in Vitro Toxicity Data in Hazard and Risk Assessment: Current Limitations and Future Perspectives." *Toxicology letters* 180, no. 2: 81-84.
- Boonstra, Johannes, and Jan Andries Post. 2004. "Molecular Events Associated with Reactive Oxygen Species and Cell Cycle Progression in Mammalian Cells." *Gene* 337: 1-13.
- Brugarolas, James, Chitra Chandrasekaran, Jeffrey I Gordon, David Beach, Tyler Jacks, and Gregory J Hannon. 1995. "Radiation-Induced Cell Cycle Arrest Compromised by P21 Deficiency." *Nature* 377, no. 6549: 552-557.
- Bunz, F., A. Dutriaux, C. Lengauer, T. Waldman, S. Zhou, J. P. Brown, J. M. Sedivy, K. W. Kinzler, and B. Vogelstein. 1998. "Requirement for P53 and P21 to Sustain G2 Arrest after DNA Damage." *Science* 282, no. 5393: 1497-1501.  
<https://dx.doi.org/10.1126/science.282.5393.1497>.
- Burhans, William C, and Nicholas H Heintz. 2009. "The Cell Cycle Is a Redox Cycle: Linking Phase-Specific Targets to Cell Fate." *Free Radical Biology and Medicine* 47, no. 9: 1282-1293.
- Carere, A, A Stammati, and F Zucco. 2002. "In Vitro Toxicology Methods: Impact on Regulation from Technical and Scientific Advancements." *Toxicology letters* 127, no. 1-3: 153-160.
- Cohen, Joel M, Justin G Teeguarden, and Philip Demokritou. 2014. "An Integrated Approach for the in Vitro Dosimetry of Engineered Nanomaterials." *Particle and fibre toxicology* 11, no. 1: 20.
- Diamond, M. S., D. Edgil, T. G. Roberts, B. Lu, and E. Harris. 2000. "Infection of Human Cells by Dengue Virus Is Modulated by Different Cell Types and Viral Strains." *Journal of Virology* 74, no. 17: 7814-7823.  
<https://dx.doi.org/10.1128/JVI.74.17.7814-7823.2000>.
- Eom, H. J., and J. Choi. 2010. "P38 Mapk Activation, DNA Damage, Cell Cycle Arrest and Apoptosis as Mechanisms of Toxicity of Silver Nanoparticles in Jurkat T Cells." *Environmental Science and Technology* 44, no. 21: 8337-8342.  
<https://dx.doi.org/10.1021/es1020668>.

- Fernandes, Tiago G, Maria Margarida Diogo, Douglas S Clark, Jonathan S Dordick, and Joaquim MS Cabral. 2009. "High-Throughput Cellular Microarray Platforms: Applications in Drug Discovery, Toxicology and Stem Cell Research." *Trends in biotechnology* 27, no. 6: 342-349.
- Finkel, Toren, and Nikki J Holbrook. 2000. "Oxidants, Oxidative Stress and the Biology of Ageing." *nature* 408, no. 6809: 239-247.
- Foldbjerg, Rasmus, Duy Anh Dang, and Herman Autrup. 2011. "Cytotoxicity and Genotoxicity of Silver Nanoparticles in the Human Lung Cancer Cell Line, A549." *Archives of toxicology* 85, no. 7: 743-750.
- Godoy, Patricio, Nicola J Hewitt, Ute Albrecht, Melvin E Andersen, Nariman Ansari, Sudin Bhattacharya, Johannes Georg Bode, Jennifer Bolleyn, Christoph Borner, and Jan Boettger. 2013. "Recent Advances in 2d and 3d in Vitro Systems Using Primary Hepatocytes, Alternative Hepatocyte Sources and Non-Parenchymal Liver Cells and Their Use in Investigating Mechanisms of Hepatotoxicity, Cell Signaling and Adme." *Archives of toxicology* 87, no. 8: 1315-1530.
- Goldberg, Alan M, and John M Frazier. 1989. "Alternatives to Animals in Toxicity Testing." *Scientific American* 261, no. 2: 24-31.
- Guillouzo, André, and Christiane Guguen-Guillouzo. 2008. "Evolving Concepts in Liver Tissue Modeling and Implications for in Vitro Toxicology." *Expert opinion on drug metabolism & toxicology* 4, no. 10: 1279-1294.
- Guo, B., R. Zebda, S. J. Drake, and C. M. Sayes. 2009. "Synergistic Effect of Co-Exposure to Carbon Black and Fe<sub>2</sub>O<sub>3</sub> Nanoparticles on Oxidative Stress in Cultured Lung Epithelial Cells." *Particle and Fibre Toxicology* 6. <https://dx.doi.org/10.1186/1743-8977-6-4>.
- Gupta, S. C., D. Hevia, S. Patchva, B. Park, W. Koh, and B. B. Aggarwal. 2012. "Upsides and Downsides of Reactive Oxygen Species for Cancer: The Roles of Reactive Oxygen Species in Tumorigenesis, Prevention, and Therapy." *Antioxidants and Redox Signaling* 16, no. 11: 1295-1322. <https://dx.doi.org/10.1089/ars.2011.4414>.
- Hahn, William C, Christopher M Counter, Ante S Lundberg, Roderick L Beijersbergen, Mary W Brooks, and Robert A Weinberg. 1999. "Creation of Human Tumour Cells with Defined Genetic Elements." *Nature* 400, no. 6743: 464-468.
- Hahn, William C, Scott K Dessain, Mary W Brooks, Jessie E King, Brian Elenbaas, David M Sabatini, James A DeCaprio, and Robert A Weinberg. 2002. "Enumeration of the Simian Virus 40 Early Region Elements Necessary for Human Cell Transformation." *Molecular and cellular biology* 22, no. 7: 2111-2123.

- Hanahan, Douglas, and Robert A Weinberg. 2000. "The Hallmarks of Cancer." *cell* 100, no. 1: 57-70.
- . 2011. "Hallmarks of Cancer: The Next Generation." *cell* 144, no. 5: 646-674.
- Hartung, Thomas, and George Daston. 2009. "Are in Vitro Tests Suitable for Regulatory Use?" *Toxicological sciences* 111, no. 2: 233-237.
- Hatch, Theodore F., Paul Gross. 2013. "Pulmonary Deposition and Retention of Inhaled Aerosols." *Elsevier*.
- Heiden, M. G. V., L. C. Cantley, and C. B. Thompson. 2009. "Understanding the Warburg Effect: The Metabolic Requirements of Cell Proliferation." *Science* 324, no. 5930: 1029-1033. <https://dx.doi.org/10.1126/science.1160809>.
- Hussain, S. M., K. L. Hess, J. M. Gearhart, K. T. Geiss, and J. J. Schlager. 2005. "In Vitro Toxicity of Nanoparticles in Brl 3a Rat Liver Cells." *Toxicology in Vitro* 19, no. 7: 975-983. <https://dx.doi.org/10.1016/j.tiv.2005.06.034>.
- Ishii, T., K. Yasuda, A. Akatsuka, O. Hino, P. S. Hartman, and N. Ishii. 2005. "A Mutation in the Sdhc Gene of Complex Ii Increases Oxidative Stress, Resulting in Apoptosis and Tumorigenesis." *Cancer Research* 65, no. 1: 203-209. <https://www.scopus.com/inward/record.uri?eid=2-s2.0-11244279161&partnerID=40&md5=bf6b75f34b095776fd7522091474488e>.
- Kroll, Alexandra, Mike H Pillukat, Daniela Hahn, and Jürgen Schnekenburger. 2009. "Current in Vitro Methods in Nanoparticle Risk Assessment: Limitations and Challenges." *European journal of Pharmaceutics and Biopharmaceutics* 72, no. 2: 370-377.
- Liebsch, Manfred, and Horst Spielmann. 2002. "Currently Available in Vitro Methods Used in the Regulatory Toxicology." *Toxicology letters* 127, no. 1-3: 127-134.
- Lin, Ruei-Zhen, and Hwan-You Chang. 2008. "Recent Advances in Three-Dimensional Multicellular Spheroid Culture for Biomedical Research." *Biotechnology Journal: Healthcare Nutrition Technology* 3, no. 9-10: 1172-1184.
- Liu, Y. J. 2001. "Dendritic Cell Subsets and Lineages, and Their Functions in Innate and Adaptive Immunity." *Cell* 106, no. 3: 259-262. [https://dx.doi.org/10.1016/S0092-8674\(01\)00456-1](https://dx.doi.org/10.1016/S0092-8674(01)00456-1).
- Menon, SG, and PC Goswami. 2007. "A Redox Cycle within the Cell Cycle: Ring in the Old with the New." *Oncogene* 26, no. 8: 1101-1109.

- Michael Berg, J., A. A. Romoser, D. E. Figueroa, C. Spencer West, and C. M. Sayes. 2013. "Comparative Cytological Responses of Lung Epithelial and Pleural Mesothelial Cells Following in Vitro Exposure to Nanoscale Sio<sub>2</sub>." *Toxicology in Vitro* 27, no. 1: 24-33. <https://dx.doi.org/10.1016/j.tiv.2012.09.002>.
- Mooi, WJ, and DS Peeper. 2006. "Oncogene-Induced Cell Senescence—Halting on the Road to Cancer." *New England Journal of Medicine* 355, no. 10: 1037-1046.
- Murphy, Michael P. 2009. "How Mitochondria Produce Reactive Oxygen Species." *Biochemical Journal* 417, no. 1: 1-13.
- Nemmar, Abderrahim, Jørn A Holme, Irma Rosas, Per E Schwarze, and Ernesto Alfaro-Moreno. 2013. "Recent Advances in Particulate Matter and Nanoparticle Toxicology: A Review of the in Vivo and in Vitro Studies." *BioMed research international* 2013.
- Nohl, H., L. Gille, and K. Staniek. 2005. "Intracellular Generation of Reactive Oxygen Species by Mitochondria." *Biochemical Pharmacology* 69, no. 5: 719-723. <https://dx.doi.org/10.1016/j.bcp.2004.12.002>.
- Oberdörster, G. 2010. "Safety Assessment for Nanotechnology and Nanomedicine: Concepts of Nanotoxicology." *Journal of Internal Medicine* 267, no. 1: 89-105. <https://dx.doi.org/10.1111/j.1365-2796.2009.02187.x>.
- Oberdörster, G., A. Maynard, K. Donaldson, V. Castranova, J. Fitzpatrick, K. Ausman, J. Carter, B. Karn, W. Kreyling, D. Lai, S. Olin, N. Monteiro-Riviere, D. Warheit, and H. Yang. 2005a. "Principles for Characterizing the Potential Human Health Effects from Exposure to Nanomaterials: Elements of a Screening Strategy." *Particle and Fibre Toxicology* 2. <https://dx.doi.org/10.1186/1743-8977-2-8>.
- Pedley, T. J. 1977. "Pulmonary Fluid Dynamics." *Annual Review of Fluid Mechanics* 9 no. 1: 229-274.
- Phalen, Robert F, Michael J Oldham, and Andre E Nel. 2006. "Tracheobronchial Particle Dose Considerations for in Vitro Toxicology Studies." *Toxicological Sciences* 92, no. 1: 126-132.
- Ravuri, C., G. Svineng, S. Pankiv, and N. E. Huseby. 2011. "Endogenous Production of Reactive Oxygen Species by the Nadph Oxidase Complexes Is a Determinant of  $\Gamma$ -Glutamyltransferase Expression." *Free Radical Research* 45, no. 5: 600-610. <https://dx.doi.org/10.3109/10715762.2011.564164>.
- Sauer, Heinrich, Maria Wartenberg, and Juergen Hescheler. 2001. "Reactive Oxygen Species as Intracellular Messengers During Cell Growth and Differentiation." *Cellular physiology and biochemistry* 11, no. 4: 173-186.

- Sayes, C. M., H. Staats, and A. J. Hickey. 2014. "Scale of Health: Indices of Safety and Efficacy in the Evolving Environment of Large Biological Datasets." *Pharmaceutical Research* 31, no. 9: 2256-2265. <https://dx.doi.org/10.1007/s11095-014-1415-2>.
- Thiery, J. P., H. Acloque, R. Y. J. Huang, and M. A. Nieto. 2009. "Epithelial-Mesenchymal Transitions in Development and Disease." *Cell* 139, no. 5: 871-890. <https://dx.doi.org/10.1016/j.cell.2009.11.007>.
- Vousden, K. H., and X. Lu. 2002. "Live or Let Die: The Cell's Response to P53." *Nature Reviews Cancer* 2, no. 8: 594-604. <https://dx.doi.org/10.1038/nrc864>.
- Warburg, O. 1956. "On the Origin of Cancer Cells." *Science* 123, no. 3191: 309-314. <https://dx.doi.org/10.1126/science.123.3191.309>.
- Wei, Z., and H. T. Liu. 2002. "Mapk Signal Pathways in the Regulation of Cell Proliferation in Mammalian Cells." *Cell Research* 12, no. 1: 9-18. <https://dx.doi.org/10.1038/sj.cr.7290105>.
- Wu, Jie, Jiao Sun, and Yang Xue. 2010. "Involvement of Jnk and P53 Activation in G2/M Cell Cycle Arrest and Apoptosis Induced by Titanium Dioxide Nanoparticles in Neuron Cells." *Toxicology letters* 199, no. 3: 269-276.
- Yu, Byung Pal. 1994. "Cellular Defenses against Damage from Reactive Oxygen Species." *Physiological reviews* 74, no. 1: 139-162.

## CHAPTER THREE

### **Lung Cell Phenotype Impacts Mitochondrial Health After Exposure to Aluminum Nanoparticles**

This chapter published as: Lujan, H., Mulenos, M.R., Carrasco, D., Zechmann, B., Hussain, S.M., and Sayes, C.M., 2020. Lung Cell Phenotype Impacts Mitochondrial Health After Exposure to Aluminum Nanoparticles. ACS nano.

#### *Abstract*

The main role of mitochondria is to generate the energy necessary for the cell to survive and adapt to different environmental stresses. Energy demand varies depending on the phenotype of the cell. To efficiently meet metabolic demands, mitochondria require a specific proton homeostasis and defined membrane structures to facilitate adenosine triphosphate production. A homeostatic environment is constantly challenged as mitochondria are a major target for damage after exposure to environmental contaminants. Mitochondrial damage induces mitochondrial dysregulation which leads to dysfunctional metabolic conditions. In this study, microscopy was used to investigate mitochondria-related toxicity of aluminum nanoparticles (AlNPs) exposed to three different lung cell-types, namely primary tracheal bronchial epithelial cells (PTBE), adenocarcinoma epithelial cells (A549), and asthma derived bronchial epithelial cells (DHBE-As). Endpoint analyses include nanoparticle intracellular uptake; measured changes in mitochondrial size, shape, and ultrastructure; and confirmation of autophagosome formation. Results show that AlNPs (1 ppm) exposure to primary and asthma cells incurred significant mitochondrial deformation and increases in mitophagy, while cancer cells exhibited only slight changes in mitochondrial morphology and an

increase in lipid body formation. These results support previously published microscopic investigations that show low-dose nanomaterial exposure induces subtle changes in mitochondria.

### *Introduction*

The major role of mitochondria is to produce adenosine triphosphate (ATP) as an energy source through the process of oxidative phosphorylation (OXPHOS) (Brevini et al. 2005; Schousboe et al. 2011). The energy production within mitochondria is directly dependent upon the structural integrity of the inner and outer mitochondrial membrane as OXPHOS occurs along the inner membrane (i.e. cristae structure) through the electron transport chain (ETC). A homeostatic proton gradient requires an intact cristae structure to function properly (Rampelt et al. 2017). The energy demand is determined by the phenotype of the cell and the morphology of mitochondria. Primary cells (i.e. cells taken from healthy tissue) are translatable to a healthy human as compared to immortalized cell lines; however, using diseased cell-type models offer a unique opportunity to decipher variable outcomes after nanomaterial exposures in sensitive subpopulations (Kirkpatrick and Mittermayer 1990; Esch, Bahinski, and Huh 2015; Huang et al. 2009). For example, excess oxidative stress and inflammation in asthmatic epithelial cells has been shown to cause mitochondrial dysfunction earlier than in primary lung epithelial cells (Mabalirajan and Ghosh 2013; Cloonan and Choi 2016). Observations of mitochondrial ultrastructure have linked mitochondrial fission and fusion imbalance to the loss of cristae structure in the asthma cell phenotype (Mabalirajan and Ghosh 2013). Other studies have shown that lung cells with other phenotypes have different baseline characteristics inclusive of proliferation, over-expressed versus inactive biochemical pathways, antioxidant capacity,

and cell cycle distributions – all of which effect toxicological responses (Lujan et al. 2019). These cellular health indices define mitochondrial health.

Mitochondrial activity and bioenergetics are tightly linked to morphology and internal cristae structure (Zick, Rabl, and Reichert 2009). Examining these structures microscopically can unveil endpoints related to mitochondrial dysfunction based on ultrastructural changes before versus after exposure to environmental contaminants. One emerging contaminant of concern is aluminum nanoparticles (AlNPs) (Darlington et al. 2009). AlNPs are currently in formulations for surface coatings, high combustion fuel, and explosives because these materials promote increased energy release in combustion reactions, thermal stability, corrosion resistance, and increased plasmonic resonance as compared to bulk aluminum (Kim et al. 2012). Aluminum particles less than 100 nanometers in diameter aerosolize easily, transport across large distances, and are frequently inhaled in occupational settings causing concern for pulmonary toxicity (Brar et al. 2010; Darlington, et al. 2009). Aluminum negatively impact mitochondrial health and charged with increasing the onset of metabolic diseases; however, the extent of mitochondrial damage induced by AlNP exposure has yet to be investigated (Niu et al. 2005; Murakami and Yoshino 2004; Ghribi et al. 2001; Mirshafa et al. 2018).

Studies have shown that mitochondria are central targets of a large number of environmental contaminants (Dreier et al. 2019). Both engineered and incidental nanoparticles have been implicated in mitochondrial dysregulation through mitophagy (Zhang et al. 2010). Mitophagy is the selective degradation of healthy or damaged mitochondria to either regulate under normal conditions or isolate damaged mitochondria into membranes for fusion with a lysosome (Youle and Narendra 2011). The process of

mitophagy then continues by selectively degrading damaged mitochondria via shuttling into autophagosomes for fusion with lysosomes (Youle and Narendra 2011). Low-dose exposures to AlNPs follow this mechanism, i.e. accumulation in mitochondria, alteration of the inner and outer membrane structure, and generation of reactive oxygen species (ROS) disrupting ETC homeostasis (Chevallet et al. 2016). Aluminum ions disrupt mitochondria function through an imbalance of ions in membrane channels as well as inducing ROS (Sharma and Mishra 2006). The mito-toxic effects of AlNP may be intensified compared to other forms of aluminum because of the innate ability of nanoparticles to passively diffuse into cells, intercalate within lipid membranes, and disguise themselves as electrophilic species (Balbus et al. 2007; Elsaesser and Howard 2012). The data presented in the paper are the first evidence of aluminum nanoparticles as inducers of mitophagy.

## Results and Discussion

*Polydisperse aluminum nanoparticles induce mitophagy.* The mechanism of mitochondrial dysregulation, along with the physicochemical properties of aluminum nanoparticles, is shown in Figure 3.1. The polydisperse nature of aluminum nanoparticles (AlNPs) enables three different ways that nanoparticles can enter a cell. Individual particles can passively diffuse across the cytoplasmic membrane; particles less than 30 nm in diameter can undergo clathrin and caveolin mediated uptake and particles greater than 200 nm undergo phagocytosis and macro-pinocytosis (Lujan and Sayes 2017). Aggregates of particles are shuttled into the cell in a vesicle that is then fused with a lysosome. Within the lysosome nanoparticles become ionized due to the acid

environment (Stern, Adisheshaiah, and Crist 2012). Degraded particles, resultant ion, and even individual particles (<20 nm in size) interact with mitochondria causing the induction of fission and fusion leading to mitophagy (Twig and Shirihai 2011).

Nanoparticles interact with mitochondria causing damage inducing increased fission or fusion. The damaged mitochondria are isolated and fused with a lysosome for degradation. These damaged mitochondria can contain particles that will then ionize within the acidic vesicle. The cycle of particle uptake, mitochondrial damage, and isolation within acidic vesicles creates a positive feedback loop of continued mitophagy.

Each of these steps in the loop - ranging aluminum exposure to mitochondrial dysfunction - was examined using microscopy techniques. The physicochemical characteristics of AlNPs were characterized before and after exposure to cells in culture. Before exposure, dynamic light scattering was used to measure the dispersity index ( $0.422 \pm 0.018$ ) which indicated a moderately polydisperse size population (i.e. value could range 0 to 1, where 0 indicates monodispersity). Polydispersity in particle size was confirmed with transmission electron microscopy (TEM) (Figure 3.1B), where the average particle size of AlNPs were determined to be 80 nm. The hydrodynamic diameter was  $455.77 \pm 16.47$  nm, which indicates a high level of particle agglomeration. This is due to the hydrophobic nature of the nanopowder when force suspended in ultrapure water. Zeta potential was  $8.44 \pm 0.49$  mV indicating colloidal instability (i.e. values >30 mV or <-30 mV indicate stability; values between -30 and 30 mV indicate instability). The particles were measured as 99.99% pure aluminum via inductively coupled plasma-mass spectrometry (Figure 3.1C).

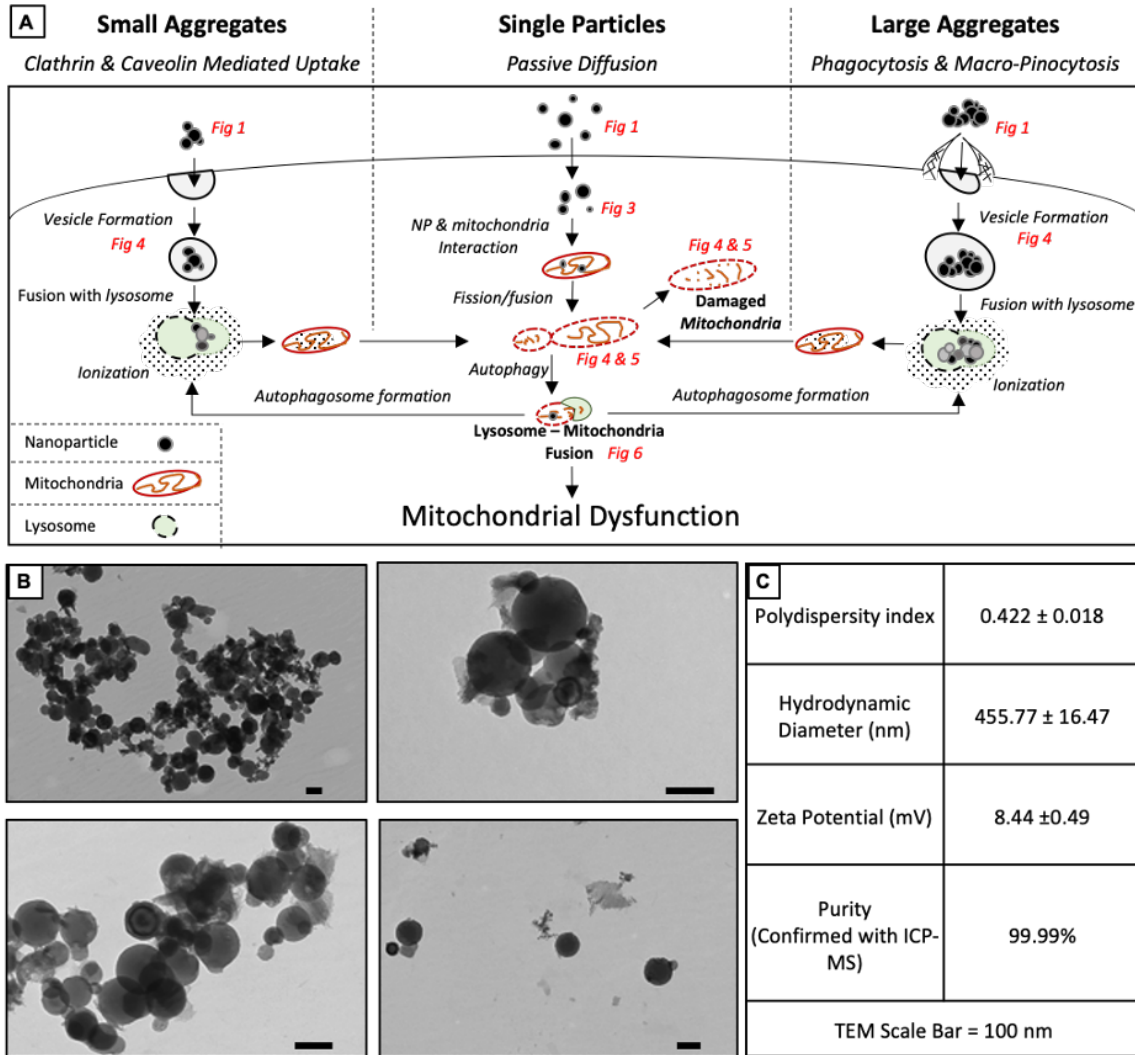


Figure 3.1. Mechanisms of mitochondrial dysregulation after aluminum nanoparticle exposure. The hypothesized mechanism (A) shows the different routes of uptake and the possible pathway of aluminum nanoparticle toxicity to mitochondria. Steps along the pathway are denoted with the figure within the paper that visualize the step in the pathway. TEM micrograph of aluminum nanoparticles (B) show an average size of around 100nm with different sizes due to agglomeration. The table (C) shows the polydispersity index indicates that the particles are polydisperse with an average hydrodynamic diameter of 455.77 nm. The zeta potential of 8.44 denotes that the particles are relatively unstable in suspension. The purity of the nanoparticles was confirmed via ICP-MS to be 99.99% pure. Scale Bar = 100 nm.

*Primary, cancer, and asthma lung cell-types exhibit differential mitochondrial morphologies.* Representative transmission electron micrographs depicting the typical morphologies of mitochondria in primary (PTBE), cancer (A549), and asthma (DHBE-As) lung cell lines are shown in Figure 3.2. Quantitative analyses of micrographs reveal differences in the size (*i.e.* diameter) and shape (*i.e.* roundness) among the different cells. Mitochondrial roundness was measured as a ratio of length to width, where  $x = 0$  represents a perfect circle,  $0 < x \leq 0.4$  represents an oval shape, and  $0.4 < x < 1$  represents elongated shapes. Figures 3.2D and 3.2E display mitochondrial roundness as either a histogram showing the frequency of the measured shapes or a box plot to visualize the distributions among the ratios. Figures 3.2F and 3.2G display the diameter measurements (*i.e.* the value used for length in the roundness measurements) of mitochondria, also as a histogram and a box plot. Specific to the box plots, ends of each box represent 25% and 75% of the distributions, while the middle line represents the median. The whiskers show the minimum and maximum values measured and the symbols represent outlier values.

All three cell-types have varied distributions in their size and shape. The primary cell-type was seen to be the smallest in diameter ( $0.49 \pm 0.02 \mu\text{m}$ ), most of which were oval in shape ( $0.35 \pm 0.02$ ). When compared to the primary cell-type, mitochondria within the cancer cells were significantly larger in diameter ( $0.68 \pm 0.03 \mu\text{m}$ ) where most of which were significantly more circular in shape ( $0.28 \pm 0.02$ ). When compared to the primary cell-type, the asthma cell-type possessed the significantly longest mitochondria ( $1.59 \pm 0.12 \mu\text{m}$ ). Interestingly, the shape of asthma cell-type mitochondria was not

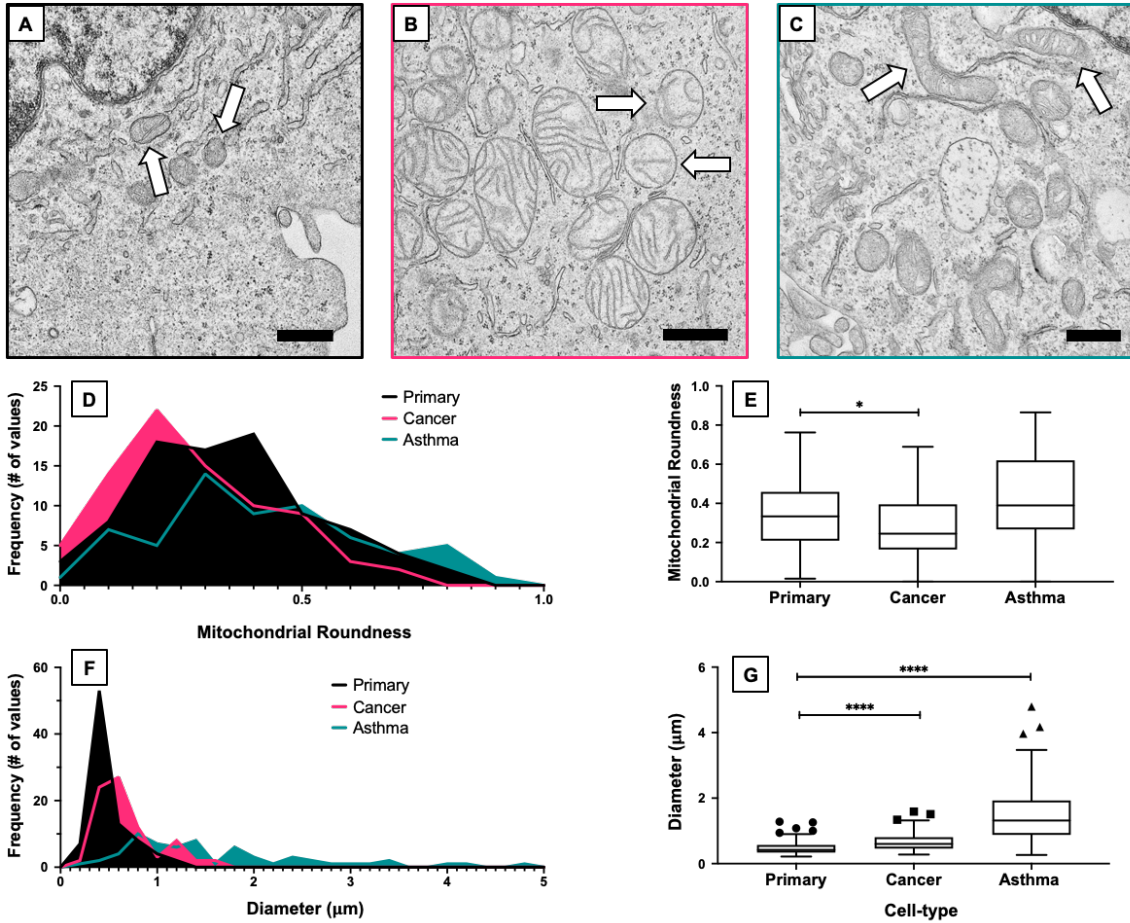


Figure 3.2. Characterization of mitochondrial morphology in untreated primary, cancer, and asthma lung cell-types. TEM micrographs visualizing the typical baseline morphology of mitochondria are shown for (A) primary, (B) cancer, and (C) asthma cell-types. The arrows in each image point to the representative mitochondria. Mitochondrial roundness (length and width ratio) is displayed through histograms (D) and corresponding boxplot (E). Compared to the primary cells, mitochondria in the cancer cells tend to be rounder while asthma have elongated mitochondria. Mitochondrial length is also displayed as a histogram (F) and boxplot (G). Compared to the primary cell-type, mitochondria in cancer cells have a longer diameter and mitochondria in asthma cells have a longer diameter than the cancer cell-type. \* $P \leq 0.05$ ; \*\*\*\* $P \leq 0.0001$  versus control (Primary cell-type). The symbols above the box plots (i.e. circles, squares, and triangles) represent outliers as defined by the Tukey method. Scale bar = 500nm.

significant when compared to either the primary or cancer cells ( $0.42 \pm 0.03$ ). Data was corroborated through the Brown-Forsythe ANOVA test comparing shape and size. The p-values of 0.002 and  $<0.0001$  for shape and size denote highly statistically significant differences in the morphology of mitochondria within the three cell types. All values, standard error of the mean (SEM), and P values from this analysis are cataloged in Table 3.1.

The baseline mitochondrial morphologies of each cell type, even when grown under the same growth conditions, demonstrate different mitochondrial morphology profiles that need to be considered within *in vitro* studies. The differences in the size and shape of mitochondria are attributed to the phenotype of the cell and will influence studies aimed at uncovering mechanisms of mitochondrial dysregulation.

*Uptake of aluminum nanoparticles into different cell-types.* Enhanced darkfield hyperspectral imaging was used to confirm the uptake of AlNPs in primary, cancer, and asthma cell-types. Figure 3.3 shows images of each cell exposed to AlNPs (1 ppm) and corresponding hyperspectral analysis. Over 30 regions of interest (ROIs) were selected of nanoparticles taken up into the cells. Nanoparticle spectra of lower wavelengths (520 nm and below) indicate discrete individual particles, while spectra of higher wavelength (720 nm and above) indicate agglomerated nanoparticles intracellularly (Mortimer et al. 2014; Zucker et al. 2019). Primary and asthma cell-types internalize individual and agglomerated AlNPs as seen in the Gaussian-like distribution around 500 nm. Cancer cell-type primarily internalize agglomerated AlNPs as seen in the predominant right shouldered spectrum.

Table 3.1. Statistical analysis of mitochondrial size and shape among different cell-types.

Measurand	Figure	Parameter	Cell-Type			Significance	<i>p</i> -value
			Primary Mean (SEM)	Cancer Mean (SEM)	Asthma Mean (SEM)		
Mitochondrial roundness of unexposed cells	3.2E	Brown-Forsythe ANOVA test	0.3488 (0.0192)	0.2792 (0.0185)	0.4166 (0.0279)	***	0.0002
		Games-Howell's post hoc test Primary versus Cancer	“	“	N/A	*	0.0267
		Games-Howell's post hoc test Primary versus Asthma	“	N/A	“	ns	0.1165
Mitochondrial Diameter of unexposed cells	3.2G	Brown-Forsythe ANOVA test	0.4873 (0.0237)	0.6843 (0.0339)	1.592 (0.1242)	****	<0.0001
		Games-Howell's post hoc test Primary versus Cancer	“	“	N/A	****	<0.0001
		Games-Howell's post hoc test Primary versus Asthma	“	N/A	“	****	<0.0001
Mitochondrial Roundness of exposed cells	3.4E	Brown-Forsythe ANOVA test	0.4008 (0.0261)	0.3525 (0.0193)	0.3504 (0.0225)	ns	0.2023
		Games-Howell's post hoc test Primary versus Cancer	“	“	N/A	ns	0.3016
		Games-Howell's post hoc test Primary versus Asthma	“	N/A	“	ns	0.3136
Mitochondrial Diameter of exposed cells	3.4G	Brown-Forsythe ANOVA test	0.4363 (0.0287)	0.5325 (0.0261)	0.6307 (0.0352)	****	<0.0001
		Games-Howell's post hoc test Primary versus Cancer	“	“	N/A	*	0.0385
		Games-Howell's post hoc test Primary versus Asthma	“	N/A	“	***	0.0001

The intensity of the peak, or peak height, is related to the concentration of nanoparticles. Asthma cells internalized the most nanoparticles whereas cancer cells had the least amount of uptake in the cells. This could be due to different uptake mechanisms among the different cell-types. Studies have found that different cell-types (i.e. healthy versus cancer derived) will differential uptake macro and nano sized particles (Patiño et al. 2015). The larger clusters of particles seen in the primary and asthma lung cell images (i.e. the bright clusters with shape peaks) are indicative of the increased levels of mitophagy seen in the two cells lines while the lower concentration of particles seen in the cancer cells (i.e. more dispersed particles with weak signal) explain the reduced impact on mitochondrial morphology of the cell.

*Mitochondrial morphology is altered after aluminum nanoparticle exposure.*

Figure 3.4 show representative mitochondrial features of each cell-type exposed to 1 ppm of AlNPs for 24 hours. Each cell-type incurred different morphological changes that were identifiable via TEM. The shape of mitochondria in each cell type is displayed in Figure 3.4D and E as the mean shape of mitochondria for the primary, cancer, and asthma cell-types clustered around  $0.40 \pm 0.03$ ,  $0.35 \pm 0.02$ , and  $0.35 \pm 0.02$  representing an oval shape. The difference in average shape of mitochondria amongst each cell-type was not significant.

The mitochondrial diameter in each cell-type is shown in Figure 3.4F and G. The mean mitochondrial diameter of the primary, cancer, and asthma cell-types were  $0.43 \pm 0.03 \mu\text{m}$ ,  $0.53 \pm 0.03 \mu\text{m}$ , and  $0.63 \pm 0.04 \mu\text{m}$ , respectively. Compared to the primary cell-type, the cancer and asthma cells possessed larger mitochondria (asthma cell

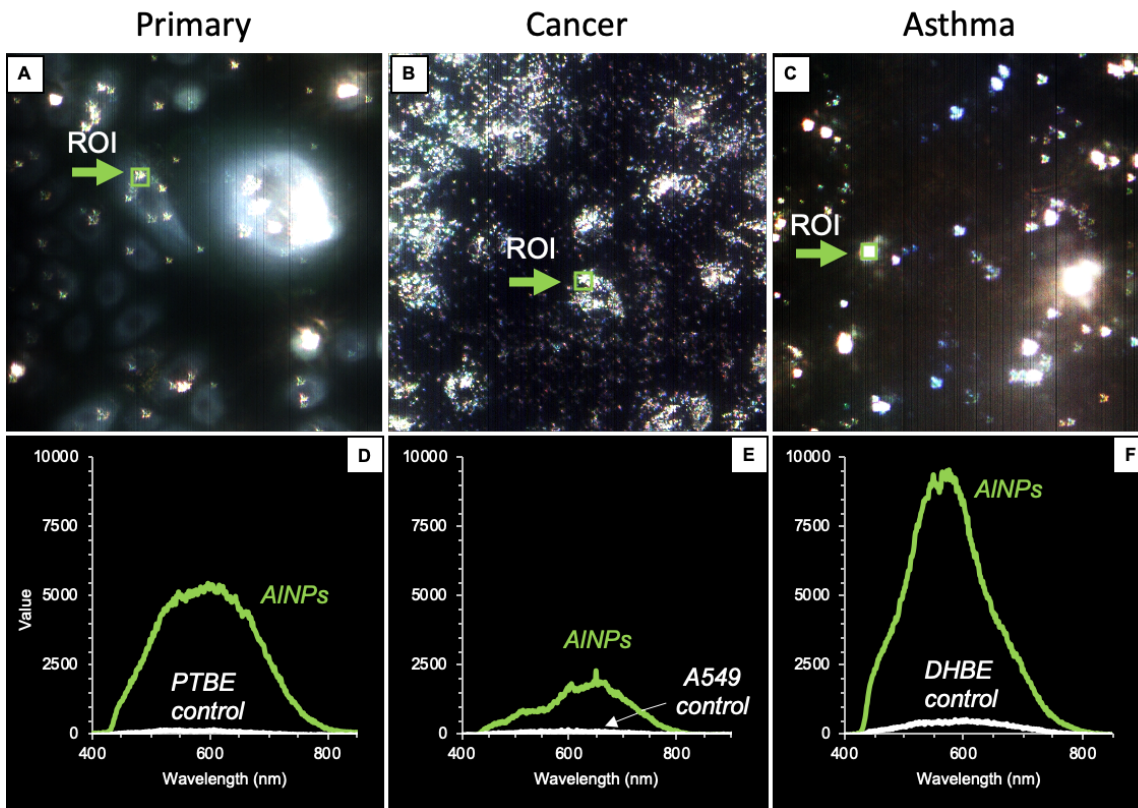


Figure 3.3. Confirmation of aluminum nanoparticle intracellular internalization. Enhanced Dark-field microscopy was used to determine a region of interest (ROI) in all three cell lines (A-C). Hyperspectral imaging is presented (D-F) as spectra from aluminum nanoparticles exposed to the cells. From this data we can confirm the uptake of aluminum into the cells and be able to understand its phase and quantity. Aluminum in primary and asthma cells seem to be a mixture of discrete and agglomerated particles, at 520 and 720 nm respectively. There is a gaussian-like distribution between the wavelengths indicating that there are multiple forms. Aluminum in the cancer cells contains more agglomerated particle forms due to the right shoulder.

mitochondria were significantly larger than primary cell mitochondria). Data was corroborated through the Brown-Forsythe ANOVA test. The shape of mitochondria was not significantly different (P value of 0.2023), but the maximum diameter was highly significantly different among the three cell types. This indicates that exposure to aluminum nanoparticles caused mitochondria to regulate into different sized ovals. This could be an indicator of the energy demand of the cell when stressed by an exogenous

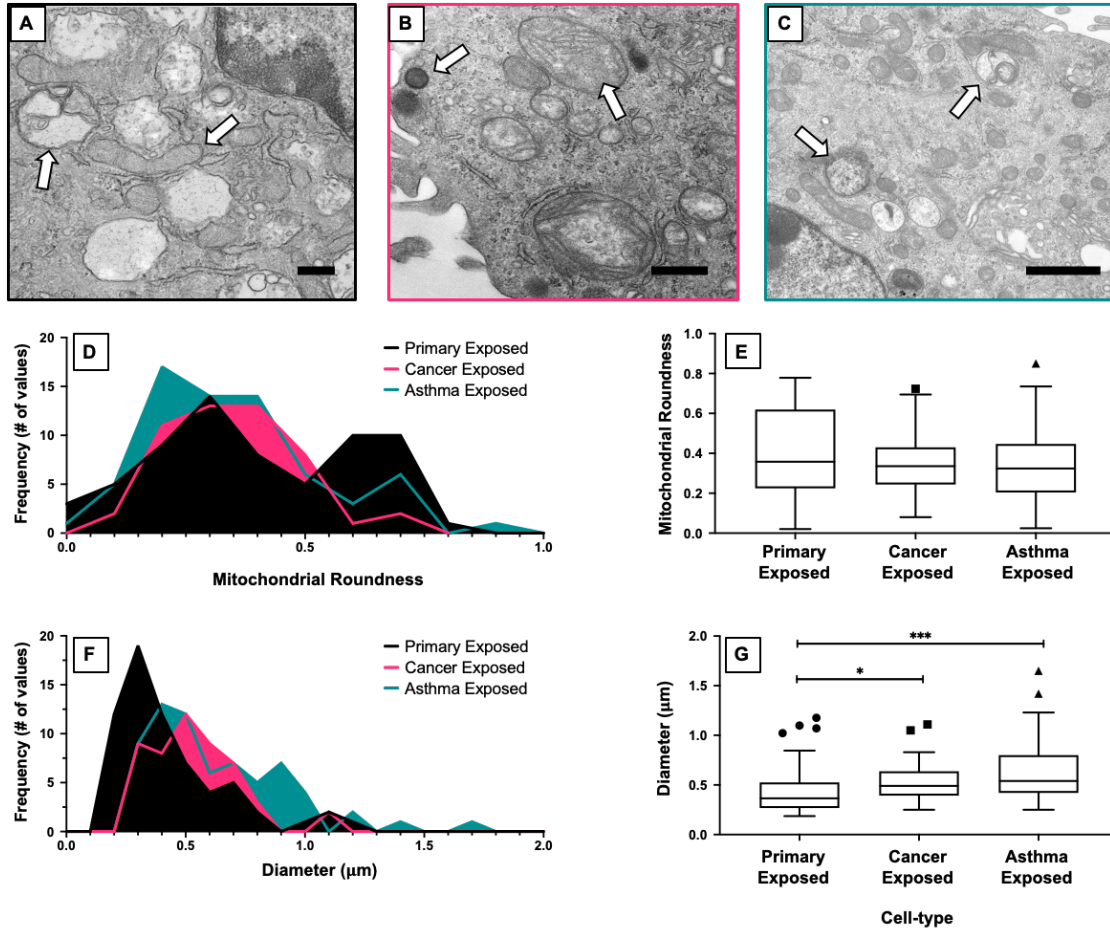


Figure 3.4. Morphological changes in mitochondria among aluminum nanoparticle treated cell-types. TEM micrographs visualizing morphology of mitochondria after exposure to aluminum nanoparticle are shown for (A) primary, (B) cancer, and (C) asthma cell-types. The arrows in each image point to characteristic changes in each cell. Primary cells experience an increase in membrane bound vesicles and elongated mitochondria. Cancer cells have decreased cristae integrity and the presence of lipid bodies. Asthma cells have an increase in membrane bound vesicles and decrease in the size of mitochondria. Mitochondrial roundness is displayed through histograms (D) and corresponding boxplot (E). Compared to the primary cells, mitochondria in each cell-type cluster around the same shape with the primary cells having an increase in elongated mitochondria. Mitochondrial length is also displayed as a histogram (F) and boxplot (G). Compared to the primary cell-type, mitochondria in cancer cells have a slightly longer diameter and mitochondria in asthma cells have a longer diameter than the cancer cell-type. \* $P \leq 0.05$ ; \*\*\* $P \leq 0.001$  versus control (Primary cell-type). The symbols above the box plots (i.e. circles, squares, and triangles) represent outliers as defined by the Tukey method. Scale bar = 500nm.

material as it relates to disease state. All values, SEM, and P values are shown in Table 3.1.

There is evidence that changes in mitochondria shape and size over time generally translates to changes in changes in bioenergetic activity (Yu, Wang, and Yoon 2015). Shape changes generally correspond to changes in ROS levels and altered energy production (Yu, Robotham, and Yoon 2006). Alterations in mitochondrial morphology results in decreased cellular metabolism which accelerates aging, apoptosis, and autophagy (Karbowski and Youle 2003; Sastre et al. 2000). Therefore, if exposure to aluminum nanoparticles change mitochondria shape, then exposure to AINPs can induce mitophagy, decrease ATP production, and decrease metabolism.

*Mitochondria in primary, cancer, and asthma cells respond differently to aluminum nanoparticle exposure.* The mitochondrial roundness and diameter of mitochondria before and after exposure to AINPs in each cell type is summarized in Figure 3.5. The boxplots in Figure 3.5C tabulate the data shown in Figure 3.5A. Mitochondria in the primary and cancer cell-types experienced a 14.89% and 26.24% increase in elongation of mitochondria, respectively, while mitochondria in the asthma cell-type experienced a 15.90% shift towards more circular shaped mitochondria. The change in average mitochondrial roundness within the cancer cells was significant (P value of 0.0070) as calculated via Welch's t test.

The boxplots in Figure 3.5D tabulate the data shown in Figure 3.5B. After exposure, the diameter of mitochondria within each cell-type decreased. Mitochondria within the primary cell-type decreased by 10.46%; mitochondria within the cancer cells decreased by 22.19%; and mitochondria within the asthma cells decreased by 60.39%.

The decrease in the average length of the mitochondria diameter in the cancer and asthma cell-types were found to be highly significant (P value of 0.0005 and  $< 0.0001$ , respectively) as seen in the Welch's t test. Lastly, primary cells did not incur mitochondrial changes in the average size or shape, while the other two cell-types did. All roundness ratios, diameters, SEM, and P values are shown in Table 3.2.

Mitochondria within primary cells seem strictly regulated to a specific morphology while mitochondria in other cell-types are more fluid. Specifically, the decreased size of mitochondria in the cancer and asthma cell-types (due to increased fission) is associated with mitochondrial dysfunction (Jheng et al. 2012). The increased fragmentation of mitochondria (i.e. fission) is likely due to AINP exposure and subsequent increased in ROS. Other studies have found that increased ROS is implicated in fragmenting mitochondria (Wu et al. 2011).

*Exposure to aluminum nanoparticles triggers mitochondria and lysosome interactions.* Fluorescent images of primary, cancer, and asthma cells before and after exposure to AINPs were captured in an effort to compare the overlap of the fluorescently tagged mitochondria and lysosomes. Figure 3.6 shows the images and the associated scatterplot and overlap coefficient values ( $M_1$  and  $M_2$ ). The overlap, or colocalization, of the red dye (MitoTracker Red CM-H2Xros) and the green dye (lysosomal associated membrane protein 1 (LAMP1)) were designed to examine the interaction of mitochondria and lysosomes because the close proximity between and encapsulation of mitochondria within lysosomes is a crucial step in mitophagy, i.e. the mitochondrial degradation pathway. Colocalization analysis measures the spatial overlap of two dyes of interest. The bright gold color in the images represents the areas in the cell where the green

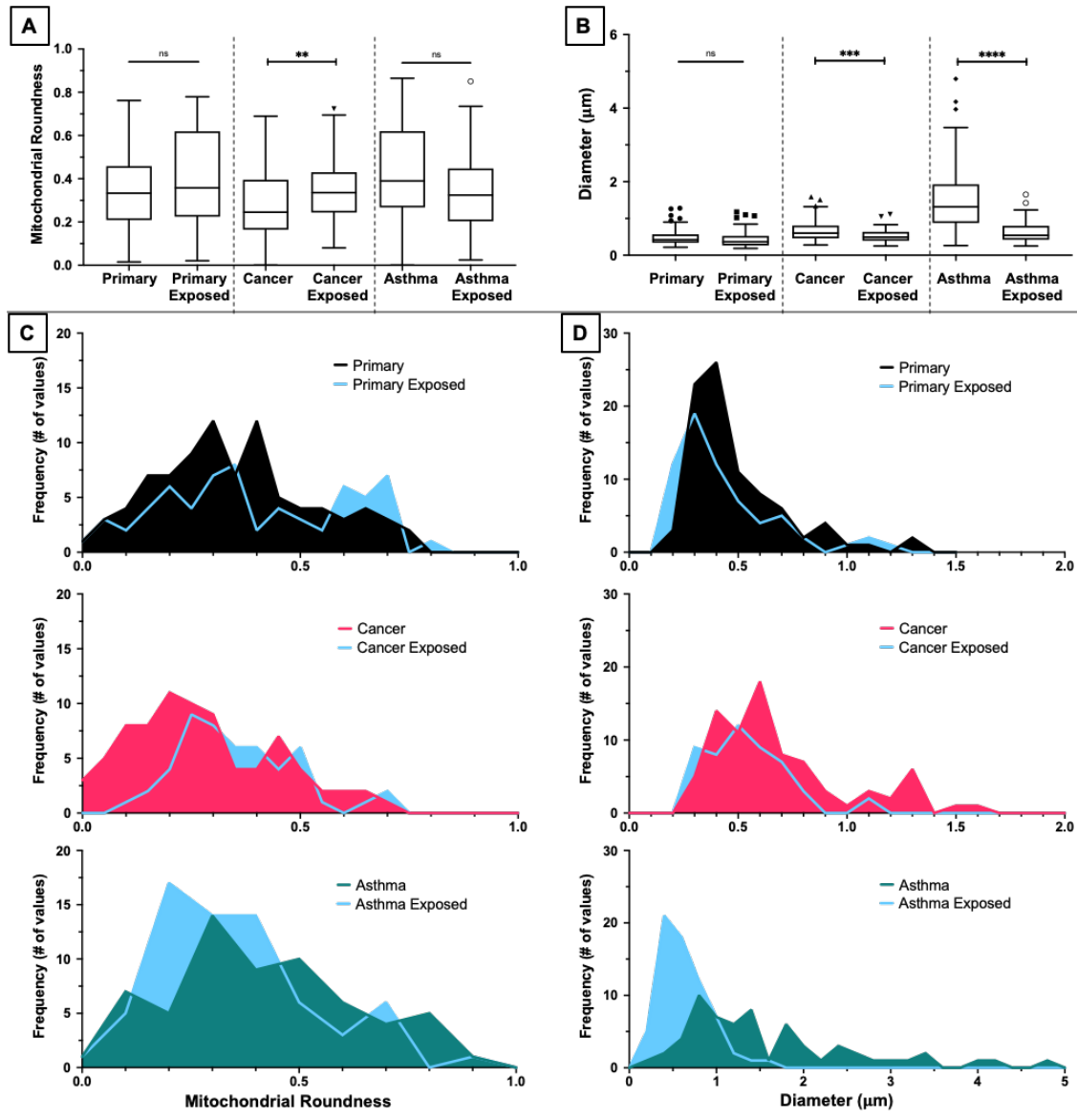


Figure 3.5. Cross comparisons within each cell-type before and after aluminum nanoparticle exposure. Comparisons between the mitochondrial roundness of each cell-type is shown as a box plot (A) and histograms (C). The primary and cancer cells both experienced a shift towards slightly more elongated mitochondria compared to their baseline while the asthma cells experienced a shift towards more circular mitochondria. Comparisons between the length of mitochondria in each cell-type is shown as a box plot (B) and histograms (D). In general, each cell type experienced an overall decrease in the length of their mitochondria with the cancer and asthma cells experiencing the largest decreases.  $**P \leq 0.01$ ;  $***P \leq 0.001$ ;  $****P \leq 0.0001$  versus control (Primary cell-type). The symbols above the box plots (i.e. circles, squares, and triangles) represent outliers as defined by the Tukey method.

Table 3.2. Statistical analysis of mitochondrial size and shape before versus after aluminum nanoparticle exposure among different cell-types.

Measurand	Figure	Parameter	Cell-Type	Exposure Group		Significance	<i>p</i> -value
				Unexposed (SEM)	Exposed (SEM)		
Mitochondria roundness	3.5A	Welch's t test	Primary	0.3488 (0.0192)	0.4008 (0.0261)	ns	0.1117
			Cancer	0.2792 (0.0185)	0.3525 (0.0193)	**	0.0070
			Asthma	0.4166 (0.0280)	0.3504 (0.0225)	ns	0.0673
Mitochondria diameter	3.5B	Welch's t test	Primary	0.4873 (0.0237)	0.4363 (0.0287)	ns	0.1733
			Cancer	0.6843 (0.0339)	0.5325 (0.0261)	***	0.0005
			Asthma	1.5923 (0.1242)	0.6307 (0.0352)	****	<0.0001
Colocalization	3.6B	Tukey's honestly significant difference test	Primary (M <sub>1</sub> )	0.0253 (0.0080)	0.3900 (0.1069)	****	<0.0001
			Primary (M <sub>2</sub> )	0.0200 (0.0068)	0.3170 (0.0997)	####	<0.0001
			Cancer (M <sub>1</sub> )	0.0200 (0.0094)	0.0900 (0.0317)	ns	0.8587
			Cancer (M <sub>2</sub> )	0.0064 (0.0034)	0.0582 (0.0249)	ns	0.9571
			Asthma (M <sub>1</sub> )	0.1014 (0.0522)	0.3627 (0.0337)	***	0.005
			Asthma (M <sub>2</sub> )	0.0750 (0.0407)	0.2155 (0.0265)	ns	0.1970

(lysosomes) and red (mitochondria) dye colocalize in the same location. M values are denoted in Figure 3.6B where the open green circle (M<sub>1</sub>) represents the lysosomal dye and the closed red circle (M<sub>2</sub>) represents the mitochondrial dye.

An ordinary two-way ANOVA showed that there is a highly significant interaction between cell types with a P value of <0.0001, which indicates that the cell-type determines the degree of colocalization in the two selected dyes. This interaction

was followed by a Tukey's honestly significant difference (HSD) test to investigate statistical significance between means of the same cell-type before and after exposure to aluminum nanoparticles. The colocalization of both  $M_1$  and  $M_2$  in primary cells are highly significant as each had a P value of  $<0.0001$ . There was no significant difference in colocalization in the cancer cell lines. Asthma cells incurred an increase in  $M_1$  and  $M_2$ , however only the change in  $M_1$  (lysosome) was significant with a P value of 0.005. The results of the Tukey's HSD test are outlined in Table 3.2.

Upon visual analysis of fluorescent images, it is clear that stress is most apparent in the primary cell population as the overall morphology has changed and there is a large increase in colocalization. Primary and asthma cells are the most affected from exposure to AINPs while the cancer cell population shows no noticeable signs of change in the fluorescent images.

Taken together, exposure to AINPs resulted in (1) all cell-types having oval shaped mitochondria, (2) primary cells with the same mitochondrial diameter before and after exposure, but with a large increase in mitophagy, (3) cancer cells with decreased mitochondrial diameter with no increase in mitophagy, and (4) asthma cells had decreased mitochondrial diameter and also experienced an increase in mitophagy. This data suggests that (A) primary cells readily undergo mitophagy to avoid excess mitochondrial damage, (B) cancer cells mitigate mitochondrial damage by increasing fission but avoid mitophagy, and (C) asthma cells are most susceptible to mitochondrial damage due to the increase in both fission and mitophagy that was seen. The different endpoints that were measured via TEM and fluorescent microscopy highlights the importance of the microscopic analysis conducted for each cell-type.

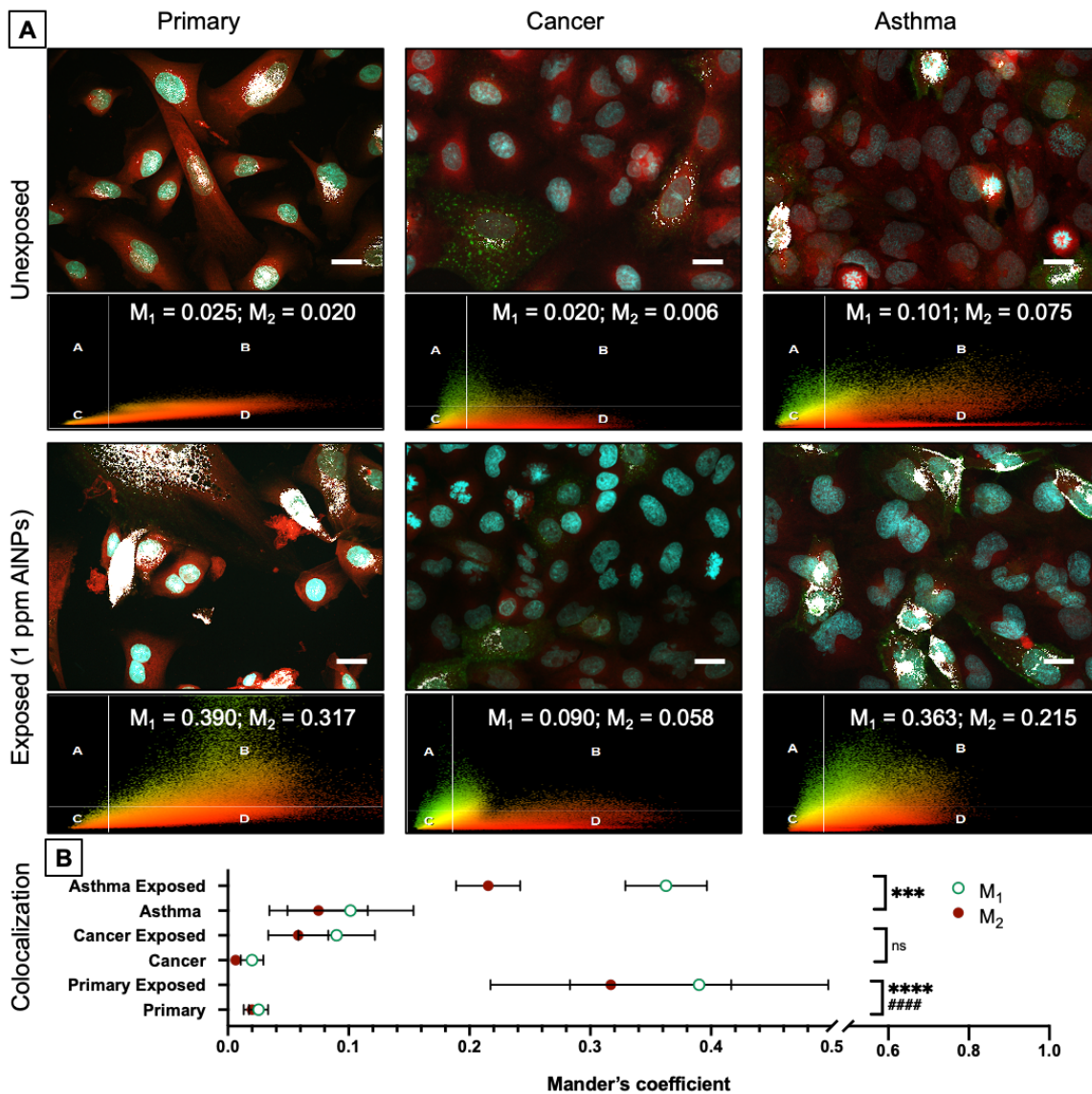


Figure 3.6. Colocalization of lysosomes and mitochondria. Fluorescent images of primary, cancer, and asthma cells before exposure to AINPs were captured to compare the overlap of the mitochondrial and lysosomal dyes. Scatterplot data from colocalization analysis as well as  $M_1$  and  $M_2$  values are also shown (A). The blue dye (Hoechst 33342) stains the nucleus, the red dye (MitoTracker Red CM-H2Xros) accumulates in mitochondria, and the green dye (CellLight Lysosomes-GFP) is transduced into the cell and targets lysosomal associated membrane protein 1 (LAMP1). The bright white color represents the areas in the cell where the green (lysosomes) and red (mitochondria) dye colocalize in the cell above the set threshold. These overlap coefficients before and after exposure are visualized in the graph (B). Before exposure small amount of colocalization occur in each cell-type with the asthma cells having a small amount of colocalization before exposure. After exposure colocalization increases in the primary and asthma cells while cancer cells do not experience a significant increase. Scale bar =  $20\mu\text{m}$ .

## *Conclusion*

We have shown that exposure to aluminum nanoparticles to lung cells with different disease phenotypes can generate mitochondrial specific adverse health effects. This data highlights the importance of probing endpoints beyond general live:dead cell counts. In this study, the interaction between nanoparticles and mitochondria was investigated using microscopy to visualize changes in mitochondria structure.

Mitochondrial structure is directly linked to mitochondrial function and energy production. Adenosine triphosphate (ATP) is the product and is the predominant energy source for the cell. The cristae structure, inclusive of the folds of inner membranes responsible for electron transport, as well as the amount and shape of mitochondria can be measured and used as indicators of metabolic energy efficiency and cellular health. The data presented in this paper demonstrates that the ultrastructural integrity of mitochondria can be visualized by transmission electron microscopy, confocal laser scanning microscopy (CLSM), and hyperspectral imaging; data generated from these techniques can be quantified and used as indicators of effect.

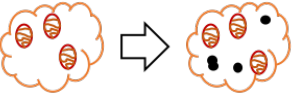
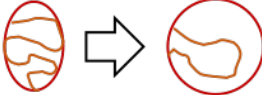
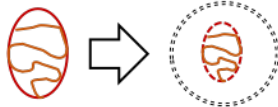
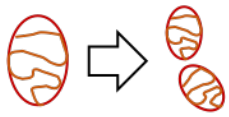
Mitophagy was visualized in the TEM images as membrane bound vesicles. Vesicle formation was corroborated via CLSM imaging and colocalization analysis. Images showed vesicles that range in appearance from small structures void of contents to larger autophagosomes containing degrading cellular material. We interpreted this as aluminum nanoparticle damaged mitochondria shuttled into autophagosomes to fuse with lysosomes for degradation. This phenomenon was confirmed via CLSM where stains targeted the overlap of mitochondria and lysosomes; aluminum nanoparticle exposure caused an increase in colocalization of both dyes.

TEM length and width analysis of cells cultured under control growth conditions revealed that primary, cancer, and asthma cells have different mitochondrial morphologies before AINP treatment, but mostly tend to be slightly oval in shape. The primary cells have the highest abundance of oval mitochondria, cancer cells are more circular in nature, and asthma cells range from oval to highly elongated mitochondria. The differences in mitochondrial morphologies can be explained by the differences in disease phenotypes that alter the normal energy demand of the cell (Table 3.3).

Visualization and analysis of cellular ultrastructure by TEM is an unparalleled technique that depicts changes in morphology that would otherwise go unnoticed. Due to the strong link between mitochondrial ATP production efficiency and mitochondrial structure, it is imperative that structural analysis of mitochondria be included in toxicological assessments. Additionally, it is important to include different phenotypes in respiratory health studies as they have increased susceptibility to metabolic dysfunction from exposure to environmental stressors that target and damaging mitochondria (Wei et al. 2016). Mitochondrial damage has a wide range of negative consequences that include reduced bioenergetics and cell death at the cellular level as well as Alzheimer's disease, Parkinson's disease, chronic fatigue, diabetes, and obesity at the organism level (Kowaltowski and Vercesi 1999; Chattopadhyay et al. 2015).

The information gleaned from TEM analysis provide insight into mitochondrial and overall cell health to produce a more complete story of metabolic perturbations after exposure to environmental contaminants for primary detection of mitochondrial damage before the onset of downstream disease states.

Table 3. Physiological consequences of altered mitochondrial properties.

Type of damage assess via TEM	Pictogram	Potential Physiological consequence	References to support claim
Loss of cristae		Impaired cellular metabolism	Cogliati, Sara, Jose A. Enriquez, and Luca Scorrano. "Mitochondrial cristae: where beauty meets functionality." <i>Trends in biochemical sciences</i> 41.3 (2016): 261-273.
Lipid bodies		Obesity; diabetes	Murphy, Denis J., and Jean Vance. "Mechanisms of lipid-body formation." <i>Trends in biochemical sciences</i> 24.3 (1999): 109-115.
Mitochondrial swelling		Impaired energy metabolism	Li, Ruijin, et al. "Mitochondrial damage: an important mechanism of ambient PM2.5 exposure-induced acute heart injury in rats." <i>Journal of hazardous materials</i> 287 (2015): 392-401.
Vacuole formation		Impaired cell function; cell death indicator	Shintani, Takahiro, and Daniel J. Klionsky. "Autophagy in health and disease: a double-edged sword." <i>Science</i> 306.5698 (2004): 990-995.
Increased fission		Huntingtons disease; dysregulation of mitochondrial dynamics	Chan, David C. "Fusion and fission: interlinked processes critical for mitochondrial health." <i>Annual review of genetics</i> 46 (2012): 265-287.

## *Methods*

*Experimental Design.* The approach to this study was to detect and measure changes in mitochondrial structure in three different lung cell-types before versus after exposure to aluminum nanoparticles using transmission electron microscopy (TEM). Specifically, we conducted assessments using primary tracheal bronchial epithelial cells (PTBE), human lung epithelial carcinoma (A549) cells, and asthma diseased human bronchial/tracheal epithelial (DHBE-As) cells. The nanoparticles were characterized for physicochemical properties before exposure. All exposure scenarios were carried out for 24 hours at a concentration of 1 ppm.

*Nanoparticle Physicochemical Characterization.* A stock suspension of aluminum nanoparticles (50 nm particle size; SkySpring Nanomaterials, Inc., Houston, Texas, USA) was generated by mixing the particles in ultrapure water at a concentration of 100 ppm. The resultant nanoparticle suspension was produced and sonicated at 37 kHz for 10 min immediately before exposure to cells.

For dynamic light scattering analyses, the stock suspension was diluted in ultrapure water in a ratio of 1:2 to generate a 50-ppm concentration. The sample was loaded into a zeta cell and analyzed for hydrodynamic size, polydispersity index, and zeta potential over the course of 30 trials using a ZetaSizer (Malvern Pananalytical; Malvern, United Kingdom).

For electron microscopy analysis, approximately 10  $\mu$ L of the stock suspension was placed onto a copper grid with formvar/carbon film 200 nm (Electron Microscopy

Sciences; Hatfield, Pennsylvania, USA). The nanoparticles were air-dried before image analysis on a JEM-1010 TEM (JEOL Inc.; Tokyo, Japan).

*Maintaining Cell Culture.* PTBE cells (PCS-300-010, American Type Culture Collection (ATCC); Manassas, Virginia, USA) were cultured using airway epithelial cell basal medium (ATCC) supplemented as detailed by ATCC. A549 cells (CCL-185, ATCC) and DHBE-As cells (00194911, Lonza; Basel, Switzerland) were cultured using a 1:1 mixture of Dulbecco's Modified Eagle's Medium and Ham's F-12 Nutrient Mixture (DMEM/F12; Gibco, Waltham, Massachusetts, USA) supplemented with 10% fetal bovine serum (FBS; Equitech-Bio, Inc. Kerrville, Texas, USA) and 1% antibiotic cocktail of Penicillin-Streptomycin (MP Biomedical; Solon, Ohio, USA). All cells were cultured at 37°C in an air-jacketed humidified incubator with 5% CO<sub>2</sub>.

*Cell Preparation for TEM Image Analyses.* PTBE, A549, and DHBE cells were treated with 1 ppm aluminum nanoparticle suspension for 24 h. The inoculated cell culture media was then removed and the cells were rinsed with phosphate buffered saline (PBS; Gibco) prior to collection. The samples were then collected after incubation by placing trypsin onto the cells for 5 minutes at 37°C and then equal parts media was added to the cells to neutralize the trypsin. The collected cell suspension was then centrifuged at 200 g for 5 min to create a pellet. The supernatant was replaced with a 2.5% glutaraldehyde solution (Electron Microscopy Sciences; Hatfield, Pennsylvania, USA) in a pH 7.2 adjusted 0.1 M sodium cacodylate buffer (Electron Microscopy Sciences) and cells were fixed for 30 min. The glutaraldehyde solution was removed and the pellet was washed with cacodylate buffer three times for 10 min each wash.

The cells were then subjected to secondary fixation for 30 min. Fixation was performed with a solution of 1% osmium tetroxide, 0.1 M cacodylate buffer, 3mM calcium chloride, and 0.8% potassium ferrocyanide (Electron Microscopy Sciences). The solution was removed and the cells were washed with cacodylate buffer three times for 10 min each. Post-fixation staining was then carried out in 1% uranyl acetate (Electron Microscopy Sciences) for 30 min after washing with cacodylate buffer. The samples were washed and dehydrated in increasing concentrations of acetone. This dehydration series consisted of two incubations in 50% acetone in de-ionized water for 10 min, two incubations in 70% acetone in de-ionized water for 10 min, two incubations in 90% acetone in de-ionized water for 15 min, and two incubations in 100% acetone for 15 min.

An Embed 812 epoxy resin was then prepared using Embed 812, dodecenylsuccinic anhydride (DDSA), methyl nadic anhydride (MNA), and benzyldimethylamine (BDMA) (Electron Microscopy Sciences) as the accelerant. The samples were then infiltrated with increasing concentrations (1:2, 1:1, 2:1) of the Embed 812 resin and acetone. The samples were then placed in 100 % Embed 812 resin and pelleted in preparation of polymerization (incubation in 60°C oven for 48 h). Following polymerization, the blocks were trimmed, sectioned, and placed on copper mesh grids. Post-staining was performed with lead citrate (Electron Microscopy Sciences) for 5 min, and 1% uranyl acetate for 15 min. The grids were then imaged with a TEM (JEM-1010; JEOL Inc., Tokyo, Japan)

*Hyperspectral Imaging.* All cells types were seeded and incubated into one of 4 wells of a chamber slide (Lab-Tek II, Rochester, New York) for 24 h to allow adhesion and acclimation. Cells were treated with 1 ppm aluminum nanoparticle suspension for 24

h. The cells were fixed and permeabilized as described in the Image-it Fix-Perm kit (Molecular Probes, Eugene, Oregon). Each well was then washed with PBS solution three more times and fixed with two drops of ProLong Diamond Anti-fade Mountant (Molecular Probes). A glass cover slip was then carefully placed on the slide and set for 24 h. Images of the cells were first taken using hyperspectral imaging (CytoViva Inc., Auburn, Alabama) with the accompanying ENVI software (Advanced Scientific Camera Control Version 1.0).

*Cell Preparation for Confocal Laser Scanning Microscopy.* All cells types were seeded and incubated into a 4 well chamber slide (Lab-Tek II, Rochester, New York) for 24 h to allow adhesion and acclimation. Cells were treated with 1 ppm aluminum nanoparticle suspension for 24 h. At the same time the cells were incubated with 30 particles per cell of Lysosomes-GFP (molecular probes) reagent (12 uL). The cells were then washed, fixed, and permeabilized as described in the Image-it Fix-Perm kit (Molecular Probes, Eugene, Oregon). Staining of the nucleus and mitochondria was then carried out by adding MitoTracker Red CM-H2XRos and NucBlue Live Cell Stain Ready Probes reagent (Molecular Probes) for 15 minutes at room temperature. Each well was then washed with PBS solution three more times and fixed with two drops of ProLong Diamond Anti-fade Mountant (Molecular Probes). A glass cover slip was then carefully placed on the slide and set for 24 h. Each of the steps were conducted away from harsh light to preserve the fluorescent dyes. Image were taken on an Olympus Confocal Laser Scanning Microscope FV-3000 (Olympus America Inc., Center Valley, Pennsylvania, USA)

*Post Imaging Analysis.* The length and width of mitochondria were measured using the Olympus CellSens Dimension software (Olympus America Inc., Version 2.2). Before analysis, mitochondria were numbered in each picture to maintain consistent cataloging. Length and width of each mitochondria was measured using the polyline tool in the Olympus CellSens software. The data collected from the CellSens software data retrieval tool was exported for subsequent analyses. Colocalization of lysosomes and mitochondria was also carried out using the CellSens software colocalization tool. Specifically, the maximum Z projection image was obtained through the software and regions of interest were created to increase the power of the colocalization function. The three unexposed cell-types were utilized to designate the parameters of the scatterplots and follow up calculation of overlap coefficients  $M_1$  and  $M_2$ .  $M_1$  represents the contribution of the green fluorescence (lysosome) to the colocalized area while  $M_2$  represents the red fluorescence (mitochondria) to the colocalized area. Values range from 0 to 1 and signify the percentage of pixels from one channel that colocalize with the other channel.

To obtain a ratio that represents the “roundness” of mitochondria, the length was divided by the width of a mitochondria and subtracted from one. The absolute value of this number was then used to generate all positive numbers (**Equation 1**). A value of zero represents a perfectly round mitochondria while values approaching one represent different degrees of elongation.

$$R_{Mitochondria} = \left| 1 - \frac{L_{Mitochondria}}{W_{Mitochondria}} \right| \quad [1]$$

Where  $R_{Mitochondria}$  is the value representing the average roundness,  $L_{Mitochondria}$  is the average length, and  $W_{Mitochondria}$  is the average width of each mitochondria within an analyzed cell.

*Data visualization and statistical analysis.* Figure creation, data analysis, and statistical analysis was completed using GraphPad Prism (GraphPad software, Version 8.4.2., San Diego, California, USA). All values are annotated with their standard error of mean (SEM). Statistical analysis for figures 3.1 and 3.3, data sets comparing cancer and asthma cell-types to the primary cell-type as a control group, used Brown-Forsythe one-way analysis of variance (one-way ANOVA) with a 95% confidence interval. Games-Howell's followup test was used to identify group means that are significantly different from the control. To compare the baseline and exposed mitochondrial morphologies within one cell type, an unpaired parametric t test with Welch's correction at the 95% confidence level was used. Statistical significance in both tests are defined as having a p value of less than 0.05. Statistical analysis for Figure 3.6 utilized a two-way ANOVA with Tukey's honestly significant difference (HSD) follow up test to compare unexposed and exposed  $M_1$  and  $M_2$  values. All statistical data is shown in Table 3.1 and 3.2.

## References

- Balbus, J.M., A.D. Maynard, V.L. Colvin, V. Castranova, G.P. Daston, R.A. Denison, K.L. Dreher, P.L. Goering, A.M. Goldberg, K.M. Kulinowski, N.A. Monteiro-Riviere, G. Oberdörster, G.S. Omenn, K.E. Pinkerton, K.S. Ramos, K.M. Rest, J.B. Sass, E.K. Silbergeld, and B.A. Wong. 2007. "Meeting Report: Hazard Assessment for Nanoparticles-Report from an Interdisciplinary Workshop." *Environmental Health Perspectives* 115, no. 11 (Nov): 1654-9. <https://dx.doi.org/10.1289/ehp.10327>.
- Brar, S. K., M. Verma, R. D. Tyagi, and R. Y. Surampalli. 2010. "Engineered Nanoparticles in Wastewater and Wastewater Sludge--Evidence and Impacts." *Waste Manag* 30, no. 3 (Mar): 504-20. <https://dx.doi.org/10.1016/j.wasman.2009.10.012>.
- Brevini, Tiziana AL, Rita Vassena, Chiara Francisci, and Fulvio Gandolfi. 2005. "Role of Adenosine Triphosphate, Active Mitochondria, and Microtubules in the Acquisition of Developmental Competence of Parthenogenetically Activated Pig Oocytes." *Biology of reproduction* 72, no. 5: 1218-1223.
- Chattopadhyay, M., V. K. Khemka, G. Chatterjee, A. Ganguly, S. Mukhopadhyay, and S. Chakrabarti. 2015. "Enhanced Ros Production and Oxidative Damage in Subcutaneous White Adipose Tissue Mitochondria in Obese and Type 2 Diabetes Subjects." *Mol Cell Biochem* 399, no. 1-2 (Jan): 95-103. <https://dx.doi.org/10.1007/s11010-014-2236-7>.
- Chevallet, M, Benoit Gallet, A Fuchs, PH Jouneau, K Um, E Mintz, and I Michaud-Soret. 2016. "Metal Homeostasis Disruption and Mitochondrial Dysfunction in Hepatocytes Exposed to Sub-Toxic Doses of Zinc Oxide Nanoparticles." *Nanoscale* 8, no. 43: 18495-18506.
- Cloonan, S. M., and A. M. Choi. 2016. "Mitochondria in Lung Disease." *J Clin Invest* 126, no. 3 (Mar): 809-20. <https://dx.doi.org/10.1172/JCI81113>.
- Darlington, T. K., A. M. Neigh, M. T. Spencer, O. T. Nguyen, and S. J. Oldenburg. 2009. "Nanoparticle Characteristics Affecting Environmental Fate and Transport through Soil." *Environ Toxicol Chem* 28, no. 6 (Jun): 1191-9. <https://dx.doi.org/10.1897/08-341.1>.
- Dreier, David A, Danielle F Mello, Joel N Meyer, and Christopher J Martyniuk. 2019. "Linking Mitochondrial Dysfunction to Organismal and Population Health in the Context of Environmental Pollutants: Progress and Considerations for Mitochondrial Adverse Outcome Pathways." *Environmental toxicology and chemistry* 38, no. 8: 1625-1634.

- Elsaesser, A., and C. V. Howard. 2012. "Toxicology of Nanoparticles." *Adv Drug Deliv Rev* 64, no. 2 (Feb): 129-37. <https://dx.doi.org/10.1016/j.addr.2011.09.001>.
- Esch, E. W., A. Bahinski, and D. Huh. 2015. "Organs-on-Chips at the Frontiers of Drug Discovery." *Nat Rev Drug Discov* 14, no. 4 (Apr): 248-60. <https://dx.doi.org/10.1038/nrd4539>.
- Ghribi, Othman, David A DeWitt, Michael S Forbes, Mary M Herman, and John Savory. 2001. "Co-Involvement of Mitochondria and Endoplasmic Reticulum in Regulation of Apoptosis: Changes in Cytochrome C, Bcl-2 and Bax in the Hippocampus of Aluminum-Treated Rabbits." *Brain research* 903, no. 1-2: 66-73.
- Huang, Song, Ludovic Wiszniewski, Jean-Paul Derouette, and Samuel Constant. 2009. "In Vitro Organ Culture Models of Asthma." *Drug Discovery Today: Disease Models* 6, no. 4: 137-144.
- Jheng, Huei-Fen, Pei-Jane Tsai, Syue-Maio Guo, Li-Hua Kuo, Cherng-Shyang Chang, Ih-Jen Su, Chuang-Rung Chang, and Yau-Sheng Tsai. 2012. "Mitochondrial Fission Contributes to Mitochondrial Dysfunction and Insulin Resistance in Skeletal Muscle." *Molecular and cellular biology* 32, no. 2: 309-319.
- Karbowski, M, and RJ Youle. 2003. "Dynamics of Mitochondrial Morphology in Healthy Cells and During Apoptosis." *Cell Death & Differentiation* 10, no. 8: 870-880.
- Kim, HJ, DH Jung, IH Jung, JI Cifuentes, KY Rhee, and D Hui. 2012. "Enhancement of Mechanical Properties of Aluminium/Epoxy Composites with Silane Functionalization of Aluminium Powder." *Composites Part B-Engineering* 43, no. 4 (JUN 2012): 1743-1748. <https://dx.doi.org/10.1016/j.compositesb.2011.12.010>.
- Kirkpatrick, CJ, and Ch Mittermayer. 1990. "Theoretical and Practical Aspects of Testing Potential Biomaterialsin Vitro." *Journal of Materials Science: Materials in Medicine* 1, no. 1: 9-13.
- Kowaltowski, A. J., and A. E. Vercesi. 1999. "Mitochondrial Damage Induced by Conditions of Oxidative Stress." *Free Radic Biol Med* 26, no. 3-4 (Feb): 463-71. <https://www.ncbi.nlm.nih.gov/pubmed/9895239>.
- Lujan, H., M. F. Criscitiello, A. S. Hering, and C. M. Sayes. 2019. "Refining in Vitro Toxicity Models: Comparing Baseline Characteristics of Lung Cell Types." *Toxicol Sci* 168, no. 2 (Apr): 302-314. <https://dx.doi.org/10.1093/toxsci/kfz001>.
- Lujan, Henry, and Christie M Sayes. 2017. "Cytotoxicological Pathways Induced after Nanoparticle Exposure: Studies of Oxidative Stress at the 'Nano-Bio' interface." *Toxicology research* 6, no. 5: 580-594.

- Mabalarajan, U., and B. Ghosh. 2013. "Mitochondrial Dysfunction in Metabolic Syndrome and Asthma." *J Allergy (Cairo)* 2013: 340476. <https://dx.doi.org/10.1155/2013/340476>.
- Mirshafa, Atefeh, Mehdi Nazari, Daniel Jahani, and Fatemeh Shaki. 2018. "Size-Dependent Neurotoxicity of Aluminum Oxide Particles: A Comparison between Nano-and Micrometer Size on the Basis of Mitochondrial Oxidative Damage." *Biological trace element research* 183, no. 2: 261-269.
- Mortimer, Monika, Alexander Gogos, Nora Bartolomé, Anne Kahru, Thomas D Bucheli, and Vera I Slaveykova. 2014. "Potential of Hyperspectral Imaging Microscopy for Semi-Quantitative Analysis of Nanoparticle Uptake by Protozoa." *Environmental science & technology* 48, no. 15: 8760-8767.
- Murakami, Keiko, and Masataka Yoshino. 2004. "Aluminum Decreases the Glutathione Regeneration by the Inhibition of NADP-Isocitrate Dehydrogenase in Mitochondria." *Journal of Cellular Biochemistry* 93, no. 6: 1267-1271.
- Niu, PY, Q Niu, QL Zhang, LP Wang, SC He, TC Wu, P Conti, M Di Gioacchino, and P Boscolo. 2005. "Aluminum Impairs Rat Neural Cell Mitochondria in Vitro." *International journal of immunopathology and pharmacology* 18, no. 4: 683-689.
- Patiño, Tania, Jorge Soriano, Leonard Barrios, Elena Ibáñez, and Carme Nogués. 2015. "Surface Modification of Microparticles Causes Differential Uptake Responses in Normal and Tumoral Human Breast Epithelial Cells." *Scientific reports* 5: 11371.
- Rampelt, Heike, Ralf M Zerbes, Martin van der Laan, and Nikolaus Pfanner. 2017. "Role of the Mitochondrial Contact Site and Cristae Organizing System in Membrane Architecture and Dynamics." *Biochimica et Biophysica Acta (BBA)-Molecular Cell Research* 1864, no. 4: 737-746.
- Sastre, Juan, Federico V Pallardó, José García de la Asunción, and José Viña. 2000. "Mitochondria, Oxidative Stress and Aging." *Free radical research* 32, no. 3: 189-198.
- Schousboe, Arne, HM Sickmann, Lasse Kristoffer Bak, I Schousboe, FS Jajo, SAA Faek, and Helle S Waagepetersen. 2011. "Neuron–Glia Interactions in Glutamatergic Neurotransmission: Roles of Oxidative and Glycolytic Adenosine Triphosphate as Energy Source." *Journal of neuroscience research* 89, no. 12: 1926-1934.
- Sharma, P., and K. P. Mishra. 2006. "Aluminum-Induced Maternal and Developmental Toxicity and Oxidative Stress in Rat Brain: Response to Combined Administration of Tiron and Glutathione." *Reprod Toxicol* 21, no. 3 (Apr): 313-21. <https://dx.doi.org/10.1016/j.reprotox.2005.06.004>.

- Stern, Stephan T, Pavan P Adisheshaiah, and Rachael M Crist. 2012. "Autophagy and Lysosomal Dysfunction as Emerging Mechanisms of Nanomaterial Toxicity." *Particle and fibre toxicology* 9, no. 1: 20.
- Twig, Gilad, and Orian S Shirihai. 2011. "The Interplay between Mitochondrial Dynamics and Mitophagy." *Antioxidants & redox signaling* 14, no. 10: 1939-1951.
- Wei, Y., J. J. Zhang, Z. Li, A. Gow, K. F. Chung, M. Hu, Z. Sun, L. Zeng, T. Zhu, G. Jia, X. Li, M. Duarte, and X. Tang. 2016. "Chronic Exposure to Air Pollution Particles Increases the Risk of Obesity and Metabolic Syndrome: Findings from a Natural Experiment in Beijing." *FASEB J* 30, no. 6 (06): 2115-22. <https://dx.doi.org/10.1096/fj.201500142>.
- Wu, Shengnan, Feifan Zhou, Zhenzhen Zhang, and Da Xing. 2011. "Mitochondrial Oxidative Stress Causes Mitochondrial Fragmentation Via Differential Modulation of Mitochondrial Fission–Fusion Proteins." *The FEBS journal* 278, no. 6: 941-954.
- Youle, Richard J, and Derek P Narendra. 2011. "Mechanisms of Mitophagy." *Nature reviews Molecular cell biology* 12, no. 1: 9-14.
- Yu, Tianzheng, James L Robotham, and Yisang Yoon. 2006. "Increased Production of Reactive Oxygen Species in Hyperglycemic Conditions Requires Dynamic Change of Mitochondrial Morphology." *Proceedings of the National Academy of Sciences* 103, no. 8: 2653-2658.
- Yu, Tianzheng, Li Wang, and Yisang Yoon. 2015. "Morphological Control of Mitochondrial Bioenergetics." *Frontiers in bioscience (Landmark edition)* 20: 229.
- Zhang, Ying, Chenguang Yu, Guanyi Huang, Changli Wang, and Longping Wen. 2010. "Nano Rare-Earth Oxides Induced Size-Dependent Vacuolization: An Independent Pathway from Autophagy." *International journal of nanomedicine* 5: 601.
- Zick, Michael, Regina Rabl, and Andreas S Reichert. 2009. "Cristae Formation—Linking Ultrastructure and Function of Mitochondria." *Biochimica et Biophysica Acta (BBA)-Molecular Cell Research* 1793, no. 1: 5-19.
- Zucker, Robert M, Jayna Ortenzio, Laura L Degn, Jeremy M Lerner, and William K Boyes. 2019. "Biophysical Comparison of Four Silver Nanoparticles Coatings Using Microscopy, Hyperspectral Imaging and Flow Cytometry." *PloS one* 14, no. 7: e0219078.

## CHAPTER FOUR

### General Discussion and Conclusions

In the field of *in vitro* nanotoxicology an increase in reactive oxygen species due to nanomaterial exposure is the most cited cause for changes in cellular health. Increases in reactive oxygen species most commonly trigger toxicological pathways of inflammation, antioxidant response, and cell cycle arrest. Furthermore, nanomaterial exposure has the potential to alter mitochondrial structure and function as a result of their uptake and toxicity within cell cultures. Once inside the cell, the increased levels of reactive oxygen species are particularly detrimental to the mitochondria. These negative effects can be mitigated by identifying and evaluating potential adverse health effects at the molecular and cellular level. Mapping pathways of toxicity allows scientists to make more informed decisions when measuring and assessing hazards, recommending protective measures, setting acceptable exposure levels, developing guidelines, policies, regulations, and communicating health and safety educational and training materials to workers and consumers of nano-enabled products.

While limiting the unintended and accidental exposures to hazardous agents should be the ultimate goal, interpreting the results of nanotoxicological experiments can be critical in protecting both healthy and susceptible human (and animal) populations. To this end, studying the cytotoxicological pathways induced after nanoparticle exposures aids in the development of nanomaterial-specific adverse outcome pathways (AOPs) by linking molecular initiating events (MIEs) to adverse outcome (AOs) health effects.

Pathway analysis is relative to nano-enabled product development by establishing a framework for optimizing product efficiency, ensuring safe manufacturing practices, promoting the product's intentional use, and avoiding environmental health hazards. Understanding perturbations in gene, protein, and mitochondrial health endpoints aids in multiple aspects of environmental and human health specifically for generating AOPs, however these datasets are hindered by the varied use of cell-types without background characterization used in nanotoxicological studies.

In our study, baseline comparisons between seven different cell types from the upper and lower airway with either primary, transformed, cancer, or asthma phenotype uncovered key biochemical and morphological differences that impact current and future nanotoxicology testing. The differences in the gene and protein expression of inflammatory markers (IL-6) and antioxidant capacity (GSR) in cells from the upper and lower airway are attributed to the types of in vitro exposure. Upper airways cells are designed to interact with and mitigate stress from everything that is inhaled, which was seen in the data through the low expression of inflammatory marker IL-6. Lower airways cells are only exposed to small size scale particles such as ultrafine and nanosized particles. The difference in the amount and frequency of exposure may help explain the sensitivity to ROS that was seen in the constant expression of IL-6, GSR, and oxidative stress that was seen in all lower airway cell-types. The modeling of inhalation, deposition and clearance of respirable particles into the lung is still a new and developing field that may further explain the inherent differences in upper versus lower airway cells (Hvelplund et al. 2020).

Cell cycle regulation is also attributed to differences in toxicological outcomes. Specifically, mutations in the cell cycle genes *TP53* and *CDKN1A* potentially inhibit cell death mechanisms in cancer cells. For example, A549 upper airway cancer cells are wild-type *TP53* while Calu-3 lower airway cancer cells are mutated in *TP53*. Additionally, SV40 large T antigen induces immortalization by binding to the protein produced by the *TP53* gene to delay senescence (Bryan and Redder 1994). Previous studies mention that different *TP53* mutations alter the sensitivity of the cell to p53 specific drugs. This may inhibit differentiation or reduce cellular adhesion and tight junction formation (Maj et al. 2019; Zhang, Yan, and Chen 2011). *TP53* and *CDKN1A* function must be considered before use, particularly when used in co-culture studies that rely on cellular differentiation and tight junction formation to recapitulate the air-liquid interface of the epithelial lining in the lung.

Exposure to aerosolized nanoparticles through inhalation can generate differential adverse effects depending on the elemental composition and surface chemistry of the particle. Furthermore, the health (or disease state) of the affected cells plays a critical role in the resultant toxicities. For this reason, it is important to probe beyond general cytotoxicity and investigate complex interactions at the nano-bio interface. For example, the interactions between the nanoparticle and the mitochondria within cells of varying phenotypes were investigated to determine the extent the phenotype altered mito-toxic endpoints.

The strong link between mitochondrial ATP production efficiency, mitochondrial morphology, and disease state makes the mitochondria a valuable endpoint in determining how disease state affects the cells response to stress. It is important to

include different disease states in toxicological studies as they have increased susceptibility to metabolic dysfunction from exposure to environmental stressors (i.e. aluminum nanoparticles) that target and damaging the mitochondria.

Healthy cells maintain oval to circular shaped mitochondria while diseased cells have increased fission which are exacerbated after environmental pollutant exposure. Our studies showed that the different cell-types are not similar in their mitochondrial morphology, which indicates that they have differential metabolic activity. Furthermore, responses to aluminum nanoparticle exposure varied among the different cell types due to the different amount of aluminum that was internalized in the cell. Mitochondria within primary, cancer, and asthma cells each responded differently to the exposure which resulted in varying degrees of changes in shape and size of the mitochondria. Additionally, mitophagy occurred at varying degrees in the different cell-types.

The information gleaned from analysis of TEM micrographs and fluorescent images provide insight into mitochondrial and overall cell health to produce a more complete story of metabolic perturbations after exposure to environmental contaminants for primary detection of mitochondrial damage before the onset of downstream disease states. Future research projects will investigate how nanoparticles affect mitochondrial function. Specifically, gene, protein, and extracellular flux analysis will be used to map changes in mitochondrial activity. This future research effort will work to create a mitochondrial structure function relationship that can be used as a guide for human health metabolic risk assessments after nanoparticle exposure.

## *Future Direction*

### *Linking Mitochondrial Health to Organ-Level Effects*

Mitochondrial dysregulation (i.e. alteration of normal mitochondrial function) has severe implications in the reduction of metabolic health, physical performance, and cognitive function. Mitochondrial dysregulation is rapidly gaining interest because of the wide array of exogenous stressors associated with adverse health outcomes. These stressors include chemical fumes (diesel exhaust and jet fuel additives), aerosols (particulate matter and nanoparticles), and environmental stressors (heat or low oxygen). Currently, researchers are probing mitochondria-specific endpoints to determine how changes in the function impact overall human health. Changes in both mitochondrial structure and function induced by exogenous stressors influence cytokine signaling and the onset of metabolic diseases that may reduce human health and performance.

Future research efforts are aimed at creating a structure-function relationship in both healthy and stressed cell-based models. The purpose of this research is to define the differences and similarities of normal mitochondria function against abnormal function (induced after exposure to chemical and particle stressors). This will be accomplished by measuring changes in mitochondrial ultrastructure, cytokine signaling, oxygen consumption, and mitochondrial DNA integrity as depicted in Figure 4.1. Metabolic health is influenced by both the structure and function of the mitochondria, thus assessing normal function with electron microscopy, oxygen consumption, and genomic engineering will capture significant and minute mitochondria changes. The techniques that will be used along with their rationales are listed in Table 4.1.

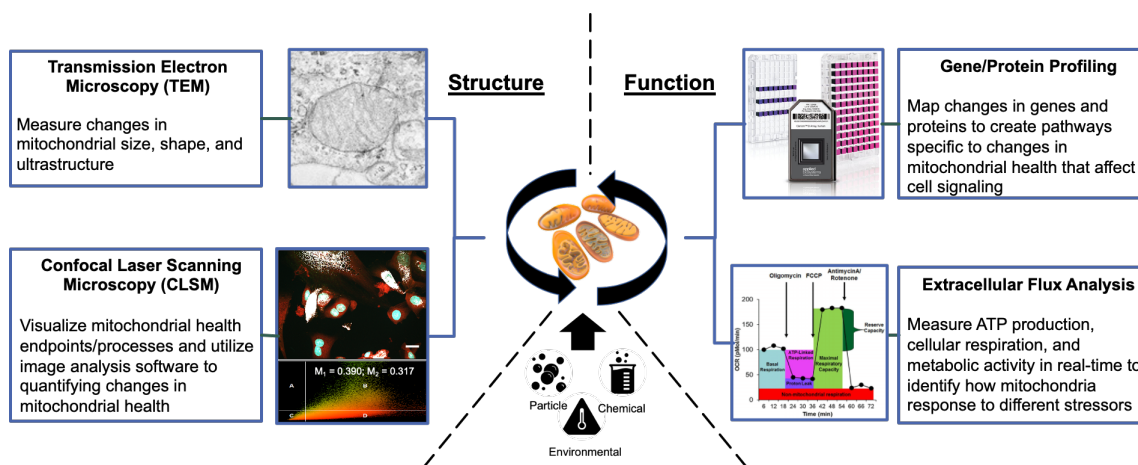


Figure 4.1. Building a mitochondrial structure function relationship. Mitochondrial health is measured before and after exposure to stressors (particle, chemical, or environmental) to build a mitochondrial structure-function relationship. Mitochondrial structure will continue to be examined via transmission electron microscopy and confocal laser scanning microscopy. Mitochondrial function will be probed using biochemical assays to map changes in mitochondrial specific gene/protein expression and extracellular flux analysis to measure the efficiency of the electron transport chain.

Table 4.1. Techniques used to characterize indices of metabolic health.

Technique	Endpoint	Information Gained & Rationale
Cryo-transmission electron microscopy (Cryo-TEM)	Mitochondrial ultrastructure	Size, structure, and crystallinity; Cryo-TEM is the most advanced method to preserve and image cellular ultrastructure
Confocal laser scanning microscopy (CLSM)	Oxidative stress, membrane polarity, DNA damage,	The presence of different mitochondrial damage endpoints and real time processes can be measured
Extracellular Flux analysis	Oxygen consumption	Electron transport chain efficiency and ATP production; The technique measures overall metabolic health
Polymerase Chain Reaction (PCR) – Clariom D	Gene array specific to mitochondrial health endpoints	Detection and quantification of gene and cytokine signaling specific to the mitochondria
Enzyme-Linked Immunosorbent assay (ELISA)	Protein analysis of selected genes	Protein quantification; Gene of interest will be selected and tested for protein production

Mitochondrial gene and protein profiling will create hypothesized cytokine signaling pathways perturbed after mitochondrial damage. The extent to which cytokine signaling affects overall mitochondrial health will then be investigated. While the mitochondria are responsible for the energy production within the cell, changes in mitochondrial health also affects downstream cytokine signaling pathways (Cadenas 2004). Understanding post exposure changes in metabolic health will require an investigation into how different stressors alter cytokine signaling in cell cultures of varying complexity (i.e. monoculture, co-culture, or organoid/tissue cultures). The data collected from PCR and ELISA assays will be used to design mechanistic pathways outlining common adverse outcomes allowing for mitigation strategies to be developed to protect metabolic health.

The resultant hypothesized mechanisms of mitochondrial damage will be validated via CRISPR/Cas9 genomic engineering as shown in figure 4.2. The most commonly cited mechanisms of toxic action after exposure to nanoparticles is oxidative stress. Oxidative stress involves a plethora of genes and proteins and the exact mechanism(s) are not clearly defined. Precise mechanisms of toxicity and oxidative stress in the mitochondria can be revealed using an emerging laboratory technique referred to as CRISPR (clustered regularly interspaced short palindromic repeats). The advent of CRISPR/Cas9 gene editing enables functional and toxicological approaches to understand the relationship between changes in mitochondrial health and cellular signaling. CRISPR based approaches to gene and protein analysis will more robustly decipher molecular toxicological mechanisms. (Shen et al. 2015). For example, previous studies have been able to better understand the role of Nrf2 in preserving mitochondrial

health through CRISPR technologies (O'Mealey, Berry, and Plafker 2017).

CRISPR/Cas9-derived functional toxicity endpoints enable more sophisticated multi-variant analyses that have the potential to definitively link exposure to adverse outcome endpoints through specific mechanisms of toxic action (Lujan et al. 2020). While Nrf2 is a potential target for knock out, other genes of interest will be selected from the initial PCR analysis.

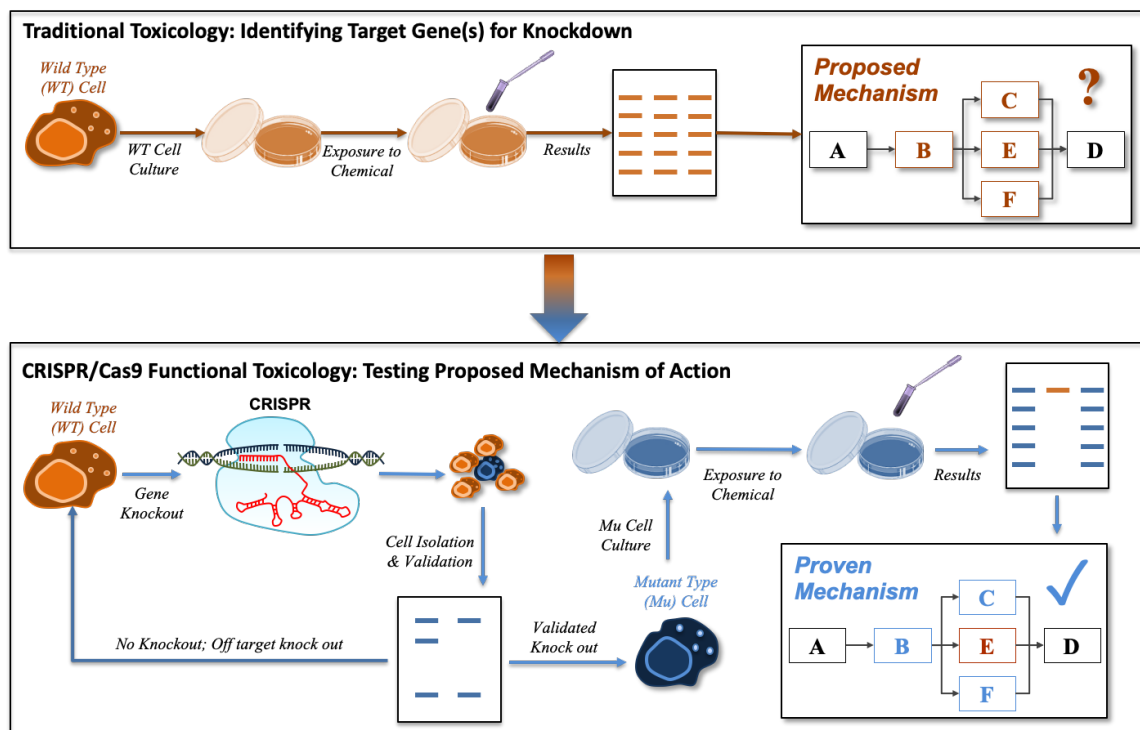


Figure 4.2. Experimental design for mechanistic pathway analysis. Derived from the experimental designs of papers that utilized a general mechanistic design to streamline CRISPR/Cas9 for toxicology studies. Briefly, wild-type cells undergo gene modifications via CRISPR; the gene knock-out is then validated after cell isolation, exposed to a toxicant, and then analyzed for changes in a determined endpoint compared with the control studies using wild-type cells. Next-generation sequencing, gel electrophoresis, PCR, or chemical selection must be used to confirm knock-out prior to exposure studies. Knock-out cells must be isolated from wild-type cells via limiting dilution and/or cell sorting (Lujan, et al. 2020).

Mitochondria within human cells are in a constant flux and change along a spectrum of different morphologies in response to physical and environmental stressors (Van der Blik, Shen, and Kawajiri 2013; Youle and Van Der Blik 2012). This change in morphology is directly related to energy production as adenosine triphosphate (ATP). ATP is the main energy unit of the cell and is produced along the electron transport chain located on the inner membrane of the mitochondria. When there are changes in ATP demand, the mitochondria adapt through changes in their morphology. The process of oxidative phosphorylation (OXPHOS) is shown in Figure 4.3 along with endpoints related to mitochondrial health.

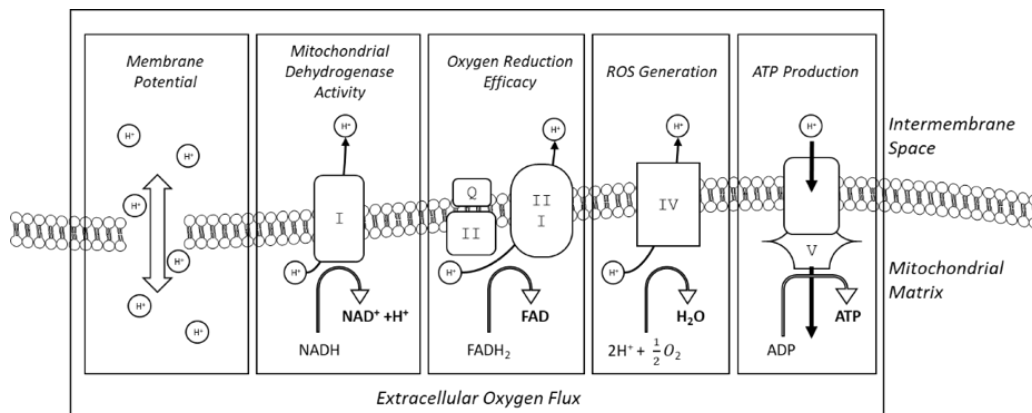


Figure 4.3. Overview of the electron transport chain and processes that can be measured. Measuring the membrane potential of the mitochondria is important because the integrity of the membrane affects each step of the ETC. Each complex of the ETC can be probed individually by different assays or evaluated together through extracellular flux analysis.

Extracellular flux analysis is a technique which can probe each compartment of the electron transport chain (ETC) in one assay. This technique gives information regarding mitochondrial respiration. Data from this technique can help aid in understanding the relationship between the structure and function of the mitochondria to elucidate how different stressors alter mitochondrial health, and by extension the overall

cellular health. Multiple techniques can be employed with increasing levels of biomolecular granularity (i.e. from biomolecular probes to single cell analysis to cell population health) to monitor these changes. Preliminary data has shown that aluminum nanoparticle alter the efficiency of the electron transport chain in A549 cancer lung cells. Interestingly, mitochondrial activity is seen to increase after exposure to the aluminum nanoparticles. Key indicators of mitochondrial activity (max respiration, spare capacity, and ATP production) are elevated at each concentration of aluminum nanoparticle exposure. This mirrors the results seen in the morphological assessment of mitochondria after exposure to 1 ppm of aluminum nanoparticles, which showed minimal changes to mitochondrial size or shape and an increase in lipid body formation. In the literature, it is widely seen that lipid body formation is a key indicator of cancer cell stress response and altered metabolism.

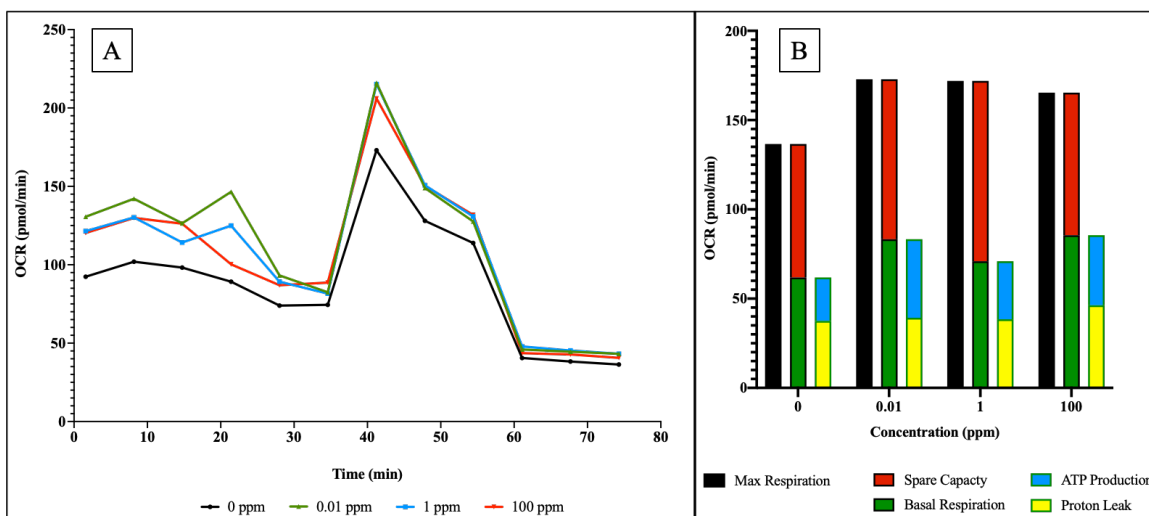


Figure 4.4. Extracellular flux analysis of A549 lung cancer cells after exposure to aluminum nanoparticles. Oxygen consumptions rates versus time (A) shows the differential states of metabolic activity of A549 lung cancer cells to increasing concentrations of aluminum nanoparticles. Analysis of the oxygen consumption rates over time (B) details the max respiration, spare capacity, and ATP production in the different samples. Exposure to aluminum nanoparticles seems to trigger increased mitochondrial activity in this cancer cell-type.

The key to understanding pathogenesis from a physically or mentally healthy state to unhealthy state lies in the health of the mitochondria. The results of current and future research will contribute to creating a framework to translate changes in mitochondrial health indices in response to different stressors to evaluate and prevent stressor induced metabolic decay. Developing the mitochondrial structure function relationship, identifying key cytokine signaling pathways in response to stressors, and building a framework for mitochondrial specific toxicity testing will bridge the gap between mitochondrial health & organ-level effects resulting in a model that will be able to rapidly predict adverse health outcomes from early stage changes in mitochondrial structure and function.

## References

- Bryan, Tracy, and Roger R Redder. 1994. "Sv40-Induced immortalization of Human Cells." *Critical Reviews™ in Oncogenesis* 5, no. 4.
- Cadenas, Enrique. 2004. "Mitochondrial Free Radical Production and Cell Signaling." *Molecular aspects of medicine* 25, no. 1-2: 17-26.
- Hvelplund, Malthe H, Li Liu, Kirstine M Frandsen, Hua Qian, Peter V Nielsen, Yuan Dai, Leitao Wen, and Yingqi Zhang. 2020. "Numerical Investigation of the Lower Airway Exposure to Indoor Particulate Contaminants." *Indoor and Built Environment* 29, no. 4: 575-586.
- Lujan, Henry, Eric Romer, Richard Salisbury, Saber Hussain, and Christie Sayes. 2020. "Determining the Biological Mechanisms of Action for Environmental Exposures: Applying Crispr/Cas9 to Toxicological Assessments." *Toxicological Sciences* 175, no. 1: 5-18.
- Maj, Ewa, Justyna Trynda, Beata Maj, Katarzyna Gębura, Katarzyna Bogunia-Kubik, Michał Chodyński, Andrzej Kutner, and Joanna Wietrzyk. 2019. "Differential Response of Lung Cancer Cell Lines to Vitamin D Derivatives Depending on Egfr, Kras, P53 Mutation Status and Vdr Polymorphism." *The Journal of steroid biochemistry and molecular biology* 193: 105431.
- O'Mealey, Gary B, William L Berry, and Scott M Plafker. 2017. "Sulforaphane Is a Nrf2-Independent Inhibitor of Mitochondrial Fission." *Redox biology* 11: 103-110.
- Shen, Hua, Cliona M McHale, Martyn T Smith, and Luoping Zhang. 2015. "Functional Genomic Screening Approaches in Mechanistic Toxicology and Potential Future Applications of Crispr-Cas9." *Mutation Research/Reviews in Mutation Research* 764: 31-42.
- Van der Blik, Alexander M, Qinfang Shen, and Sumihiro Kawajiri. 2013. "Mechanisms of Mitochondrial Fission and Fusion." *Cold Spring Harbor perspectives in biology* 5, no. 6: a011072.
- Youle, Richard J, and Alexander M Van Der Blik. 2012. "Mitochondrial Fission, Fusion, and Stress." *Science* 337, no. 6098: 1062-1065.
- Zhang, Yanhong, Wensheng Yan, and Xinbin Chen. 2011. "Mutant P53 Disrupts Mcf-10a Cell Polarity in Three-Dimensional Culture Via Epithelial-to-Mesenchymal Transitions." *Journal of Biological Chemistry* 286, no. 18: 16218-16228.

## BIBLIOGRAPHY

- Agarwal, Munna L, Archana Agarwal, William R Taylor, and George R Stark. 1995. "P53 Controls Both the G2/M and the G1 Cell Cycle Checkpoints and Mediates Reversible Growth Arrest in Human Fibroblasts." *Proceedings of the National Academy of Sciences* 92, no. 18: 8493-8497.
- Akira, Shizuo, Satoshi Uematsu, and Osamu Takeuchi. 2006. "Pathogen Recognition and Innate Immunity." *Cell* 124, no. 4: 783-801.
- Albanese, Alexandre, Peter S Tang, and Warren CW Chan. 2012. "The Effect of Nanoparticle Size, Shape, and Surface Chemistry on Biological Systems." *Annual review of biomedical engineering* 14: 1-16.
- Ankley, G.T., R.S. Bennett, R.J. Erickson, D.J. Hoff, M.W. Hornung, R.D. Johnson, D.R. Mount, J.W. Nichols, C.L. Russom, and P.K. Schmieder. 2010. "Adverse Outcome Pathways: A Conceptual Framework to Support Ecotoxicology Research and Risk Assessment." *Environmental Toxicology and Chemistry* 29, no. 3: 730-741.
- Attisano, L., and J.L. Wrana. 2002. "Signal Transduction by the Tgf-B Superfamily." *Science* 296, no. 5573: 1646-1647.
- Aueviriyavit, Sasitorn, Duangkamol Phummiratch, and Rawiwan Maniratanachote. 2014. "Mechanistic Study on the Biological Effects of Silver and Gold Nanoparticles in Caco-2 Cells—Induction of the Nrf2/Ho-1 Pathway by High Concentrations of Silver Nanoparticles." *Toxicology letters* 224, no. 1: 73-83.
- Balbus, J.M., A.D. Maynard, V.L. Colvin, V. Castranova, G.P. Daston, R.A. Denison, K.L. Dreher, P.L. Goering, A.M. Goldberg, K.M. Kulinowski, N.A. Monteiro-Riviere, G. Oberdörster, G.S. Omenn, K.E. Pinkerton, K.S. Ramos, K.M. Rest, J.B. Sass, E.K. Silbergeld, and B.A. Wong. 2007. "Meeting Report: Hazard Assessment for Nanoparticles-Report from an Interdisciplinary Workshop." *Environmental Health Perspectives* 115, no. 11 (Nov): 1654-9. <https://dx.doi.org/10.1289/ehp.10327>.
- Berg, J.M., A.A. Romoser, D.E. Figueroa, C.S. West, and C.M. Sayes. 2013. "Comparative Cytological Responses of Lung Epithelial and Pleural Mesothelial Cells Following in Vitro Exposure to Nanoscale Sio2." *Toxicology in Vitro* 27, no. 1: 24-33.

- Betts, K.S. 2013. "Tox21 to Date: Steps toward Modernizing Human Hazard Characterization." *Environmental Health Perspectives* 121, no. 7: A228.
- Blaauboer, Bas J. 2008. "The Contribution of in Vitro Toxicity Data in Hazard and Risk Assessment: Current Limitations and Future Perspectives." *Toxicology letters* 180, no. 2: 81-84.
- Boonstra, Johannes, and Jan Andries Post. 2004. "Molecular Events Associated with Reactive Oxygen Species and Cell Cycle Progression in Mammalian Cells." *Gene* 337: 1-13.
- Brar, S. K., M. Verma, R. D. Tyagi, and R. Y. Surampalli. 2010. "Engineered Nanoparticles in Wastewater and Wastewater Sludge--Evidence and Impacts." *Waste Manag* 30, no. 3 (Mar): 504-20.  
<https://dx.doi.org/10.1016/j.wasman.2009.10.012>.
- Brevini, Tiziana AL, Rita Vassena, Chiara Francisci, and Fulvio Gandolfi. 2005. "Role of Adenosine Triphosphate, Active Mitochondria, and Microtubules in the Acquisition of Developmental Competence of Parthenogenetically Activated Pig Oocytes." *Biology of reproduction* 72, no. 5: 1218-1223.
- Brugarolas, James, Chitra Chandrasekaran, Jeffrey I Gordon, David Beach, Tyler Jacks, and Gregory J Hannon. 1995. "Radiation-Induced Cell Cycle Arrest Compromised by P21 Deficiency." *Nature* 377, no. 6549: 552-557.
- Bryan, Tracy, and Roger R Redder. 1994. "Sv40-Induced Immortalization of Human Cells." *Critical Reviews™ in Oncogenesis* 5, no. 4.
- Bunz, F., A. Dutriaux, C. Lengauer, T. Waldman, S. Zhou, J. P. Brown, J. M. Sedivy, K. W. Kinzler, and B. Vogelstein. 1998. "Requirement for P53 and P21 to Sustain G2 Arrest after DNA Damage." *Science* 282, no. 5393: 1497-1501.  
<https://dx.doi.org/10.1126/science.282.5393.1497>.
- Burhans, William C, and Nicholas H Heintz. 2009. "The Cell Cycle Is a Redox Cycle: Linking Phase-Specific Targets to Cell Fate." *Free Radical Biology and Medicine* 47, no. 9: 1282-1293.
- Cadenas, Enrique. 2004. "Mitochondrial Free Radical Production and Cell Signaling." *Molecular aspects of medicine* 25, no. 1-2: 17-26.
- Carere, A, A Stammati, and F Zucco. 2002. "In Vitro Toxicology Methods: Impact on Regulation from Technical and Scientific Advancements." *Toxicology letters* 127, no. 1-3: 153-160.

- Chattopadhyay, M., V. K. Khemka, G. Chatterjee, A. Ganguly, S. Mukhopadhyay, and S. Chakrabarti. 2015. "Enhanced Ros Production and Oxidative Damage in Subcutaneous White Adipose Tissue Mitochondria in Obese and Type 2 Diabetes Subjects." *Mol Cell Biochem* 399, no. 1-2 (Jan): 95-103. <https://dx.doi.org/10.1007/s11010-014-2236-7>.
- Chevallet, M, Benoit Gallet, A Fuchs, PH Jouneau, K Um, E Mintz, and I Michaud-Soret. 2016. "Metal Homeostasis Disruption and Mitochondrial Dysfunction in Hepatocytes Exposed to Sub-Toxic Doses of Zinc Oxide Nanoparticles." *Nanoscale* 8, no. 43: 18495-18506.
- Chithrani, B Devika, and Warren CW Chan. 2007. "Elucidating the Mechanism of Cellular Uptake and Removal of Protein-Coated Gold Nanoparticles of Different Sizes and Shapes." *Nano letters* 7, no. 6: 1542-1550.
- Chithrani, B Devika, Arezou A Ghazani, and Warren CW Chan. 2006. "Determining the Size and Shape Dependence of Gold Nanoparticle Uptake into Mammalian Cells." *Nano letters* 6, no. 4: 662-668.
- Cho, Wan-Seob, Rodger Duffin, Mark Bradley, Ian L Megson, William MacNee, Jong Kwon Lee, Jayoung Jeong, and Ken Donaldson. 2013. "Predictive Value of in Vitro Assays Depends on the Mechanism of Toxicity of Metal Oxide Nanoparticles." *Particle and fibre toxicology* 10, no. 1: 55.
- Chou, L.Y.T., K. Ming, and W.C.W. Chan. 2011. "Strategies for the Intracellular Delivery of Nanoparticles." *Chemical Society Reviews* 40, no. 1: 233-245.
- Cloonan, S. M., and A. M. Choi. 2016. "Mitochondria in Lung Disease." *J Clin Invest* 126, no. 3 (Mar): 809-20. <https://dx.doi.org/10.1172/JCI81113>.
- Cohen, Joel M, Justin G Teeguarden, and Philip Demokritou. 2014. "An Integrated Approach for the in Vitro Dosimetry of Engineered Nanomaterials." *Particle and fibre toxicology* 11, no. 1: 20.
- Colvin, V.L. 2003. "The Potential Environmental Impact of Engineered Nanomaterials." *Nature Biotechnology* 21, no. 10: 1166-1170.
- Darlington, T. K., A. M. Neigh, M. T. Spencer, O. T. Nguyen, and S. J. Oldenburg. 2009. "Nanoparticle Characteristics Affecting Environmental Fate and Transport through Soil." *Environ Toxicol Chem* 28, no. 6 (Jun): 1191-9. <https://dx.doi.org/10.1897/08-341.1>.

- Delgado-Buenrostro, N.L., E.I. Medina-Reyes, I. Lastres-Becker, V. Freyre-Fonseca, Z. Ji, R. Hernández-Pando, B. Marquina, J. Pedraza-Chaverri, S. Espada, and A. Cuadrado. 2015. "Nrf2 Protects the Lung against Inflammation Induced by Titanium Dioxide Nanoparticles: A Positive Regulator Role of Nrf2 on Cytokine Release." *Environmental Toxicology* 30, no. 7: 782-792.
- Deli, Mária A, Csongor S Ábrahám, Yasufumi Kataoka, and Masami Niwa. 2005. "Permeability Studies on in Vitro Blood–Brain Barrier Models: Physiology, Pathology, and Pharmacology." *Cellular and molecular neurobiology* 25, no. 1: 59-127.
- Diamond, M. S., D. Edgil, T. G. Roberts, B. Lu, and E. Harris. 2000. "Infection of Human Cells by Dengue Virus Is Modulated by Different Cell Types and Viral Strains." *Journal of Virology* 74, no. 17: 7814-7823. <https://dx.doi.org/10.1128/JVI.74.17.7814-7823.2000>.
- Ding, L., J. Stilwell, T. Zhang, O. Elboudwarej, H. Jiang, J.P. Selegue, P.A. Cooke, J.W. Gray, and F.F. Chen. 2005. "Molecular Characterization of the Cytotoxic Mechanism of Multiwall Carbon Nanotubes and Nano-Onions on Human Skin Fibroblast." *Nano Letters* 5, no. 12: 2448-2464.
- Donaldson, K., V. Stone, C.L. Tran, W. Kreyling, and P.J.A. Borm. 2004. *Nanotoxicology*: BMJ Publishing Group Ltd.
- Donehower, Lawrence A, and Michele Harvey. 1992. "Mice Deficient for P53 Are Developmentally Normal but Susceptible to Spontaneous Tumours." *Nature* 356, no. 6366: 215.
- Dreier, David A, Danielle F Mello, Joel N Meyer, and Christopher J Martyniuk. 2019. "Linking Mitochondrial Dysfunction to Organismal and Population Health in the Context of Environmental Pollutants: Progress and Considerations for Mitochondrial Adverse Outcome Pathways." *Environmental toxicology and chemistry* 38, no. 8: 1625-1634.
- Duan, J., Y. Yu, Y. Li, Y. Yu, Y. Li, X. Zhou, P. Huang, and Z. Sun. 2013. "Toxic Effect of Silica Nanoparticles on Endothelial Cells through DNA Damage Response Via Chk1-Dependent G2/M Checkpoint." *PloS One* 8, no. 4: e62087.
- Elliott, R.L., and G.C. Blobe. 2005. "Role of Transforming Growth Factor Beta in Human Cancer." *Journal of Clinical Oncology* 23, no. 9: 2078-2093.
- Elsaesser, A., and C. V. Howard. 2012. "Toxicology of Nanoparticles." *Adv Drug Deliv Rev* 64, no. 2 (Feb): 129-37. <https://dx.doi.org/10.1016/j.addr.2011.09.001>.

- Eom, H. J., and J. Choi. 2010. "P38 Mapk Activation, DNA Damage, Cell Cycle Arrest and Apoptosis as Mechanisms of Toxicity of Silver Nanoparticles in Jurkat T Cells." *Environmental Science and Technology* 44, no. 21: 8337-8342. <https://dx.doi.org/10.1021/es1020668>.
- Eom, Hyun-Jeong, and Jinhee Choi. 2010. "P38 Mapk Activation, DNA Damage, Cell Cycle Arrest and Apoptosis as Mechanisms of Toxicity of Silver Nanoparticles in Jurkat T Cells." *Environmental science & technology* 44, no. 21: 8337-8342.
- Esch, E. W., A. Bahinski, and D. Huh. 2015. "Organs-on-Chips at the Frontiers of Drug Discovery." *Nat Rev Drug Discov* 14, no. 4 (Apr): 248-60. <https://dx.doi.org/10.1038/nrd4539>.
- Farokhzad, Omid C, and Robert Langer. 2009. "Impact of Nanotechnology on Drug Delivery." *ACS nano* 3, no. 1: 16-20.
- Fernandes, Tiago G, Maria Margarida Diogo, Douglas S Clark, Jonathan S Dordick, and Joaquim MS Cabral. 2009. "High-Throughput Cellular Microarray Platforms: Applications in Drug Discovery, Toxicology and Stem Cell Research." *Trends in biotechnology* 27, no. 6: 342-349.
- Finkel, Toren, and Nikki J Holbrook. 2000. "Oxidants, Oxidative Stress and the Biology of Ageing." *nature* 408, no. 6809: 239-247.
- Foldbjerg, Rasmus, Duy Anh Dang, and Herman Autrup. 2011. "Cytotoxicity and Genotoxicity of Silver Nanoparticles in the Human Lung Cancer Cell Line, A549." *Archives of toxicology* 85, no. 7: 743-750.
- Ghribi, Othman, David A DeWitt, Michael S Forbes, Mary M Herman, and John Savory. 2001. "Co-Involvement of Mitochondria and Endoplasmic Reticulum in Regulation of Apoptosis: Changes in Cytochrome C, Bcl-2 and Bax in the Hippocampus of Aluminum-Treated Rabbits." *Brain research* 903, no. 1-2: 66-73.
- Gliga, Anda R, Sara Skoglund, Inger Odnevall Wallinder, Bengt Fadeel, and Hanna L Karlsson. 2014. "Size-Dependent Cytotoxicity of Silver Nanoparticles in Human Lung Cells: The Role of Cellular Uptake, Agglomeration and Ag Release." *Particle and fibre toxicology* 11, no. 1: 1-17.
- Godoy, Patricio, Nicola J Hewitt, Ute Albrecht, Melvin E Andersen, Nariman Ansari, Sudin Bhattacharya, Johannes Georg Bode, Jennifer Bolleyn, Christoph Borner, and Jan Boettger. 2013. "Recent Advances in 2d and 3d in Vitro Systems Using Primary Hepatocytes, Alternative Hepatocyte Sources and Non-Parenchymal Liver Cells and Their Use in Investigating Mechanisms of Hepatotoxicity, Cell Signaling and Adme." *Archives of toxicology* 87, no. 8: 1315-1530.

- Gold, R., L. Kappos, D.L. Arnold, A. Bar-Or, G. Giovannoni, K. Selmaj, C. Tornatore, M.T. Sweetser, M. Yang, and S.I. Sheikh. 2012. "Placebo-Controlled Phase 3 Study of Oral Bg-12 for Relapsing Multiple Sclerosis." *New England Journal of Medicine* 367, no. 12: 1098-1107.
- Goldberg, Alan M, and John M Frazier. 1989. "Alternatives to Animals in Toxicity Testing." *Scientific American* 261, no. 2: 24-31.
- Grossmann, J., S. Mohr, E.G. Lapetina, C. Fiocchi, and A.D. Levine. 1998. "Sequential and Rapid Activation of Select Caspases During Apoptosis of Normal Intestinal Epithelial Cells." *American Journal of Physiology-Gastrointestinal and Liver Physiology* 274, no. 6: G1117-G1124.
- Gui, S., B. Li, X. Zhao, L. Sheng, J. Hong, X. Yu, X. Sang, Q. Sun, Y. Ze, and L. Wang. 2013. "Renal Injury and Nrf2 Modulation in Mouse Kidney Following Chronic Exposure to TiO2 Nanoparticles." *Journal of Agricultural and Food Chemistry* 61, no. 37: 8959-8968.
- Guillouzo, André, and Christiane Guguen-Guillouzo. 2008. "Evolving Concepts in Liver Tissue Modeling and Implications for in Vitro Toxicology." *Expert opinion on drug metabolism & toxicology* 4, no. 10: 1279-1294.
- Guo, B., R. Zebda, S. J. Drake, and C. M. Sayes. 2009. "Synergistic Effect of Co-Exposure to Carbon Black and Fe<sub>2</sub>O<sub>3</sub> Nanoparticles on Oxidative Stress in Cultured Lung Epithelial Cells." *Particle and Fibre Toxicology* 6. <https://dx.doi.org/10.1186/1743-8977-6-4>.
- Guo, C., Y. Xia, P. Niu, L. Jiang, J. Duan, Y. Yu, X. Zhou, Y. Li, and Z. Sun. 2015. "Silica Nanoparticles Induce Oxidative Stress, Inflammation, and Endothelial Dysfunction in Vitro Via Activation of the Mapk/Nrf2 Pathway and Nuclear Factor-Kb Signaling." *International Journal of Nanomedicine* 10: 1463.
- Gupta, S. C., D. Hevia, S. Patchva, B. Park, W. Koh, and B. B. Aggarwal. 2012. "Upsides and Downsides of Reactive Oxygen Species for Cancer: The Roles of Reactive Oxygen Species in Tumorigenesis, Prevention, and Therapy." *Antioxidants and Redox Signaling* 16, no. 11: 1295-1322. <https://dx.doi.org/10.1089/ars.2011.4414>.
- Hahn, William C, Christopher M Counter, Ante S Lundberg, Roderick L Beijersbergen, Mary W Brooks, and Robert A Weinberg. 1999. "Creation of Human Tumour Cells with Defined Genetic Elements." *Nature* 400, no. 6743: 464-468.

- Hahn, William C, Scott K Dessain, Mary W Brooks, Jessie E King, Brian Elenbaas, David M Sabatini, James A DeCaprio, and Robert A Weinberg. 2002. "Enumeration of the Simian Virus 40 Early Region Elements Necessary for Human Cell Transformation." *Molecular and cellular biology* 22, no. 7: 2111-2123.
- Hanahan, Douglas, and Robert A Weinberg. 2000. "The Hallmarks of Cancer." *cell* 100, no. 1: 57-70.
- . 2011. "Hallmarks of Cancer: The Next Generation." *cell* 144, no. 5: 646-674.
- Harris, S.L., and A.J. Levine. 2005. "The P53 Pathway: Positive and Negative Feedback Loops." *Oncogene* 24, no. 17: 2899-2908.
- Hartung, Thomas, and George Daston. 2009. "Are in Vitro Tests Suitable for Regulatory Use?" *Toxicological sciences* 111, no. 2: 233-237.
- Harush-Frenkel, Oshrat, Nir Debotton, Simon Benita, and Yoram Altschuler. 2007. "Targeting of Nanoparticles to the Clathrin-Mediated Endocytic Pathway." *Biochemical and biophysical research communications* 353, no. 1: 26-32.
- Hatch, Theodore F., Paul Gross. 2013. "Pulmonary Deposition and Retention of Inhaled Aerosols." *Elsevier*.
- Heiden, M. G. V., L. C. Cantley, and C. B. Thompson. 2009. "Understanding the Warburg Effect: The Metabolic Requirements of Cell Proliferation." *Science* 324, no. 5930: 1029-1033. <https://dx.doi.org/10.1126/science.1160809>.
- Huang, Song, Ludovic Wiszniewski, Jean-Paul Derouette, and Samuel Constant. 2009. "In Vitro Organ Culture Models of Asthma." *Drug Discovery Today: Disease Models* 6, no. 4: 137-144.
- Hussain, S. M., K. L. Hess, J. M. Gearhart, K. T. Geiss, and J. J. Schlager. 2005. "In Vitro Toxicity of Nanoparticles in Brl 3a Rat Liver Cells." *Toxicology in Vitro* 19, no. 7: 975-983. <https://dx.doi.org/10.1016/j.tiv.2005.06.034>.
- Huynh, N.T., E. Roger, N. Lautram, J.-P. Benoît, and C. Passirani. 2010. "The Rise and Rise of Stealth Nanocarriers for Cancer Therapy: Passive Versus Active Targeting." *Nanomedicine* 5, no. 9: 1415-1433.
- Hvelplund, Malthe H, Li Liu, Kirstine M Frandsen, Hua Qian, Peter V Nielsen, Yuan Dai, Leitao Wen, and Yingqi Zhang. 2020. "Numerical Investigation of the Lower Airway Exposure to Indoor Particulate Contaminants." *Indoor and Built Environment* 29, no. 4: 575-586.

- Ishii, T., K. Yasuda, A. Akatsuka, O. Hino, P. S. Hartman, and N. Ishii. 2005. "A Mutation in the Sdhc Gene of Complex Ii Increases Oxidative Stress, Resulting in Apoptosis and Tumorigenesis." *Cancer Research* 65, no. 1: 203-209.  
<https://www.scopus.com/inward/record.uri?eid=2-s2.0-11244279161&partnerID=40&md5=bf6b75f34b095776fd7522091474488e>.
- Itoh, Ken, Tomoki Chiba, Satoru Takahashi, Tetsuro Ishii, Kazuhiko Igarashi, Yasutake Katoh, Tatsuya Oyake, Norio Hayashi, Kimihiko Satoh, and Ichiro Hatayama. 1997. "An Nrf2/Small Maf Heterodimer Mediates the Induction of Phase Ii Detoxifying Enzyme Genes through Antioxidant Response Elements." *Biochemical and biophysical research communications* 236, no. 2: 313-322.
- Jheng, Huei-Fen, Pei-Jane Tsai, Syue-Maio Guo, Li-Hua Kuo, Cherng-Shyang Chang, Ih-Jen Su, Chuang-Rung Chang, and Yau-Sheng Tsai. 2012. "Mitochondrial Fission Contributes to Mitochondrial Dysfunction and Insulin Resistance in Skeletal Muscle." *Molecular and cellular biology* 32, no. 2: 309-319.
- Johnson, G.L., and R. Lapadat. 2002. "Mitogen-Activated Protein Kinase Pathways Mediated by Erk, Jnk, and P38 Protein Kinases." *Science* 298, no. 5600: 1911-1912.
- Kang, S.J., B.M. Kim, Y.J. Lee, and H.W. Chung. 2008. "Titanium Dioxide Nanoparticles Trigger P53-Mediated Damage Response in Peripheral Blood Lymphocytes." *Environmental and Molecular Mutagenesis* 49, no. 5: 399-405.
- Kang, S.J., Y.J. Lee, E.-K. Lee, and M.-K. Kwak. 2012. "Silver Nanoparticles-Mediated G2/M Cycle Arrest of Renal Epithelial Cells Is Associated with Nrf2-Gsh Signaling." *Toxicology Letters* 211, no. 3: 334-341.
- Kang, Su Jin, In-geun Ryoo, Young Joon Lee, and Mi-Kyoung Kwak. 2012. "Role of the Nrf2-Heme Oxygenase-1 Pathway in Silver Nanoparticle-Mediated Cytotoxicity." *Toxicology and applied pharmacology* 258, no. 1: 89-98.
- Karbowski, M, and RJ Youle. 2003. "Dynamics of Mitochondrial Morphology in Healthy Cells and During Apoptosis." *Cell Death & Differentiation* 10, no. 8: 870-880.
- Kastan, M.B., Q. Zhan, W.S. El-Deiry, F. Carrier, T. Jacks, W.V. Walsh, B.S. Plunkett, B. Vogelstein, and A.J. Fornace. 1992. "A Mammalian Cell Cycle Checkpoint Pathway Utilizing P53 and Gadd45 Is Defective in Ataxia-Telangiectasia." *Cell* 71, no. 4: 587-597.
- Khan, J.A., T.K. Mandal, T.K. Das, Y. Singh, B. Pillai, and S. Maiti. 2011. "Magnetite (Fe<sub>3</sub>O<sub>4</sub>) Nanocrystals Affect the Expression of Genes Involved in the Tgf-Beta Signalling Pathway." *Molecular BioSystems* 7, no. 5: 1481-1486.

- Kim, HJ, DH Jung, IH Jung, JI Cifuentes, KY Rhee, and D Hui. 2012. "Enhancement of Mechanical Properties of Aluminium/Epoxy Composites with Silane Functionalization of Aluminium Powder." *Composites Part B-Engineering* 43, no. 4 (JUN 2012): 1743-1748. <https://dx.doi.org/10.1016/j.compositesb.2011.12.010>.
- Kirkpatrick, C James, Sabine Fuchs, and Ronald E Unger. 2011. "Co-Culture Systems for Vascularization—Learning from Nature." *Advanced drug delivery reviews* 63, no. 4-5: 291-299.
- Kirkpatrick, CJ, and Ch Mittermayer. 1990. "Theoretical and Practical Aspects of Testing Potential Biomaterialsin Vitro." *Journal of Materials Science: Materials in Medicine* 1, no. 1: 9-13.
- Kobayashi, Makoto, and Masayuki Yamamoto. 2005. "Molecular Mechanisms Activating the Nrf2-Keap1 Pathway of Antioxidant Gene Regulation." *Antioxidants & redox signaling* 7, no. 3-4: 385-394.
- Kostadinova, Radina, Franziska Boess, Dawn Applegate, Laura Suter, Thomas Weiser, Thomas Singer, Brian Naughton, and Adrian Roth. 2013. "A Long-Term Three Dimensional Liver Co-Culture System for Improved Prediction of Clinically Relevant Drug-Induced Hepatotoxicity." *Toxicology and applied pharmacology* 268, no. 1: 1-16.
- Kowaltowski, A. J., and A. E. Vercesi. 1999. "Mitochondrial Damage Induced by Conditions of Oxidative Stress." *Free Radic Biol Med* 26, no. 3-4 (Feb): 463-71. <https://www.ncbi.nlm.nih.gov/pubmed/9895239>.
- Kroll, Alexandra, Mike H Pillukat, Daniela Hahn, and Jürgen Schnekenburger. 2009. "Current in Vitro Methods in Nanoparticle Risk Assessment: Limitations and Challenges." *European journal of Pharmaceutics and Biopharmaceutics* 72, no. 2: 370-377.
- Lawrence, T. 2009. "The Nuclear Factor Nf-Kb Pathway in Inflammation." *Cold Spring Harbor Perspectives in Biology* 1, no. 6: a001651.
- Levine, Arnold J. 1997. "P53, the Cellular Gatekeeper for Growth and Division." *cell* 88, no. 3: 323-331.
- Li, J., X. Wang, C. Wang, B. Chen, Y. Dai, R. Zhang, M. Song, G. Lv, and D. Fu. 2007. "The Enhancement Effect of Gold Nanoparticles in Drug Delivery and as Biomarkers of Drug-Resistant Cancer Cells." *ChemMedChem* 2, no. 3: 374-378.
- Liebsch, Manfred, and Horst Spielmann. 2002. "Currently Available in Vitro Methods Used in the Regulatory Toxicology." *Toxicology letters* 127, no. 1-3: 127-134.

- Limbach, Ludwig K, Peter Wick, Pius Manser, Robert N Grass, Arie Bruinink, and Wendelin J Stark. 2007. "Exposure of Engineered Nanoparticles to Human Lung Epithelial Cells: Influence of Chemical Composition and Catalytic Activity on Oxidative Stress." *Environmental science & technology* 41, no. 11: 4158-4163.
- Lin, J., H. Zhang, Z. Chen, and Y. Zheng. 2010. "Penetration of Lipid Membranes by Gold Nanoparticles: Insights into Cellular Uptake, Cytotoxicity, and Their Relationship." *ACS Nano* 4, no. 9: 5421-5429.
- Lin, Rwei-Zhen, and Hwan-You Chang. 2008. "Recent Advances in Three-Dimensional Multicellular Spheroid Culture for Biomedical Research." *Biotechnology Journal: Healthcare Nutrition Technology* 3, no. 9-10: 1172-1184.
- Liu, Jingyu, and Robert H Hurt. 2010. "Ion Release Kinetics and Particle Persistence in Aqueous Nano-Silver Colloids." *Environmental science & technology* 44, no. 6: 2169-2175.
- Liu, X., and J. Sun. 2010. "Endothelial Cells Dysfunction Induced by Silica Nanoparticles through Oxidative Stress Via Jnk/P53 and Nf-Kb Pathways." *Biomaterials* 31, no. 32: 8198-8209.
- Liu, Y. J. 2001. "Dendritic Cell Subsets and Lineages, and Their Functions in Innate and Adaptive Immunity." *Cell* 106, no. 3: 259-262. [https://dx.doi.org/10.1016/S0092-8674\(01\)00456-1](https://dx.doi.org/10.1016/S0092-8674(01)00456-1).
- Lujan, H., M. F. Criscitiello, A. S. Hering, and C. M. Sayes. 2019. "Refining in Vitro Toxicity Models: Comparing Baseline Characteristics of Lung Cell Types." *Toxicol Sci* 168, no. 2 (Apr): 302-314. <https://dx.doi.org/10.1093/toxsci/kfz001>.
- Lujan, Henry, Eric Romer, Richard Salisbury, Saber Hussain, and Christie Sayes. 2020. "Determining the Biological Mechanisms of Action for Environmental Exposures: Applying Crispr/Cas9 to Toxicological Assessments." *Toxicological Sciences* 175, no. 1: 5-18.
- Lujan, Henry, and Christie M Sayes. 2017. "Cytotoxicological Pathways Induced after Nanoparticle Exposure: Studies of Oxidative Stress at the 'Nano-Bio' interface." *Toxicology research* 6, no. 5: 580-594.
- Lundqvist, Martin, Johannes Stigler, Giuliano Elia, Iseult Lynch, Tommy Cedervall, and Kenneth A Dawson. 2008. "Nanoparticle Size and Surface Properties Determine the Protein Corona with Possible Implications for Biological Impacts." *Proceedings of the National Academy of Sciences* 105, no. 38: 14265-14270.
- Mabalirajan, U., and B. Ghosh. 2013. "Mitochondrial Dysfunction in Metabolic Syndrome and Asthma." *J Allergy (Cairo)* 2013: 340476. <https://dx.doi.org/10.1155/2013/340476>.

- Maj, Ewa, Justyna Trynda, Beata Maj, Katarzyna Gębura, Katarzyna Bogunia-Kubik, Michał Chodyński, Andrzej Kutner, and Joanna Wietrzyk. 2019. "Differential Response of Lung Cancer Cell Lines to Vitamin D Derivatives Depending on Egfr, Kras, P53 Mutation Status and Vdr Polymorphism." *The Journal of steroid biochemistry and molecular biology* 193: 105431.
- Marambio-Jones, Catalina, and Eric MV Hoek. 2010. "A Review of the Antibacterial Effects of Silver Nanomaterials and Potential Implications for Human Health and the Environment." *Journal of Nanoparticle Research* 12, no. 5: 1531-1551.
- Martindale, J.L., and N.J. Holbrook. 2002. "Cellular Response to Oxidative Stress: Signaling for Suicide and Survival." *Journal of Cellular Physiology* 192, no. 1: 1-15.
- Menon, SG, and PC Goswami. 2007. "A Redox Cycle within the Cell Cycle: Ring in the Old with the New." *Oncogene* 26, no. 8: 1101-1109.
- Michael Berg, J., A. A. Romoser, D. E. Figueroa, C. Spencer West, and C. M. Sayes. 2013. "Comparative Cytological Responses of Lung Epithelial and Pleural Mesothelial Cells Following in Vitro Exposure to Nanoscale Sio2." *Toxicology in Vitro* 27, no. 1: 24-33. <https://dx.doi.org/10.1016/j.tiv.2012.09.002>.
- Mirshafa, Atefeh, Mehdi Nazari, Daniel Jahani, and Fatemeh Shaki. 2018. "Size-Dependent Neurotoxicity of Aluminum Oxide Particles: A Comparison between Nano-and Micrometer Size on the Basis of Mitochondrial Oxidative Damage." *Biological trace element research* 183, no. 2: 261-269.
- Mishra, Anurag, Todd A Stueckle, Robert R Mercer, Raymond Derk, Yon Rojanasakul, Vincent Castranova, and Liying Wang. 2015. "Identification of Tgf-B Receptor-1 as a Key Regulator of Carbon Nanotube-Induced Fibrogenesis." *American Journal of Physiology-Lung Cellular and Molecular Physiology* 309, no. 8: L821-L833.
- Monopoli, Marco P, Christoffer Åberg, Anna Salvati, and Kenneth A Dawson. 2012. "Biomolecular Coronas Provide the Biological Identity of Nanosized Materials." *Nature nanotechnology* 7, no. 12: 779-786.
- Mooi, WJ, and DS Peeper. 2006. "Oncogene-Induced Cell Senescence—Halting on the Road to Cancer." *New England Journal of Medicine* 355, no. 10: 1037-1046.
- Mortimer, Monika, Alexander Gogos, Nora Bartolomé, Anne Kahru, Thomas D Bucheli, and Vera I Slaveykova. 2014. "Potential of Hyperspectral Imaging Microscopy for Semi-Quantitative Analysis of Nanoparticle Uptake by Protozoa." *Environmental science & technology* 48, no. 15: 8760-8767.

- Mout, R., D.F. Moyano, S. Rana, and V.M. Rotello. 2012. "Surface Functionalization of Nanoparticles for Nanomedicine." *Chemical Society Reviews* 41, no. 7: 2539-2544.
- Murakami, Keiko, and Masataka Yoshino. 2004. "Aluminum Decreases the Glutathione Regeneration by the Inhibition of NADP-Isocitrate Dehydrogenase in Mitochondria." *Journal of Cellular Biochemistry* 93, no. 6: 1267-1271.
- Murphy, Michael P. 2009. "How Mitochondria Produce Reactive Oxygen Species." *Biochemical Journal* 417, no. 1: 1-13.
- Nel, A., T. Xia, L. Mädler, and N. Li. 2006. "Toxic Potential of Materials at the Nanolevel." *Science* 311, no. 5761: 622-627.
- Nemmar, Abderrahim, Jørn A Holme, Irma Rosas, Per E Schwarze, and Ernesto Alfaro-Moreno. 2013. "Recent Advances in Particulate Matter and Nanoparticle Toxicology: A Review of the in Vivo and in Vitro Studies." *BioMed research international* 2013.
- Nguyen, Truyen, Paul Nioi, and Cecil B Pickett. 2009. "The Nrf2-Antioxidant Response Element Signaling Pathway and Its Activation by Oxidative Stress." *Journal of Biological Chemistry* 284, no. 20: 13291-13295.
- Niu, PY, Q Niu, QL Zhang, LP Wang, SC He, TC Wu, P Conti, M Di Gioacchino, and P Boscolo. 2005. "Aluminum Impairs Rat Neural Cell Mitochondria in Vitro." *International journal of immunopathology and pharmacology* 18, no. 4: 683-689.
- Nohl, H., L. Gille, and K. Staniek. 2005. "Intracellular Generation of Reactive Oxygen Species by Mitochondria." *Biochemical Pharmacology* 69, no. 5: 719-723. <https://dx.doi.org/10.1016/j.bcp.2004.12.002>.
- O'Mealey, Gary B, William L Berry, and Scott M Plafker. 2017. "Sulforaphane Is a Nrf2-Independent Inhibitor of Mitochondrial Fission." *Redox biology* 11: 103-110.
- O'Shea, J.J., M. Gadina, and R.D. Schreiber. 2002. "Cytokine Signaling in 2002: New Surprises in the Jak/Stat Pathway." *Cell* 109, no. 2: S121-S131.
- Oberdörster, G. 2010. "Safety Assessment for Nanotechnology and Nanomedicine: Concepts of Nanotoxicology." *Journal of Internal Medicine* 267, no. 1: 89-105. <https://dx.doi.org/10.1111/j.1365-2796.2009.02187.x>.
- Oberdörster, G., A. Maynard, K. Donaldson, V. Castranova, J. Fitzpatrick, K. Ausman, J. Carter, B. Karn, W. Kreyling, D. Lai, S. Olin, N. Monteiro-Riviere, D. Warheit, and H. Yang. 2005a. "Principles for Characterizing the Potential Human Health Effects from Exposure to Nanomaterials: Elements of a Screening Strategy." *Particle and Fibre Toxicology* 2. <https://dx.doi.org/10.1186/1743-8977-2-8>.

- Oberdörster, G., A. Maynard, K. Donaldson, Vi. Castranova, J. Fitzpatrick, K. Ausman, J. Carter, B. Karn, W. Kreyling, and D. Lai. 2005b. "Principles for Characterizing the Potential Human Health Effects from Exposure to Nanomaterials: Elements of a Screening Strategy." *Particle and Fibre Toxicology* 2, no. 1: 8.
- Oberdörster, G., E. Oberdörster, and J. Oberdörster. 2005. "Nanotoxicology: An Emerging Discipline Evolving from Studies of Ultrafine Particles." *Environmental Health Perspectives*: 823-839.
- Oberdörster, G., V. Stone, and K. Donaldson. 2007. "Toxicology of Nanoparticles: A Historical Perspective." *Nanotoxicology* 1, no. 1: 2-25.
- Park, E.-J., H.N. Umh, S.-W. Kim, M.-H. Cho, J.-H. Kim, and Y. Kim. 2014. "Erk Pathway Is Activated in Bare-Fenps-Induced Autophagy." *Archives of Toxicology* 88, no. 2: 323-336.
- Parnsamut, C, and S Brimson. 2015. "Effects of Silver Nanoparticles and Gold Nanoparticles on Il-2, Il-6, and Tnf-A Production Via Mapk Pathway in Leukemic Cell Lines." *Genet. Mol. Res* 14, no. 2: 3650.
- Patiño, Tania, Jorge Soriano, Lleonard Barrios, Elena Ibáñez, and Carme Nogués. 2015. "Surface Modification of Microparticles Causes Differential Uptake Responses in Normal and Tumoral Human Breast Epithelial Cells." *Scientific reports* 5: 11371.
- Pedley, T. J. 1977. "Pulmonary Fluid Dynamics." *Annual Review of Fluid Mechanics* 9 no. 1: 229-274.
- Phalen, Robert F, Michael J Oldham, and Andre E Nel. 2006. "Tracheobronchial Particle Dose Considerations for in Vitro Toxicology Studies." *Toxicological Sciences* 92, no. 1: 126-132.
- Piao, M.J., K.C. Kim, J.-Y. Choi, J. Choi, and J.W. Hyun. 2011. "Silver Nanoparticles Down-Regulate Nrf2-Mediated 8-Oxoguanine DNA Glycosylase 1 through Inactivation of Extracellular Regulated Kinase and Protein Kinase B in Human Chang Liver Cells." *Toxicology Letters* 207, no. 2: 143-148.
- Podila, Ramakrishna, Ran Chen, Pu Chun Ke, JM Brown, and AM Rao. 2012. "Effects of Surface Functional Groups on the Formation of Nanoparticle-Protein Corona." *Applied physics letters* 101, no. 26: 263701.
- Prives, C., and P.A. Hall. 1999. "The P53 Pathway." *Journal of Pathology* 187, no. 1: 112-126.

- Rampelt, Heike, Ralf M Zerbes, Martin van der Laan, and Nikolaus Pfanner. 2017. "Role of the Mitochondrial Contact Site and Cristae Organizing System in Membrane Architecture and Dynamics." *Biochimica et Biophysica Acta (BBA)-Molecular Cell Research* 1864, no. 4: 737-746.
- Ravuri, C., G. Svineng, S. Pankiv, and N. E. Huseby. 2011. "Endogenous Production of Reactive Oxygen Species by the NADPH Oxidase Complexes Is a Determinant of  $\Gamma$ -Glutamyltransferase Expression." *Free Radical Research* 45, no. 5: 600-610. <https://dx.doi.org/10.3109/10715762.2011.564164>.
- Rawlings, J.S., K.M. Rosler, and D.A. Harrison. 2004. "The Jak/Stat Signaling Pathway." *Journal of Cell Science* 117, no. 8: 1281-1283.
- Romoser, A.A., P.L. Chen, J.M. Berg, C. Seabury, I. Ivanov, M.F. Criscitiello, and C.M. Sayes. 2011. "Quantum Dots Trigger Immunomodulation of the NF- $\kappa$ B Pathway in Human Skin Cells." *Molecular Immunology* 48, no. 12: 1349-1359.
- Romoser, A.A., D.E. Figueroa, A. Soorash, K. Scribner, P.L. Chen, W. Porter, M.F. Criscitiello, and C.M. Sayes. 2012. "Distinct Immunomodulatory Effects of a Panel of Nanomaterials in Human Dermal Fibroblasts." *Toxicology Letters* 210, no. 3: 293-301.
- Romoser, Amelia A, Michael F Criscitiello, and Christie M Sayes. 2014. "Engineered Nanoparticles Induce DNA Damage in Primary Human Skin Cells, Even at Low Doses." *Nano Life* 4, no. 01: 1440001.
- Salatin, Sara, Solmaz Maleki Dizaj, and Ahmad Yari Khosroushahi. 2015. "Effect of the Surface Modification, Size, and Shape on Cellular Uptake of Nanoparticles." *Cell biology international* 39, no. 8: 881-890.
- Sastre, Juan, Federico V Pallardó, José García de la Asunción, and José Viña. 2000. "Mitochondria, Oxidative Stress and Aging." *Free radical research* 32, no. 3: 189-198.
- Sauer, Heinrich, Maria Wartenberg, and Juergen Hescheler. 2001. "Reactive Oxygen Species as Intracellular Messengers During Cell Growth and Differentiation." *Cellular physiology and biochemistry* 11, no. 4: 173-186.
- Sayes, C. M., H. Staats, and A. J. Hickey. 2014. "Scale of Health: Indices of Safety and Efficacy in the Evolving Environment of Large Biological Datasets." *Pharmaceutical Research* 31, no. 9: 2256-2265. <https://dx.doi.org/10.1007/s11095-014-1415-2>.
- Sayes, C.M., G.V. Aquino, and A.J. Hickey. 2017. "Nanomaterial Drug Products: Manufacturing and Analytical Perspectives." *AAPS Journal*.

- Sayes, C.M., and J.R. Child. 2015. "Nanotoxicology: Determining Nano-Bio Interactions and Evaluating Toxicity Using in Vitro Models." *Nanoengineering: Global Approaches to Health and Safety Issues*: 85.
- Sayes, Christie M, Nivedita Banerjee, and Amelia A Romoser. 2009. "The Role of Oxidative Stress in Nanotoxicology." *General, Applied and Systems Toxicology*.
- Schousboe, Arne, HM Sickmann, Lasse Kristoffer Bak, I Schousboe, FS Jajo, SAA Faek, and Helle S Waagepetersen. 2011. "Neuron–Glia Interactions in Glutamatergic Neurotransmission: Roles of Oxidative and Glycolytic Adenosine Triphosphate as Energy Source." *Journal of neuroscience research* 89, no. 12: 1926-1934.
- Sharma, P., and K. P. Mishra. 2006. "Aluminum-Induced Maternal and Developmental Toxicity and Oxidative Stress in Rat Brain: Response to Combined Administration of Tiron and Glutathione." *Reprod Toxicol* 21, no. 3 (Apr): 313-21. <https://dx.doi.org/10.1016/j.reprotox.2005.06.004>.
- Shen, Hua, Cliona M McHale, Martyn T Smith, and Luoping Zhang. 2015. "Functional Genomic Screening Approaches in Mechanistic Toxicology and Potential Future Applications of Crispr-Cas9." *Mutation Research/Reviews in Mutation Research* 764: 31-42.
- Shenoy, D., W. Fu, J. Li, C. Crasto, G. Jones, C. Dimarzio, S. Sridhar, and M. Amiji. 2006. "Surface Functionalization of Gold Nanoparticles Using Hetero-Bifunctional Poly (Ethylene Glycol) Spacer for Intracellular Tracking and Delivery." *International Journal of Nanomedicine* 1, no. 1: 51.
- Shi, Y., F. Wang, J. He, S. Yadav, and H. Wang. 2010. "Titanium Dioxide Nanoparticles Cause Apoptosis in Beas-2b Cells through the Caspase 8/T-Bid-Independent Mitochondrial Pathway." *Toxicology Letters* 196, no. 1: 21-27.
- Simbula, G., A. Columbano, G.M. Ledda-Columbano, L. Sanna, M. Deidda, A. Diana, and M. Pibiri. 2007. "Increased Ros Generation and P53 Activation in A-Lipoic Acid-Induced Apoptosis of Hepatoma Cells." *Apoptosis* 12, no. 1: 113-123.
- Slowing, I., B.G. Trewyn, and V.S.-Y. Lin. 2006. "Effect of Surface Functionalization of Mcm-41-Type Mesoporous Silica Nanoparticles on the Endocytosis by Human Cancer Cells." *Journal of the American Chemical Society* 128, no. 46: 14792-14793.
- Snyder-Talkington, Brandi N, Diane Schwegler-Berry, Vincent Castranova, Yong Qian, and Nancy L Guo. 2013. "Multi-Walled Carbon Nanotubes Induce Human Microvascular Endothelial Cellular Effects in an Alveolar-Capillary Co-Culture with Small Airway Epithelial Cells." *Particle and fibre toxicology* 10, no. 1: 1-14.

- Sperling, R.A., and W.J. Parak. 2010. "Surface Modification, Functionalization and Bioconjugation of Colloidal Inorganic Nanoparticles." *Philosophical Transactions of the Royal Society of London A: Mathematical, Physical and Engineering Sciences* 368, no. 1915: 1333-1383.
- Stępkowski, TM, K Brzóska, and M Kruszewski. 2014. "Silver Nanoparticles Induced Changes in the Expression of Nf-Kb Related Genes Are Cell Type Specific and Related to the Basal Activity of Nf-Kb." *Toxicology in Vitro* 28, no. 4: 473-478.
- Stern, Stephan T, Pavan P Adisheshaiah, and Rachael M Crist. 2012. "Autophagy and Lysosomal Dysfunction as Emerging Mechanisms of Nanomaterial Toxicity." *Particle and fibre toxicology* 9, no. 1: 20.
- Stone, Vicki, and Ken Donaldson. 2006. "Nanotoxicology: Signs of Stress." *Nature Nanotechnology* 1, no. 1: 23-24.
- Storm, G., S.O. Belliot, T. Daemen, and D.D. Lasic. 1995. "Surface Modification of Nanoparticles to Oppose Uptake by the Mononuclear Phagocyte System." *Advanced Drug Delivery Reviews* 17, no. 1: 31-48.
- Taguchi, K., H. Motohashi, and M. Yamamoto. 2011. "Molecular Mechanisms of the Keap1–Nrf2 Pathway in Stress Response and Cancer Evolution." *Genes to Cells* 16, no. 2: 123-140.
- Tenderenda, M. 2005. "A Study on the Prognostic Value of Cyclins D1 and E Expression Levels in Resectable Gastric Cancer and on Some Correlations between Cyclins Expression, Histoclinical Parameters and Selected Protein Products of Cell-Cycle Regulatory Genes." *Journal of Experimental & Cclinical Cancer Research* 24, no. 3: 405-414.
- Thiery, J. P., H. Acloque, R. Y. J. Huang, and M. A. Nieto. 2009. "Epithelial-Mesenchymal Transitions in Development and Disease." *Cell* 139, no. 5: 871-890. <https://dx.doi.org/10.1016/j.cell.2009.11.007>.
- Topuz, E., and C.A.M. van Gestel. 2015. "Toxicokinetics and Toxicodynamics of Differently Coated Silver Nanoparticles and Silver Nitrate in Enchytraeus Crypticus Upon Aqueous Exposure in an Inert Sand Medium." *Environmental Toxicology and Chemistry* 34, no. 12: 2816-2823.
- Twig, Gilad, and Orian S Shirihai. 2011. "The Interplay between Mitochondrial Dynamics and Mitophagy." *Antioxidants & redox signaling* 14, no. 10: 1939-1951.
- Van der Blik, Alexander M, Qinfang Shen, and Sumihiro Kawajiri. 2013. "Mechanisms of Mitochondrial Fission and Fusion." *Cold Spring Harbor perspectives in biology* 5, no. 6: a011072.

- Vance, M.E., T. Kuiken, E.P. Vejerano, S.P. McGinnis, M.F. Hochella, D. Rejeski, and M. S. Hull. 2015. "Nanotechnology in the Real World: Redeveloping the Nanomaterial Consumer Products Inventory." *Beilstein Journal of Nanotechnology* 6: 1769-1780. <https://dx.doi.org/10.3762/bjnano.6.181>.
- Vargas, A.J., and C.C. Harris. 2016. "Biomarker Development in the Precision Medicine Era: Lung Cancer as a Case Study." *Nature Reviews Cancer* 16, no. 8: 525-537.
- Verma, A., O. Uzun, Y. Hu, Y. Hu, H.-S. Han, N. Watson, S. Chen, D.J. Irvine, and F. Stellacci. 2008. "Surface-Structure-Regulated Cell-Membrane Penetration by Monolayer-Protected Nanoparticles." *Nature Materials* 7, no. 7: 588-595.
- Villanueva, A., M. Canete, A.G. Roca, M. Calero, S. Veintemillas-Verdaguer, C.J. Serna, M. del Puerto Morales, and R. Miranda. 2009. "The Influence of Surface Functionalization on the Enhanced Internalization of Magnetic Nanoparticles in Cancer Cells." *Nanotechnology* 20, no. 11: 115103.
- Vousden, K. H., and X. Lu. 2002. "Live or Let Die: The Cell's Response to P53." *Nature Reviews Cancer* 2, no. 8: 594-604. <https://dx.doi.org/10.1038/nrc864>.
- Warburg, O. 1956. "On the Origin of Cancer Cells." *Science* 123, no. 3191: 309-314. <https://dx.doi.org/10.1126/science.123.3191.309>.
- Warheit, D.B., R.A. Hoke, C. Finlay, E.M. Donner, K.L. Reed, and C.M. Sayes. 2007. "Development of a Base Set of Toxicity Tests Using Ultrafine TiO<sub>2</sub> Particles as a Component of Nanoparticle Risk Management." *Toxicology Letters* 171, no. 3: 99-110.
- Wei, Y., J. J. Zhang, Z. Li, A. Gow, K. F. Chung, M. Hu, Z. Sun, L. Zeng, T. Zhu, G. Jia, X. Li, M. Duarte, and X. Tang. 2016. "Chronic Exposure to Air Pollution Particles Increases the Risk of Obesity and Metabolic Syndrome: Findings from a Natural Experiment in Beijing." *FASEB J* 30, no. 6 (06): 2115-22. <https://dx.doi.org/10.1096/fj.201500142>.
- Wei, Z., and H. T. Liu. 2002. "Mapk Signal Pathways in the Regulation of Cell Proliferation in Mammalian Cells." *Cell Research* 12, no. 1: 9-18. <https://dx.doi.org/10.1038/sj.cr.7290105>.
- Wilhelmi, V., U. Fischer, H. Weighardt, K. Schulze-Osthoff, C. Nickel, B. Stahlmecke, T.A.J. Kuhlbusch, A.M. Scherbarth, C. Esser, and R.P.F. Schins. 2013. "Zinc Oxide Nanoparticles Induce Necrosis and Apoptosis in Macrophages in a P47phox-and Nrf2-Independent Manner." *PloS One* 8, no. 6: e65704.
- Wu, Jie, Jiao Sun, and Yang Xue. 2010. "Involvement of Jnk and P53 Activation in G2/M Cell Cycle Arrest and Apoptosis Induced by Titanium Dioxide Nanoparticles in Neuron Cells." *Toxicology letters* 199, no. 3: 269-276.

- Wu, Shengnan, Feifan Zhou, Zhenzhen Zhang, and Da Xing. 2011. "Mitochondrial Oxidative Stress Causes Mitochondrial Fragmentation Via Differential Modulation of Mitochondrial Fission–Fusion Proteins." *The FEBS journal* 278, no. 6: 941-954.
- Xia, Tian, Michael Kovoichich, Jonathan Brant, Matt Hotze, Joan Sempf, Terry Oberley, Constantinos Sioutas, Joanne I Yeh, Mark R Wiesner, and Andre E Nel. 2006. "Comparison of the Abilities of Ambient and Manufactured Nanoparticles to Induce Cellular Toxicity According to an Oxidative Stress Paradigm." *Nano letters* 6, no. 8: 1794-1807.
- Xia, Tian, Michael Kovoichich, Monty Liong, Lutz Mädler, Benjamin Gilbert, Haibin Shi, Joanne I Yeh, Jeffrey I Zink, and Andre E Nel. 2008. "Comparison of the Mechanism of Toxicity of Zinc Oxide and Cerium Oxide Nanoparticles Based on Dissolution and Oxidative Stress Properties." *ACS nano* 2, no. 10: 2121.
- Xu, L., X. Li, T. Takemura, N. Hanagata, G. Wu, and L.L. Chou. 2012. "Genotoxicity and Molecular Response of Silver Nanoparticle (Np)-Based Hydrogel." *Journal of Nanobiotechnology* 10, no. 1: 16.
- Yang, Hui, Chao Liu, Danfeng Yang, Huashan Zhang, and Zhuge Xi. 2009. "Comparative Study of Cytotoxicity, Oxidative Stress and Genotoxicity Induced by Four Typical Nanomaterials: The Role of Particle Size, Shape and Composition." *Journal of applied Toxicology* 29, no. 1: 69-78.
- Youle, Richard J, and Derek P Narendra. 2011. "Mechanisms of Mitophagy." *Nature reviews Molecular cell biology* 12, no. 1: 9-14.
- Youle, Richard J, and Alexander M Van Der Blik. 2012. "Mitochondrial Fission, Fusion, and Stress." *Science* 337, no. 6098: 1062-1065.
- Yu, Byung Pal. 1994. "Cellular Defenses against Damage from Reactive Oxygen Species." *Physiological reviews* 74, no. 1: 139-162.
- Yu, Tianzheng, James L Robotham, and Yisang Yoon. 2006. "Increased Production of Reactive Oxygen Species in Hyperglycemic Conditions Requires Dynamic Change of Mitochondrial Morphology." *Proceedings of the National Academy of Sciences* 103, no. 8: 2653-2658.
- Yu, Tianzheng, Li Wang, and Yisang Yoon. 2015. "Morphological Control of Mitochondrial Bioenergetics." *Frontiers in bioscience (Landmark edition)* 20: 229.
- Zhang, F., P. Durham, C.M. Sayes, B.L.T. Lau, and E.D. Bruce. 2015. "Particle Uptake Efficiency Is Significantly Affected by Type of Capping Agent and Cell Line." *Journal of Applied Toxicology* 35, no. 10: 1114-1121.

- Zhang, H., H. Liu, K.J.A. Davies, Co. Sioutas, C.E. Finch, T.E. Morgan, and H.J. Forman. 2012. "Nrf2-Regulated Phase II Enzymes Are Induced by Chronic Ambient Nanoparticle Exposure in Young Mice with Age-Related Impairments." *Free Radical Biology and Medicine* 52, no. 9: 2038-2046.
- Zhang, Sulin, Ju Li, George Lykotrafitis, Gang Bao, and Subra Suresh. 2009. "Size-Dependent Endocytosis of Nanoparticles." *Advanced materials* 21, no. 4: 419-424.
- Zhang, Yanhong, Wensheng Yan, and Xinbin Chen. 2011. "Mutant P53 Disrupts Mcf-10a Cell Polarity in Three-Dimensional Culture Via Epithelial-to-Mesenchymal Transitions." *Journal of Biological Chemistry* 286, no. 18: 16218-16228.
- Zhang, Ying, Chenguang Yu, Guanyi Huang, Changli Wang, and Longping Wen. 2010. "Nano Rare-Earth Oxides Induced Size-Dependent Vacuolization: An Independent Pathway from Autophagy." *International journal of nanomedicine* 5: 601.
- Zhao, J., L. Bowman, X. Zhang, X. Shi, B. Jiang, V. Castranova, and M. Ding. 2009. "Metallic Nickel Nano-and Fine Particles Induce Jb6 Cell Apoptosis through a Caspase-8/Aif Mediated Cytochrome C-Independent Pathway." *Journal of Nanobiotechnology* 7, no. 1: 2.
- Zick, Michael, Regina Rabl, and Andreas S Reichert. 2009. "Cristae Formation—Linking Ultrastructure and Function of Mitochondria." *Biochimica et Biophysica Acta (BBA)-Molecular Cell Research* 1793, no. 1: 5-19.
- Zucker, Robert M, Jayna Ortenzio, Laura L Degn, Jeremy M Lerner, and William K Boyes. 2019. "Biophysical Comparison of Four Silver Nanoparticles Coatings Using Microscopy, Hyperspectral Imaging and Flow Cytometry." *PloS one* 14, no. 7: e0219078.